# Review on water electro-sprays and applications of charged drops with focus on the corona-assisted cone-jet mode for High Efficiency Air Filtration by wet electro-scrubbing of aerosols

Jean-Pascal Borra

https://doi.org/10.1016/j.jaerosci.2018.04.005

# (private transmission of pre-proof version)
# for a Special Issue of *Journal Aerosol Science* on ELECTRO-SPRAYS

https://doi.org/10.1016/j.jaerosci.2018.04.005

***Highlights***:

- electrosprays is a continuous production process of self-dispersed unipolar droplets with monodisperse/unimodal size distributions ($0.2 < d_{modal} < 150$ µm)
- Applications of ES of aqueous solutions are reviewed with special attention for material production and bio-applications
- Means to achieve steady water ES are presented with respect to electrical discharges in ambient air around the liquid cone and jet
- Streamer discharges with transient and asymmetric space charges disrupt the EHD equilibrium for steady cone-jet mode, while the axisymmetric and quasi-stationary space charge is required to achieve *steady water ES in the pulseless corona-assisted cone-jet mode*
- Empirical scaling laws of droplet properties are reminded for both *steady water ES in cone-jet with a pulseless corona and without discharge*
- High filtration efficiencies of a lab-scale wet bipolar-scrubbers (>99%) supports that Water ES in corona-assisted cone-jet could be applied to low cost Air cleaning

https://doi.org/10.1016/j.jaerosci.2018.04.005

# Review on Water Electro-Sprays and applications of charged droplets with focus on the corona-assisted cone-jet mode for High Efficiency Particle Air Filtration by wet electro-scrubbing of aerosol

Jean-Pascal Borra

*Laboratoire de Physique des Gaz et Plasmas CNRS- Univ. Paris-Sud, Univ. Paris-Saclay, Orsay, F-91405, France, 00.33.1.69.15.36.74, jean-pascal.borra@u-psud.fr*

***Keywords:*** Water, Electrospray, EHD, electrical discharges, corona, wet scrubbing

***Abstract***: Electrospray of Water and aqueous solutions is a simple, steady and continuous process for the production of charged droplets. Applications of this low cost spraying process, easy to scale up and environment friendly with low water consumption are first presented.
This review addresses ***the Electro-Spray (ES) in the cone-jet mode****, with focus on water ES with or without discharges in ambient air*. The physical constraints to achieve steady water electrospray in ambient air are depicted to account for Electro-Hydro-Dynamic equilibrium required for the cone and jet formation on the one hand and to control electrical discharges in the gas around the liquid (with continuous corona or without any discharge) on the other hand. Operating conditions and empirical scaling laws between regulation parameters (liquid flow rate and corona current) and the properties of droplets such as the size and the charge are presented for the corona-assisted cone-jet mode of water electrospray in air. Subsequent working conditions to achieve the other steady water ES, without discharge, are then justified. *The interest of this corona assisted cone-jet mode of electrospray in air* for the steady production of self-dispersed unipolar water droplets (close to the Rayleigh limit) with unimodal size distribution is presented with one environmental application for filtration by bipolar-scrubbing of suspended particles from exhaust or ambient aerosols, *with lab-scale efficiencies of High Efficiency Particulate Air filters.*

## 1 Introduction

The fragmentation of bulk liquid into droplets is used in various fields of science and technology under different key-words; ‘spraying’ and sometimes ‘nebulization’, ‘pulverization’ or even ‘atomization’. In all cases, the liquid is divided into droplets by fragmentation of films or jets. In pressure nebulizer, the jet is formed by applying a pressure on the liquid flowing in a capillary nozzle. Otherwise, jets can arise from liquid menisci fragmentation in turbulent gas in pneumatic atomizers or from a flat surface by mechanical deformation under external forces in piezo-electric vibrating crystals (Ashgriz, 2011). Bursting bubbles also produce droplets from liquid jet and film fragmentation, as over ocean whitecap, source of droplets and subsequent salt nuclei involved in clouds formation. (Blanchard, 1989; Rai et al., 2017).
*This review addresses another spraying method with critical advantages among others;* ***the Electro-Spray (ES) in the cone-jet mode****, with focus on water ES with or without discharges in ambient air.*
The interest for water drops and crystals probably arose from their unexpected shapes in permanent visible evolution. Under electrical field, the deformation is even more striking, when the more or less regular rounded drop turns into conical shapes. Since Da Vinci’s description of dripping in terms of drop mass and diameter to balance the opposed inward capillary and gravity forces (Da Vinci, 1513), Savart and Plateau’s have characterized the formation and fragmentation of neutral liquid jets into droplets by purely hydrodynamic propagation of the Plateau-Rayleigh capillary instabilities (Savart, 1833). Then, Rayleigh derived a relation between droplet and jet diameters ($d_{drop}$= 1.89 $d_{jet}$) for the axisymmetric varicose jet break-up (Rayleigh, 1879). He also demonstrated that electrical repulsions in charged droplets accounts for Coulombian explosion with a size-dependent maximum charge limit (Rayleigh, 1882).
Kelvin used the ES as a Voltage generator and for printing by field driven deposition of charged droplets (Kelvin, 1867). Zeliny’s description of ES modes (Zeleny, 1917), was detailed by Vonnegut who noticed the monodispersity of droplets that can be produced in the steady cone-jet mode of ES (Vonnegut et al., 1952) from the equilibrium cone shape of conducting liquid submitted to electric field (Taylor, 1964).

As a source of charged species, ES was then also considered for its potential environmental impact on cloud, fog and haze electrification (Chalmers, 1967). In such disturbed weather, the natural electric fields up to few kV/m leads to drop deformation with subsequent local increase of the electric field in the gas around the charged liquid cones and jets. When the threshold field of gas ionization is reached, corona discharges create ions around pending, suspended or falling drops and crystals, with subsequent space charge fields (Zeleny, 1914; English, 1948; Chalmers, 1967; Janischewskyj et al., 1981; Borra et al., 1997b; Sugimoto et al., 2001; Higashiyama et al., 2013; Xu P et al., 2017).

In corona chargers and electrostatic precipitator (ESP) for filtration, particles are charged by collection of corona gaseous ions (Cross, 1987; Parker, 1997). When used with liquid aerosols, ES of liquid previously collected on electrodes accounts for the production of charged aerosol from the polarized electrodes in ESP (Marijnissen J.C.M. et al., 1993a; Marijnissen J. C. M. et al., 1993b) as in corona charger (Unger et al., 1999). Under AC polarization of pending drops on HV power lines, ES is also considered to account for power losses by ES and corona leakage currents (Hara et al., 1980; Farzaneh et al., 1985; Borra et al., 1999d; Xu P et al., 2017; Yin et al., 2017).

Various modes of hydrodynamic and Electro-Hydro Dynamic (EHD) jet formation and fragmentation are reviewed in (Rosell-Llompardt et al., 2018b) focusing on Electro-Spray modes, as defined by (Cloupeau et al., 1989, 1990; Cloupeau, 1994; Cloupeau et al., 1994) with a special attention paid to the ***cone-jet mode***, detailed in (Ganan-Calvo et al., 2018). In that case, the drop turns into a conical shape because of the surface polarization and related outward normal electrical pressure that can only be balanced by the inward capillary pressure. This equilibrium is frequently expressed as a threshold field condition for the cone-jet formation ($E_{cone\text{-}jet} \approx (\gamma / \varepsilon_0 R_{jet})^{1/2}$), versus the liquid properties (density $\rho$= 998 kg.m$^{-3}$, viscosity $\eta$= 1.002 Pa.s, surface tension $\gamma$= 65-73 mN.m$^{-1}$, relative permittivity $\varepsilon_r$= 80, for water). Since the surface charge density increases from the cone base at the tip of the capillary, the normal electric pressure increases which leads to smaller liquid radius up to the cone-jet transition zone, where the normal electric field is maximal, as expected from models of the cone and jet shapes (Hayati et al., 1987a; Hartmann et al., 1997; Yan et al., 2003), and confirmed from electrical discharge localization in the gas around the liquid (Borra et al., 1996). The surface charges are accelerated by the tangential component of the electric field along the cone surface, to the apex. Once, this EHD flow delivered from the cone to the jet is adjusted with the applied voltage to the liquid flowrate delivered to the cone, the EHD equilibrium is reached and the emerging jet breaks-up into droplets by the propagation of growing capillary instabilities. This EHD equilibrium can be maintained by increasing the voltage for lower flow rate and reversely (Hayati et al., 1987b) for all tested liquids and solutions. Even if out of scope of water ES, ES of viscous liquids has been achieved in cone-jet mode (Ku et al., 2002; Rosell-Llompardt et al., 2018a), as well as for low conductivities by charge injection (Bailey, 1988).

In this steady ***cone-jet mode of ES***, unique monodisperse/unimodal droplet size distributions can be achieved. The modal diameter can be finely tuned with liquid flowrate and conductivity and to a lower extend with the voltage, following confirmed characteristic scaling laws between the spray current of charged droplets evolving with $Q_{Liq.}^{n>0}$, as well as droplet size. Operating conditions and subsequent droplet properties (size and charge) produced by steady ES in cone-jet mode can be defined by different approaches, detailed in (Ganan-Calvo et al., 2018; Rosell-Llompardt et al., 2018b), versus liquid properties and geometry of spraying capillary nozzles. Moreover, these unipolar charged droplets are self-dispersed, with a quasi-maximal charge per drop, close to half of the Rayleigh limit.

With such critical advantages among other spraying means, ES in cone-jet mode is a low cost environment friendly production process of monodisperse droplets from any bulk liquid. With low liquid consumption and enhanced surface of such fine self-dispersed droplets, easy to scale up, the water ES has been studied for different applications presented in the first section, with emphasis on recent developments for material production and processing as well as for bio-applications.

The second section addresses the coupled physical constraints to be taken into account to achieve steady water ES in the cone-jet mode in ambient air. Indeed, with the highest surface tension around 70 mN.m$^{-1}$ in STP, higher threshold field and voltages are required to reach EHD equilibrium for water in cone-jet mode than for other solvent and solutions (Burayev et al., 1972; Smith, 1986; Cloupeau et al., 1989; Borra et al., 1999d; Hartmann et al., 1999a; Hartmann et al., 1999b). Here, the effect of transient or quasi-stationary space charges of gaseous ions created by streamers and pulseless corona discharges in the gas

https://doi.org/10.1016/j.jaerosci.2018.04.005

around the liquid on the total electric field at liquid surface are depicted and related to steady/unsteady ES modes. Common ways to avoid electrical discharges or to induce a pulseless discharge are given to achieve steady water ES in the cone-jet mode, for the production of charged water spray in ambient air.
Finally, the interest of water ES in the pulseless corona-assisted cone-jet mode is highlighted for the steady production of monodisperse/unimodal self-dispersed unipolar water droplets, close to Rayleigh charge limit to enhance wet electro-scrubbing efficiencies, as an alternative to fabric filters and ESP used for filtration**.**

https://doi.org/10.1016/j.jaerosci.2018.04.005

## *2* Interest and applications of water electro- spray

The high surface-to-volume ratio of sprays with a particular interest for low cost, environment friendly and biocompatible water ES, has been applied to various domains, for:

- propulsion by "colloidal" thruster in space, where contamination is not allowed except by water (Huberman et al., 1968; Velásquez-García et al., 2006; Alexander et al., 2007; Quang Tran Si et al., 2007; Gamero-Castaño, 2008; Tang HB et al., 2011; Borner et al., 2013; Morris et al., 2013),
- agricultural application for crop spraying of water-based solutions of pesticides on fields (Coffee, 1981; Law, 1982), as well as in greenhouses (Geerse et al., 2000),
- Gas conditioning in terms of temperature and humidity (Bailey, 1988; Cui et al., 2017), up to odor masking for domestic gas (Ganesan et al., 2016),
- gas treatment for pollution abatement of harmful gases and suspended particles in exhaust fumes and smokes, detailed in the section 4,
- water treatment as metal extraction (Parmentier et al., 2016), desalination by evaporation (Agostinho et al., 2018) or bio-decontamination (Pyrgiotakis et al., 2012; Machala et al., 2013; Kanev et al., 2014).
- monodisperse nano-particles production by ES of sucrose solutions (Chen DR et al., 1995; Kaufman, 2000) now developed and sold by TSI™ and Ramem™ as size-calibrated aerosol generators. Here, the neutralization of droplets can be achieved either with bipolar gaseous ions from radioactive, X-ray and DBD neutralizers or with unipolar ions from corona discharges or from evaporation of charged droplets (Liu BYH et al., 1974; Adachi M. et al., 1983; Adachi Motoaki et al., 1993; Chen DR et al., 1995; Morozov VN et al., 2007; Tsai et al., 2008; Fu et al., 2011; Morozov V, 2011; Fu et al., 2012; Tsai et al., 2013; Liu Q et al., 2014b; Tai et al., 2014; You et al., 2014; Mathon et al., 2017).

Jaworek (2007b, 2018), Wu and Clark (2008a, 2008b) have reviewed ES devices developed for production and processing of materials implying droplet neutralisation. Coatings have been performed by ES deposition on grounded surfaces and particle production is achieved either by injection of charged droplets in grounded liquids for composite coated particles or by neutralization of suspended droplets for the production of the dried powders.

Neutralization of droplets produced by ES in cone jet mode can be achieved either in suspension by bipolar or unipolar gaseous ions, detailed just above for monodisperse particles production, as well as by coalescence of droplets with opposite polarity from two unipolar ES for powder production (see §2.1).

### 2.1 For Materials processing

Electro-spray in the steady cone-jet mode is, to date, mainly used for materials production, with a particular interest for composite materials such as coated powders and porous membranes deposited on surfaces. Indeed, powder production starting from ES of water based solutions and suspensions of nanoparticles is already used in numerous domains of applications from food flavoring and conservation (Pyrgiotakis et al., 2016), to new materials and bio-applications (Sweet ML et al., 2014).

With highly charged droplets, ES is well adapted for electric field driven applications, either for deposition on grounded electrodes, in grounded liquids or for coagulation with opposite polarity species in suspension. Of course, the control of electrical properties of droplets is an additional advantage of ES in cone-jet for deposition processes like coatings and printing (Sweet RG, 1965; Kamphoefner, 1972; Jaworek, 2007a; Stachewicz et al., 2010; Jaworek, 2011). Furthermore, efficient interfacial processes, such as bipolar mixing for controlled kinetics of reactions in droplets formed by coalescence of two opposite polarity droplets from two unipolar ES. Taking advantage of the tunable size distributions of the droplets produced by ES in steady cone-jet modes, tailored dried particles can be achieved with controlled size, shape and density (Borra et al., 1997a; Borra et al., 1999a; Jaworek, 2007a, b). Dense to hollow dried particles are achieved with subsequent tunable porosity of final powders. This is especially critical to produce membranes with defined apparent exchange surface and composition required in most industrial domains from energy production, conversion, and storage and more generally to catalysis or polymers membranes (Castillo et al., 2018; Kelder et al., 2018; Rosell-Llompardt et al., 2018a).

The properties of the dried particles, including composition, size and morphology can be tuned by controlling the initial droplet size and the drying conditions with related droplet evaporation rates and subsequent production rates of nanoparticle suspended in the droplet on the one hand and on the other, the diffusion rate of so-formed nano-crystal. Production and transport of so-formed nuclei in the droplet

controls the size and concentration profile of nanoparticles in the droplet and the related agglomeration rate, which is critical to achieve different morphologies of the final dried particles (Vehring, 2008).
Kodas and Hampden-Smith described ***aerosol-based processes for the production of materials***, including reactive and non-reactive spray drying (Kodas et al., 1971; Messing et al., 1993; Wilhelm et al., 2003; Vehring, 2008). Some examples of reactive spray pyrolysis used for the production of oxide particles are detailed in (Rulison et al., 1994; Borra et al., 1997a; Okuyama et al., 1997; Chen CH et al., 1999; Lenggoro et al., 2000; Bastide et al., 2006; Jaworek et al., 2008; Shi et al., 2011; Xie et al., 2015; Tang J et al., 2016; Tang J et al., 2017a; Tang J et al., 2017b) and non-reactive drying of droplets leading to nano-particles from water based solutions in (Tang K et al., 1994b; Vehring, 2008; Maißer et al., 2013).
Such nuclei are formed by nucleation or crystallization when the maximum solute concentration (solubility constant) is reached, either at the surface or in the volume of the droplet. Surface nucleation occurs from evaporation or from interfacial reaction of liquid with gaseous reactants. In that case, the kinetics of product formation in the droplet depends on the surface temperature and on reactants concentrations in the liquid interface, limited by slow diffusion from gas phase. Since the same chemical reactions can be induced in volume when two droplets with opposite polarities are mixed by electro-coalescence, positive and negative ES have been used to increase the apparent reaction rate between the same reactants dissolved in controlled relative concentrations in droplets produced by ES with opposite polarities, (Borra et al., 1997a; Camelot et al., 1998; Borra et al., 1999a; Verdoold et al., 2000; Jaworek et al., 2008; Verdoold et al., 2011; Fu et al., 2012; Liu Q et al., 2014a; Xie et al., 2015; Tang J et al., 2016; Tang J et al., 2017a).
Recent production of "smart" composite materials are also based on the production of nanoparticles in liquid droplets, as described above, from drying and eventual reaction in the liquid drop but as well by the direct ES of nano-suspensions, i.e. of droplets with suspended solid nanoparticles. In that case, composite coatings including nanoparticles are deposited by ES of water-based suspension. ES deposition of living bacteria and bio-molecules and self-patterning of Carbon nanotube and graphene in watersuspension have been achieved. It is also used for the production of nano-composite materials doped with nano-oxides, polymer fibers loaded with Metal catalysts for fabrics, porous membranes for energy production with fuel-cells, conversion in solar cells and storage in capacitors, sensors for gas detection (De Juan et al., 1996; Chen CH et al., 1999; Jayasinghe et al., 2002; Jayasinghe et al., 2005a, b; Wang DZ et al., 2005; Jayasinghe, 2006; Wang DZ et al., 2007a; Yu et al., 2007; Kim K et al., 2008; Prajapati et al., 2010; Wang D et al., 2011; Wang D et al., 2013; Krella et al., 2017; Castillo et al., 2018; Kelder et al., 2018).

## 2.2 For bio-applications

Bio-applications of water-based solutions ES are expected to become soon a fruitful investment for technological companies. As an example of these tremendous markets to be developed for allergies detection and treatment, DBV Technology ™ recently achieved the fabrication of skin-compatible-patches for lactose and peanuts allergy detection by ES deposition.
To do so, ES of an aqueous protein solution is used for deposition on a patch of required amount of dried proteins per patch, with 100% efficiency i.e. without any mass loss of dissolved proteins. Moreover, the dried protein are homogeneously distributed on the patch due to electrostatic repulsions, to avoid post-deposition electro-coagulation, with their initial allergenic properties. Production capacity in the order of millions of patches per year (DBVtechno.), already enables large scale commercialization in malls rather than as performed today with long and expensive tests in specialized services of hospitals (Fig.1).

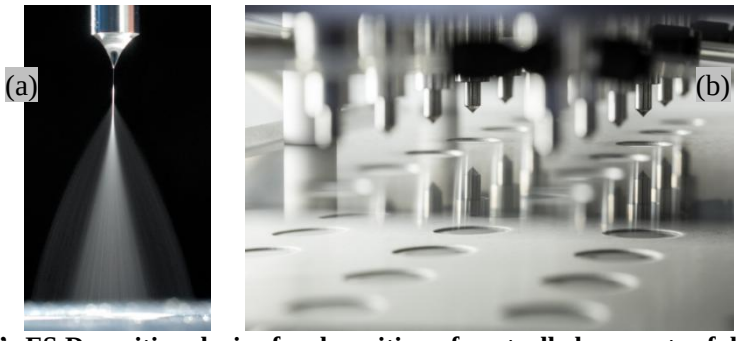


**Figure 1: DBVtechno's ES Deposition device for deposition of controlled amounts of dried allergenic proteins homogeneously distributed over the patch surface, (a) Single ES in the cone-jet mode of the aqueous solution**

**of proteins deposited after evaporation and drying along the transit to surface of the patch and (b) the multi nozzle electro-spraying machine for the large scale production of bio-functionalized skin compatible patches.**

Other medical powders are produced in the industry for pills and cream processing. Eventual coating may be used for stabilization of light sensitive materials, for accurate localization within the micrometer range resolution from electromagnetic properties, as well as for storage and transport without agglomeration from mechanical and chemical properties (Ho et al., 2012), Another important application of coated reactants or medical principles is the time-controlled delivery by diffusion across a porous coating or dissolution of the coating (Vehring, 2008). ES is also tested in drug delivery inhalers of dried powders (Tang K et al., 1994b; Ijsebaert et al., 1999; Chen DR et al., 2010; Carvalho et al., 2016), as well as for deposition of biomolecules such as genes, allergens (DBVtechno.), anticorps IgH or living bio-organisms like bacteria and viruses for chemical and bio-sensors (Boda et al., 2018; Kavadiya et al., 2018).
ES of charged droplets collected in liquid is also applied to emulsion and suspension preparation. For instance, cytocompatible capsules suspended in water are achieved by "water in water" emulsions formed when two immiscible solutes are mixed by spraying 15% dextran aqueous solution in 8% PEG aqueous solution (Song et al., 2015). This is also used for the production of composite particles suspended in liquids, e.g. with a chitosan core electrosprayed in a calcium phosphate solution for encapsulation of liquids up to living yeast cells in hydroxyapatite shell (Yunoki et al., 2014) and with polystyrene beads electrosprayed in a aqueous solution for surface functionalization and immunoassay bio-diagnostic (Foti et al., 2015).
Otherwise, water ES is also investigated for bio-decontamination of surfaces and of water. ES of aqueous suspension of bacteriophages has been achieved for for surface decontamination after collection on grounded surfaces (Jung et al., 2009). Besides, coupling the UV photo-catalysis of $TiO_2$ nanoparticles suspended in water for Reactive Oxygen Species production, decontamination of bacteria in water has been achieved using water ES without electrical discharges i.e. without plasmas (Hong et al., 2011), while water ES with electrical discharges is also used for water treatment (see below §-2.3 Other application of water electrospray with electrical discharges).
Finally, the most spread application of water-based solution ES has been developed for bio-molecules analysis. Here ES is used as an ion source to produce ionized species from liquid droplets, then analyzed either (i) by mass spectrometry, referred as ES Ionization-MS (Thompson et al., 1984; Yamashita et al., 1984; Whitehouse et al., 1985; Fenn et al., 1990; Wilm et al., 1994; Xu X et al., 1996; Juraschek et al., 1998; Pozniak et al., 2004; Loo et al., 2005; Marginean et al., 2007; Pozniak et al., 2007) used for macromolecules analysis and quantification near atmospheric pressure by online HPLC MS/MS, in both polarities or (ii) by mobility analysis of so-produced droplets/dried residues by ES-DMA for Differential Mobility Analyzers or as GEMMA for Gas-phase Electrophoretic Mobility Molecular Analyzer (Lewis et al., 1994; Kaufman et al., 1996; Mouradian et al., 1997; Kaufman, 1998; Kaufman et al., 1998; Kaufman, 2000; Bacher et al., 2001; Tsai et al., 2008; Tsai et al., 2013; Tai et al., 2014; You et al., 2014; Almaier, 2018). These analytical methods are still under development with new microfluidic facilities for "nano-emitter" to reach unequaled sensitivity for biomolecules like DNA, lipoprotein at sub-$nL.min^{-1}$ (Bacher et al., 2001; Marginean et al., 2007; Wang L et al., 2007b; Gibson et al., 2009; Marginean et al., 2014).

## 2.3 Other application of water electrospray with electrical discharges

Despite unstable negative water ES discussed in the next section, a new application of water ES with negative corona discharge targets analytical emission spectroscopy of dissolved species in water, that can be analyzed through light emitted from the discharge after evaporation and plasma excitation of initially dissolved species (Pohl et al., 2017), as performed by ICP-AES in low pressure RF plasmas.
Surface and Water bio-decontamination has been achieved using water ES with electrical discharges. Indeed, aqueous mixtures of hydrogen peroxide with formic and acetic acids and esters as well as nitrogen oxides and acids are used for surface decontamination (Alasri et al., 1992). Similar species are produced by plasma in humid air or in water droplet and films exposed to air plasma, as reported in lab-scale corona discharges (Lecuiller et al., 1988; Sisterson et al., 1990; Borra et al., 1998) as well as in the troposphere to account for fog acidification by corona point discharges from trees (Borra et al., 1997b). Post-discharge surface decontamination has thus been achieved by plasma (Hoenig et al., 1980; Odic et al., 2002) as well as by water ES with discharges for suspensions of Escherichia Coli (Lee HK, 2001; Lee H-K et al., 2005). Indeed, Reactive Oxygen and Nitrogenous Species produced by corona (Kanev et al.,

2014) and by spark (Machala et al., 2013) have been proposed by (Pyrgiotakis et al., 2014) to account for bacterial inactivation.
More generally, ES of other organic solvents than water with dissolved reactants can also be performed simultaneously with electrical discharges, as well as by post-discharge ES injection of droplets downstream a discharge to develop new plasma-based aerosol processes (see 5-Conclusion).
At last, steady water ES in a particular corona-assisted cone-jet mode can also be used as addressed in section 4.3, for particle removal from gas stream by bipolar Coulombian coagulation on scrubbing droplets, detailled in section 4.

https://doi.org/10.1016/j.jaerosci.2018.04.005

# 3 Water ES modes with and without discharges

This section focuses on *steady water ES in cone-jet mode for the unique tunable unimodal size and charge distributions, required for physical studies and applications of monodisperse non-agglomerated unipolar droplets that can be achieved in ambient air at STP conditions*. Here are depicted, the effect of electrical discharges in the gas on the electric field along the liquid surface and the consequences on the ES stability as well as means to suppress the discharges. Finally, working conditions for steady Water ES with and without discharges are discussed with respect to capillary geometry versus conductivity and flowrate.

## 3.1 ES modes characterization

The steady cone-jet is one of the ES modes detailed in (Zeleny, 1917; Vonnegut et al., 1952; Smith, 1986; Hayati et al., 1987b; Bailey, 1988; Cloupeau et al., 1989, 1990, 1994; Jaworek et al., 1999). These modes have been investigated versus functioning conditions in the flowrate-voltage space for different conductivities and capillaries, based on:

- Observation of cone and jet shapes (Bailey, 1988; Cloupeau et al., 1989, 1990, 1994; Jaworek et al., 1999), among others, with shape evolution confirmed for precession and multi-jet modes (Jaworek et al., 1996; Noymer et al., 1999), the spindle and intermittent cone-jet modes with fast and CCD imaging (Kim HH et al., 2011; Pongrác et al., 2014) and for the first droplet emission in cone-jet (Ganan-Calvo et al., 2016). In cone-jet, the cone is steady with either a steady jet for axisymmetric varicose fragmentation or a whipping jet for asymmetric kink fragmentation at larger flowrate (see 3.3.1.4).
- Measurements of the mean current versus flowrate and conductivities for comparison to scaling laws established for the cone-jet (see 3.2 and 3.3.1.4). For unsteady ES modes, oscilloscope measurements of currents are useful to define the droplet emission frequency of dripping or spindle modes, and even critical to deal with ES destabilization by transient discharges such as pre-onset streamers, streamers and sparks (Borra et al., 1996; Borra et al., 1999d; Ehouarn P. et al., 2001; Borra et al., 2004; Pongrác et al., 2014; Verdoold et al., 2014; Pongrác et al., 2016), as first reported on pending drops (see introduction) and confirmed by emission spectroscopy (Meesters et al., 1992; Jaworek et al., 2014).
- Droplets properties (size distributions, charge per drop) and spray expansion (2D velocities, fluxes and concentration profiles) evaluated from Laser Phase Doppler measurements at different radial positions from the symmetry axis of nozzle, cone, jet and spray, versus voltage, flow rate and conductivity (Cloupeau et al., 1989; Snarski et al., 1991; Dunn et al., 1992; Tang K et al., 1994b, 1995; Grace et al., 1996; Hartmann et al., 1996; Naqwi et al., 1996; Tang K et al., 1996; De Juan et al., 1997; Gañán-Calvo et al., 1997; Olumee et al., 1998; Hartmann et al., 1999a; Ku et al., 2002; Wilhelm et al., 2006).

Ideally, the cone-jet mode of ES is confirmed with all arguments. However, simple current or droplet size measurements alone is enough thanks to scaling laws specific to the cone-jet mode established and confirmed for all liquids, at least without discharges as depicted just below.

## 3.2 Scaling laws and characteristic times for operating conditions of cone-jet mode

The striking stability of ES in cone-jet mode for the continuous production of monodisperse or unimodal droplets size and charge distributions has triggered the interest of physicist and engineers. Operating conditions for ES in cone-jet mode (voltage-flowrate) have been addressed versus liquid properties.

***Scaling laws*** or empirical relations link the mean droplet charge and size, to both the liquid properties (density $\rho$= 998 kg.m$^{-3}$, viscosity $\eta$= 1.002 Pa.s, surface tension $\gamma$= 65-73 mN.m$^{-1}$, relative permittivity $\varepsilon_r$= 80) and flowrate (de la Mora et al., 1994; Chen DR et al., 1997; Gañán-Calvo, 1997; Hartmann et al., 1998; Ganán-Calvo, 2004) amongst others. All approaches are based on the EHD equilibrium required for the cone-jet formation, with scaling law of the spray current of charged droplets and droplet size evolving with a power law of the flowrate in $Q_{Liq.}^{n>0}$, with n depending on the liquid properties, discussed in (Ganan-Calvo et al., 2018; Rosell-Llompardt et al., 2018b).

***The minimal flowrate*** for steady ES in cone-jet mode depends on the liquid conductivity. It is usually defined as follow, for shorter electrical relaxation than viscous or transit times in the cone and jet to let charges drift to the cone surface (Ganan-Calvo et al., 2018). *Then the cone-jet can be established if surface charges induce the required normal electric field for balanced capillary and electrical pressures, as well as the tangential electric field induced by the voltage drop in the resistive liquid to accelerate the*

*interfacial converging liquid into a jet* (Hayati et al., 1987b; Hartmann et al., 1997; Hartmann et al., 1999b).

The electrical relaxation time ($\tau_{elec}= \varepsilon\varepsilon_0/\lambda$, *from 7µs for 0.1 mS.m*$^{-1}$ *de-ionized water to ≈70 ns for 10 mS.m*$^{-1}$ *rain or tap water),* is compared with different hydrodynamic characteristic times, depending on the considered mode. The hydrodynamic characteristic time corresponds either (i) to the time required for the formation of different volumes ($\tau_{transit/\ formation} \approx V_{drop}/\ Q_{Liq.}$) as the pending drop related to the outer diameter of the capillary (Shiryaeva et al., 1995), the cone (Hartmann et al., 1999b), the jet (Gañán-Calvo et al., 1997), the droplet emitted from the jet (Harpur et al., 1996), or (ii) to the characteristic times for jet formation ($\tau \approx \eta.d_{in}/\ \gamma$) and deformation ($\tau \approx(\rho.d^3_{in}/\ \gamma)^{0.5}$ related to inner diameter in (Jaworek et al., 1999), or (iii) to the characteristic viscous time ($\tau_{visc.}\approx r_{Liq.}^2.\rho/\eta$, (Pfeifer et al., 1968; Bailey, 1988; Shiryaeva et al., 1995; Harpur et al., 1996)). The minimum flowrate for cone-jet is defined as $Q_{min}= 10^{-2}.\gamma.\varepsilon_{Liq.}/\rho.\lambda$, from $10^{-16}$ $m^3.s^{-1}$ for 4 $S.m^{-1}$ sea water to $10^{-12}$ $m^3.s^{-1}$ for 0.1 $mS.m^{-1}$ deionized water (Gañán-Calvo et al., 2013).

Whatever the approach to define the minimum flowrate is, the maximum one for the cone-jet mode is ten times higher than this minimum one for a given capillary (Harpur et al., 1996). This range of water flowrate and related droplet properties can be enlarged, using micron-sized capillary nozzles. Indeed, the minimum flowrate of 60 $nL.min^{-1}$ (for $10^{-12}$ $m^3.s^{-1}$) calculated for 0.1 $mS.m^{-1}$ water ES in cone-jet without discharge, is larger than reported for micron-sized capillaries (0.3 $nL.min^{-1}$), but smaller than for 50/20 µm capillary (1.7 $\mu L.min^{-1}$) and far below the 3 $mL.min^{-1}$ reported in section 3.3.3 on larger capillaries (400/150 µm) for corona-assisted cone-jet, discussed below.

## 3.3 Water ES in cone-jet mode

Since Zeleny's observations of electrical discharges from water drop, ES in cone-jet was reported as destabilized or prevented by discharges (Zeleny, 1917; English, 1948; Hayati et al., 1987b; Bailey, 1988). Then, "a stabilized ES mode by the pulseless corona" has been described (Cloupeau et al., 1989, 1990), confirmed in $CO_2$ (Tang K et al., 1994b, 1995) and air (Borra et al., 1996; Jaworek et al., 1997; Borra et al., 1999d; Ehouarn P. et al., 1999; Borra et al., 2004; Lopez-Herrera et al., 2004; Jaworek et al., 2014).

Without discharges, ES works in both + and - DC as well as in AC polarities, as mentioned in the introduction to account for water ES from HV power lines. However, if corona discharges develop in the gas, ES are unstable in negative polarity due to positive ion flux to the liquid surface with high kinetic energy, while positive ES can be stabilized in the corona-assisted cone-jet mode with less energetic electron flux (Cloupeau, 1994; Borra et al., 1999d; Sugimoto et al., 2001; Higashiyama et al., 2013). Hence, only the positive water ES is addressed below, all the more that discharge onset voltage are lower for negative than for positive electrical discharge in air at STP (Loeb, 1965).

### *3.3.1 Unsteady/steady water ES induced by streamer/pulseless corona space charge fields*

Unsteady/steady water ES modes induced by impulse/pulseless corona are described and detailed in terms of discharge physics. The operating conditions of steady water ES in corona-assisted cone-jet mode and empirical relations between the properties of droplets are presented with spray characteristics.

For positive ES in liquid cone-to-plate configuration, the same succession of discharge regimes is reported as for the reference point-to-plane configuration. In such heterogeneous electric field profiles, the development of the discharge is controlled by the space charge field, well described for air corona discharges at atmospheric pressure (Goldman et al., 1978) as well as for ES to account for the development of the spray as a cloud of unipolar charged droplets (Hartmann et al., 1999a) and for different jet evolutions with less mobile positive and negative corona space charges (Pongrác et al., 2016). Then, the total electric field is the sum of the related gaseous corona ions and charged droplets space charge fields with Laplacian electric field related to the applied potential, the electrode shape and to the gap length.

#### *3.3.1.1 Description of unsteady/steady water ES induced by impulse/pulseless corona*

ES modes are presented in Figure 2 at increasing voltages for conductivities from 0.1 to 10 $mS.m^{-1}$, metal nozzle with outer diameters from 0.4 to 1.8 mm and flowrate from 30 to 200 $mL.h^{-1}$. The related current-voltage characteristic, with spray and corona currents are briefly reminded in Appendix A1 and detailed with material and methods for corona and spraying modes characterization in (Borra et al., 1999d; Ehouarn P. et al., 1999; Borra et al., 2004).

https://doi.org/10.1016/j.jaerosci.2018.04.005

The volume where the electric field overcomes the gas ionization onset can be localized from light emitted by the plasma. Electron avalanches occur for electric field higher than $2.5 \cdot 10^6$ V.m$^{-1}$ in ambient air (Lowke et al., 2003). Discharge develops as transient plasma filaments, measured as current pulses, or as a steady corona confined around the liquid cone-jet transition (Figure 2b), with pulseless current (see 3.3.1.2).

- $V_{Nozzle} < V_{Onset\ discharge}$: ***dripping and jetting without discharge*** (field profile 1 in section 3.3.1.2): Droplets are produced from the capillary or from the jet depending on the flowrate. No discharge pulse is detected.

- $V_{Onset\ discharge} < V_{Nozzle} < V_{pulseless\ corona}$ : ***unsteady dripping/jetting and intermittent cone-jet*** (Fig 2a with profile 2 ***in 3.3.1.2***): above the discharge threshold, non-self-sustained discharge first develops as transient plasma filaments, called "burst pulse or pre-onset streamer" up to self-sustained discharge onset, when no more external electron is required since the discharge feeds itself with electrons from previous avalanches leading to an additional continuous current (Goldman et al., 1978).

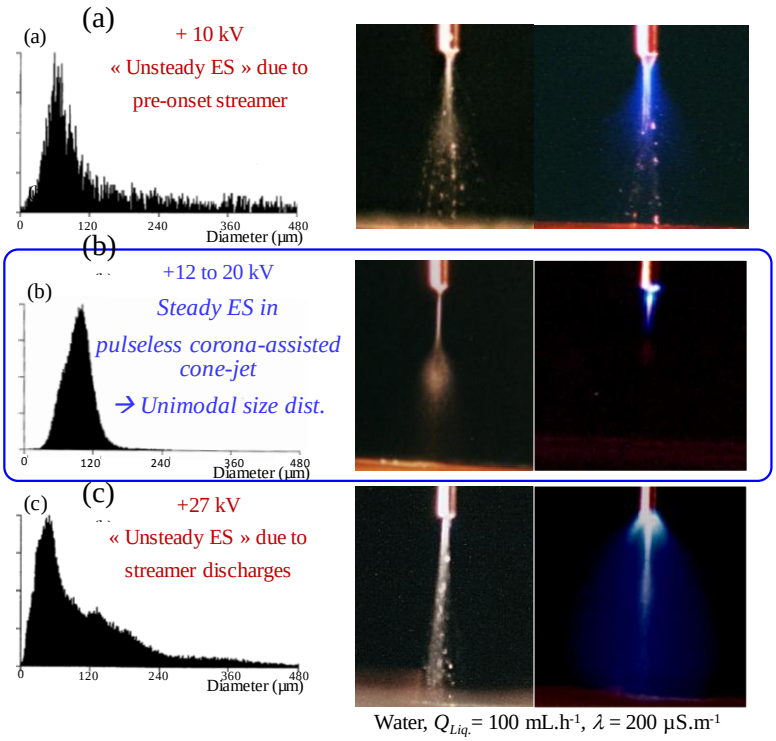


**Figure 2: correlation between discharge regime and ES modes with related size distributions (a) and (c) with (pre-onset) streamers and related transient and asymmetric surface field variations leading to unstable EHD conditions and multimodal size distributions or (b) with the stationary and axisymmetric corona space charge to achieve *steady water ES in pulseless corona-assisted cone-jet,* with unimodal droplet size distributions and geometrical standard deviation around 1.3 and daylight or 60s dark pictures of the nozzle-to-plane gap.**

Then, up to the threshold of pulseless corona, the transient space charge produced by each plasma filament induces an asymmetric, brief and local electric field variation in the gap. as well as on electrode surface (Marode, 1975b). This variation of the electric field along the liquid surfacemay disrupt the EHD equilibrium required for the cone-jet, depending on the relative space charge fields from transient streamer and steady corona and droplets (Borra et al., 2004). In that case, the steady cone-jet mode cannot be induced, as reported over huge ranges of conductivities (from a fraction of mS.m$^{-1}$ for de-ionized water to S.m$^{-1}$ for biological aqueous samples up to a few S.m$^{-1}$ for sea water) and flowrates (from nL.min$^{-1}$ to tens mL.min$^{-1}$) in air, (Juraschek et al., 1998; Sugimoto et al., 2001; Kawamoto et al., 2005; Bruggeman et al., 2007; Shirai et al., 2011; Sun et al., 2011; Shirai et al., 2014; Higashiyama et al., 2017; Xu P et al., 2017). All these modes, other than the steady cone-jet, lead to droplets emission from the capillary or/and from the jet in *dripping, micro-dripping, spindle, intermittent cone-jet, precession and (multi)-jetting modes* reported, at increasing flowrate, (Smith, 1986; Hayati et al., 1987b; Bailey, 1988; Cloupeau et al., 1994; Tang K et al., 1995; Borra et al., 1996; Jaworek et al., 1997; Ehouarn P. et al., 1999; Jaworek et al.,

2005; Pongrac et al., 2011; Jaworek et al., 2014; Kim HH et al., 2014; Pongrác et al., 2014; Pongrác et al., 2016). These modes, other than the steady corona-assisted cone-jet are here gathered under the generic expression ***"unsteady ES modes"*** even if by essence, droplet emission occurs with repetitive cycles of a necessarily unsteady liquid fragmentation zone. This terminology aims to highlight the interest of ***"steady cone-jet modes (with or without discharge)"*** *with respect to the stable shape of the liquid cone and jet (up to the fragmentation zone) and subsequent constant monodisperse droplet properties*, compared to broader or poly-modal size distributions from fluctuating electrical conditions induced by unsteady space charge fields related to transient plasma filament, as detailed below (see 3.3.1.2 Meek's criterion).

Except for the dripping mode (below the onset voltage and related threshold field of gas ionization), for all these unsteady modes of water ES in ambient air, droplets emission systematically starts or ends with a transient plasma filament. Recurrent cycles of liquid deformation and correlated discharges are reported in micro-dripping and spindle modes for lower voltages than the onset one for cone-jet: starting with a pulseless corona from the water jet elongating in the gap up to the break-up, followed after the collection of the emitted sub-millimeter sized droplet, by transient plasma filaments from the residual conical meniscus up to the next drop emission at 100-300 Hz, reported from current measurements of corona discharge around pending, falling or suspended liquid drop and electrosprays (Zeleny, 1917; English, 1948; Joffre et al., 1986; Hayati et al., 1987b; Cloupeau et al., 1990; Cloupeau, 1994; Cloupeau et al., 1994; Borra et al., 1999d; Ehouarn P. et al., 1999; Lopez-Herrera et al., 2004)

- $V_{pulseless\ steady\ corona} < V_{\text{Nozzle}} < V_{impulse\ streamer}$***: pulseless corona-assisted cone-jet mode*** (*Fig 2b with field profile 3, in* 3.3.1.2*)*. The steady pulseless corona discharge regime also referred to as Hermstein or glow (Goldman et al., 1978) corresponds to a confined faint violet plasma around the liquid in ambient air. *The pulseless corona-assisted cone-jet mode is stabilized by the stationary and axisymmetric corona space charge with related continuous current including both continuous currents of charged droplets and corona ions*, as reported for water ES in air (Cloupeau et al., 1989; Borra et al., 2004) or with at least 0.5 % $CO_2$ (Tang K et al., 1994b, 1995), as well as for glycerol in air (Borra et al., 1999d; Ku et al., 2002; Korkut et al., 2008),

The gaseous positive-corona-ion space charge lowers the normal component of the surface electric field. A slower polarization results from the lower field in the liquid, directly linked to the normal component of the field along the liquid cone and jet surface. This steady and axisymmetric corona space charge lowers the surface charge density next to the confined corona, as mentioned for water by (Cloupeau et al., 1989) and ethylene glycol by (Ku et al., 2002; Korkut et al., 2008) to account for steady ES in corona-assisted cone-jet. Korkut attributed the stability to partial neutralization of the jet by electrons from corona, while Gibson listed electro-chemical processes eventually affecting liquid ion composition and mobility.

In these steady EHD conditions, the pulseless-corona assisted cone-jet mode leads to unimodal size and charge distributions of droplets. Such well-controlled properties are critical for physical studies and applications of charged drop, with charge level from 30 to 70 % of the maximum Rayleigh charge limit.

- $V_{\text{Nozzle}} > V_{impulse\ streamer}$***: unsteady intermittent cone-jet mode*** (Fig 2c *with field profile 4 in* 3.3.1.2). In this case, the pulseless corona still exists but the higher voltage also leads to plasma filaments like streamers and sparks, as seen from the larger lightning volume extending in the gap, further than the confined corona. Then, as for pre-onset streamers, the subsequent transient and asymmetric modification of the field along the liquid surface disrupts the EHD equilibrium and the steady corona-assisted cone-jet turns into intermittent cone-jet. Size distribution are then multimodal with respect to unsteady production conditions.

*3.3.1.2 Electrical discharge physics for streamer development and pulseless corona*

• ***Meek's criterion for streamer development inducing unsteady ES***: these transient plasma filaments ("pre-onset streamer" for voltages lower than required for the continuous self-sustained corona, as well as streamer developing further in the gap than the confined corona, for higher voltages) can only occur if the so-called Meek's criterion is reached (Meek J. M., 1940; Marode, 1975a; Meek J.M. et al., 1978). Meek stated that streamer propagation in the gap implies that the space charge field of residual positive ions left by previous avalanches after the faster collection of electrons than ions, has to be at least equal to the threshold field of air ionization ($\approx 2.5 \cdot 10^6$ V.m$^{-1}$ in STP). Avalanches can then start further in the gap between the positive space charge appearing in the high field region close to the electrode with the

smaller radius of curvature and the earthed electrode, where the space charge field reinforces the total electric field. In other words, "this enables the streamer to propagate into the gap as if the high field electrode advances in the gap from the point into the low field region". Taking into account the space charge repulsion and diffusion, Raether has demonstrated that this only happens in ambient pressure when avalanches produces more than $10^{+8}$ charges. Since this number of electrons is given by $e^{(\alpha.d)}$, with *d* the ionization length (over which the total electric field overcomes the threshold field of discharge (Townsend, 1915)), and $\alpha$ the ionization coefficient, this corresponds to a *critical length of ionization around 10 µm* (for $\alpha.d$=18) considering a mean free path of electron in nitrogen of 0.5 µm at STP (Raether, 1964; Nasser, 1986). The corresponding space charge density in the front of the streamer reaches $10^{16}$ $cm^{-3}$ but decreases within nanoseconds under diffusion, repulsion and neutralization, all charges being collected within a fraction of µs (Marode, 1975a). The effect of this transient positive space charge in propagating front of streamer on the total electric field is short but intense; higher electric field develops in the gap between the space charge and the counter electrode, and reversely on the liquid surface. Hence, during streamer development in the gap, the electric field profile along the liquid surface evolves for a few tens of ns, but the EHD equilibrium is disrupted due to the asymmetric surface field evolution around the axisymmetric cone-jet, for a duration in the order of the viscous relaxation time (~ ms) required to form again the cone-jet, until next streamer. The corresponding critical amount of charges per pulse to disrupt the EHD equilibrium lies in the order of pC at the threshold voltage but increases for higher corona current, with respect to the relative space charge fields from transient streamer and both steady corona and droplets ones, as detailed in (Borra et al., 2004).

To fulfill the Meek's criterion for streamer development, avalanche has to start at least at a critical "length of ionization" from the anode surface. This accounts for the higher threshold field of positive discharges in STP air from wires with smaller diameters, as detailed from theoretical analysis of Peek's law combined with Meek's criterion (Hartman, 1984) and discussed for different electrode geometries (Lowke et al., 2003). Hartman has expressed the threshold surface electric field, the ionization length and the number of charges created along this length, versus the wire radius, down to 0.1 µm (close to the minimum jet diameter reported for water ES without discharge producing 0.2 µm droplets, see Figure 3b). More diverging fields around smaller electrode, allow higher voltages and related surface field without overcoming the Meek's criterion for pre-onset streamer development (see dashed blue field profile in Figure 3a for steady ES without discharge for $d_{out}$< 50 µm). Moreover, the critical ionization length and the related surface field increase for radius smaller than a few micrometers (Figure 3b). Then, for jet diameter smaller than few µm from capillaries with outer diameters smaller than few tens of µm, the discharge threshold voltage is offset above the cone-jet mode one and steady water ES can be achieved in air without discharges (see 3.3.2).

- ***Electrical discharge regime versus spatial evolution of the total electric field in the gas:*** the pulse or pulseless discharge regime depends on the ionization length i.e. on the field profile in the gap (see Figure 3). For any gas composition and density, this length depends on the voltage and on the radius of the high field electrode (nozzle, liquid cone and jet) with respect to the field profile in the gap (Hartman, 1984).

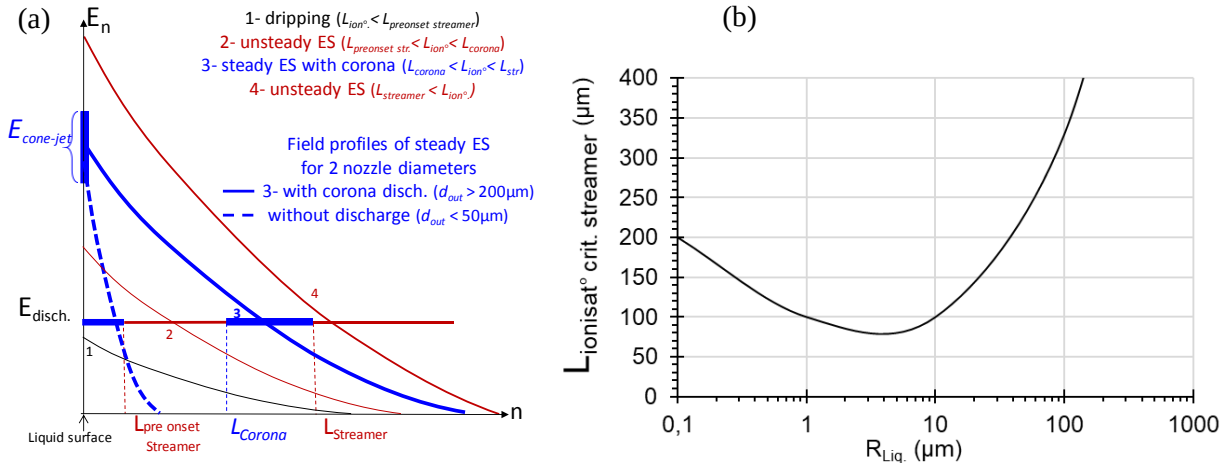


**Figure 3: Electric field profiles along the curvilinear field line from the liquid surface at increasing liquid voltages leading to different ionization lengths with impulse or pulseless discharges correlated to unsteady or**

**steady ES modes: the blue bold profile leads to steady water ES in pulseless corona-assisted cone-jet for nozzles with outer diameters from 0.4 to a 1.8 mm, liquid flow rate from 30 to 200 mL.h$^{-1}$ at 0.1 to 10 mS.m$^{-1}$, while the dashed blue one leads to steady cone-jet mode without discharge on smaller capillary down to 4 µm; (b) Critical ionization length versus the radius of curvature of the positive liquid electrode, (Hartman, 1984)**

The field profile 1 in Figure 3a applies for the dripping mode of ES (not presented on Fig. 2). It leads to a smaller ionization length than required to achieve the Meek's criterion for streamer development reported at discharge onset (Hartman, 1984). Above the onset voltage of discharge (field profile 2), the ionization length overcomes tens of micrometers and pre-onset streamers are measured as current pulses, from 1 to 100 pC per pulse, depending on the space charge density related to the continuous corona current.
For higher voltages, avalanches develop on longer lengths (field profile 3). The steady corona regime is then characterized by a continuous flux of ions from the axisymmetric corona-shaped ionization volume confined around the liquid cone-jet transition (see Figure 2b), to the grounded electrodes. The quasi-stationary space charge distributed symmetrically in the gas around the liquid cone-jet axis, retro controls the field on the anode liquid surface. As for point-to-plane gaps, no more pulse is reported. The continuous corona current evolves much less with the voltage and related Laplacian field than without corona space charge at lower voltage. This confirms the limited electrical field variation over large voltage range due to the corona space charge retro-controlling the Laplacian field in the high field region (Goldman et al., 1978).
At higher voltages (field profile 4) for unsteady ES depicted in fig. 2c, longer avalanches create enough charges leaving the confined corona to fulfill the Meek's criterion for streamer propagation further in the gap, in the low field region thanks to the transient local self-generated space charge field of streamers.
After the description of ES modes related to the discharge physics, working conditions are addressed below.

### *3.3.1.3 Operating conditions of the corona-assisted cone-jet mode in ($\lambda$, $Q_{liq}$, $V_{liq}$) space*

The nozzle-ring-plate configuration is commonly used to shield the polarized liquid cone above the production zone from electrical field variations that may arise with fluctuating surface potential when charged droplets are deposited on insulated surfaces (Tatoulian et al., 2006; Borra et al., 2010, 2012), or with space charge variations when charged particles are injected in the spray, as observed in bipolar ES coagulation for powder production (Borra et al., 1997a; Sigmund et al., 2014a; Sigmund et al., 2014b) and bipolar-scrubbing (see next section). Operating conditions of pulseless corona-assisted cone-jet for steady water ES are thus depicted in the ($\lambda$, $Q_{liq}$, $V_{liq}$) space for the same ES nozzle-to-plate, with or without a ring.

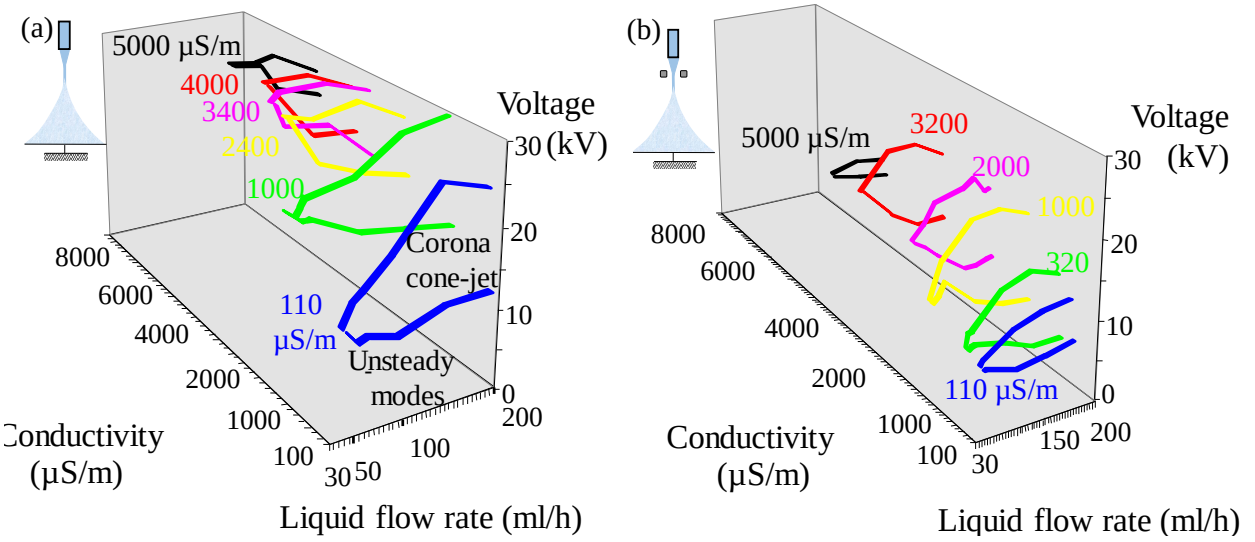


**Figure 4: Steady water ES in corona-assisted cone-jet in ($\lambda$, $Q_{Liq}$, $V_{Liq}$) space for a 4 cm gap with the nozzle ($d_{out}/d_{in}$= 0.5/ 0.25 mm) for (a) nozzle-plate and (b) nozzle-ring-plate configurations, (Borra et al., 1996; Borra et al., 1999d; Borra et al., 2004), with a ring ($d_{in}$= 10 mm) a few millimeters from the nozzle above the jet tip.**

In both configurations, impulse streamers induce "unsteady" ES modes, while the confined pulseless corona leads to steady water ES in pulseless corona-assisted cone-jet mode (cone-jet glow).

https://doi.org/10.1016/j.jaerosci.2018.04.005

***Effect of corona space charge on the minimum flowrate and voltage versus conductivity:***

- For nozzle to plate ES configuration (Fig. 4a), the succession of spraying modes reported in Figure 2 is the same for water than for liquids with lower surface tension, but shifted to higher voltages, all the more for water with the opposed space charge field from corona ions implying higher voltage to reach the same total electric field profile along the liquid surface. However, contrary to the classical cone-jet mode, which for the minimum flowrate decreases for higher conductivities, higher flowrates are required to achieve the steady ES of more conductive water in the pulseless corona-assisted cone-jet. Indeed, higher electric and balancing capillary pressures result from faster polarization of more conductive liquid cone. Then, for subcritical flowrate, the liquid is divided into unstable liquid jets before the cone formation due to excessive outward electric pressure (Cloupeau et al., 1994). Larger cone and jet at higher flowrates reduce the surface charge density and the related electric pressure at constant voltage on larger liquid area ($E_{n,\,surface} \approx \sigma$ (C.m$^{-2}$)/ $\varepsilon_0$ (F.m$^{-1}$)). Higher flowrate thus leads to longer cone with lower electric pressure in the cone base to build the field profile along the cone surface required for cone-jet formation, as described in section 3.2.

With larger cones at larger flowrates, less diverging field profiles lead to streamer development with destabilizing asymmetric and transient local space charges rather than to pulseless corona with its quasi-stationary axisymmetric space charge. Then higher voltages and related smaller cone and jet are required to induce more diverging field favorable to the pulseless corona discharge.

- For shorter gaps with the ring (Fig. 4b), the domains of steady corona ES are shifted to lower voltages. Reducing thus the energy cost of the process, rings are rather used for their stabilizing effect on the liquid cone to achieve the required steady "electrical conditions" discussed just above. Moreover, the ring with the same polarity as the liquid, lowers the normal component of the total electric field at the liquid surface to suppress the destabilizing streamer for steady water ES in air (Borra et al., 1996) as for spray focusing in ES Deposition devices for coating (Jaworek et al., 2018). For detailed information on shielding and focusing rings, these "electrostatic extractor" have been commonly used for more than a century by Lord Kelvin in his electrical power supply based on water electro-dripping/spraying (Kelvin, 1867), for electron beam focusing/deflection and for pulsed ES drop-on-demand as in ink-jet printing devices (Sweet RG, 1965; Kamphoefner, 1972; Stachewicz et al., 2010) and for material production by spray drying (Kodas et al., 1971; Rulison et al., 1994; Camelot et al., 1999). The onset voltage of corona-assisted cone-jet increases with the conductivity in nozzle-plate configuration but evolves differently with the ring (see Figure 4).

Both effects (higher minimum flowrate for higher conductivities and different evolution of the threshold voltage with and without a ring) result from the *different distributions of the corona space charge in the gap, thus retro-controlling with different intensity and dynamics the total electric field profile along the cone and the jet surface*. Indeed, the ring collects corona ions created around the liquid cone-jet or from edges of the nozzle independently of the charged droplets current, radially above the jet break-up, or as a concentric plume of ions around the droplet spray in nozzle to plate configuration.

### *3.3.1.4 Droplet properties and spray development in corona-assisted cone-jet mode of water ES*

Thanks to Phase Doppler development in the 1990's, some spray characterization can be found in literature for the classical cone-jet mode without discharges to establish or/and confirm empirical scaling laws (Gañán-Calvo et al., 1997; Hartmann et al., 1999b). Velocity, flux and diameter of droplet are usually measured to build radial profiles, which are then integrated over the section of the spray at different heights from the nozzle. The production frequency and related concentration and charge per drop can be calculated and the size distribution integrating all produced droplets is obtained, with a *modal most frequently produced droplet size in these unimodal or even monodisperse size distributions*. To highlight these unique droplet properties achieved in the less documented pulseless corona-assisted cone-jet mode, diameter and charge per drop are presented for this steady water ES in air with empirical scaling laws versus liquid conductivities, flowrates and corona current related to the applied voltage (Figure 5).

https://doi.org/10.1016/j.jaerosci.2018.04.005

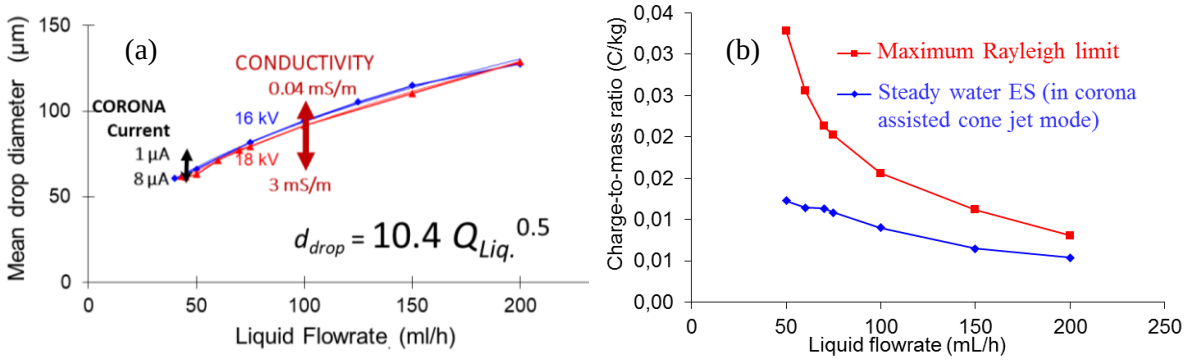


**Figure 5: (a) Modal diameter and (b) Charge-to-mass ratio of droplets and corresponding Rayleigh charge limit, versus flow rate in pulseless corona-assisted cone-jet (110 µS.m$^{-1}$ water). The diameter are represented for different conductivities, and a 15% envelop for the additional variation that can be achieved with the corona ion space charge density controlled by the voltage and the related corona current (Ehouarn P. et al., 2001)**

***Droplet diameter ($d_{droplet}$):*** The unimodal size distribution produced in pulseless corona-assisted cone-jet (Figure 2b) confirms the steady EHD conditions for droplet production. The geometric standard deviation of the size distribution (GSD≈ 1.3) is larger than for monodisperse spray produced by axisymmetric varicose fragmentation in cone-jet mode (< 1.15), as expected for water droplets produced by asymmetric kink fragmentation mode (Hartmann et al., 2000), with the characteristic whipping motion of the jet for 0.1 mS.m$^{-1}$ water ES at 100 mL.h$^{-1}$ (Ehouarn 2001). Then the modal diameter of droplet size distribution follows the empirical relation: $d_{droplet} \approx Q_{liq}^{0.5} \cdot I_{corona}^{-0.04} \cdot \lambda_{liq}^{-0.2}$

As for ES in cone-jet without discharge, in corona-assisted cone-jet, the droplet diameter evolves with the conductivity and the flowrate but as well with the corona current (see Figure 5a). Higher conductivity leads to smaller droplets at a given flow rate. Higher flow rates leads to larger droplets, as expected from classical scaling laws for the cone-jet without discharges. As for cone-jet without discharge, smaller cone-jet lead to smaller droplets at higher voltage and corona current (Ehouarn P. et al., 2001).

***Spray current and droplet charge:*** The spray current and the subsequent mean charge per drop follow the empirical fitted laws versus flowrate and corona current: $I_{spray} \approx Q_{liq}^{0.2} \cdot I_{Corona}^{0.1}$, (Ehouarn P. et al., 2001). The 0.2 exponent of the flowrate is smaller than expected from scaling laws with a 1/3 or 1/4 exponent of the flowrate. This deviation probably arises from the different field profile along the cone surface induced by the corona space charge field. The higher specific charge per drop are derived for lower flow rates from 6 to 12 mC.kg$^{-1}$, following this empirical relation: $q_{droplet}/m \approx Q_{liq}^{-0.8} \cdot I_{Corona}^{0.1}$.

The charge-to-mass ratio is close to the Rayleigh limit ($q_{Rayleigh}/m = (8\pi/m)\cdot(\varepsilon_0 \gamma r^3)^{1/2}$). Hence, the steady water ES in pulseless corona-assisted cone-jet mode produces unimodal size and charge distribution with modal diameter and specific charge of droplets from 40 to 70 % of this maximal charge.

### *3.3.1.5 Spray expansion*

With such charge levels, close to the Rayleigh limit, the corona-assisted cone-jet mode is particularly well adapted for physical studies of electrical properties of suspended droplets as well as for the development of interfacial processes based on electrical forces, such as bipolar-scrubbing of particles for filtration. To highlight the interest of unimodal water sprays for self-dispersion of unipolar droplets due to electrostatic repulsion, droplet velocity (radial profiles at different heights-z- from the nozzle) are presented for the pulseless corona-assisted cone-jet mode.

https://doi.org/10.1016/j.jaerosci.2018.04.005

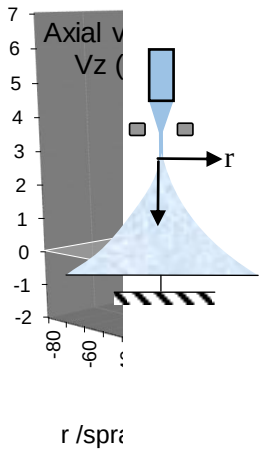


100mL/h-8kV ($I_{corona}$=11µA on a 10mm ring diam.) in a 10cm gap (100µS/m, $d_{out/in}$= 0.5/0.25mm)

**Figure 6: Radial profiles of droplet velocity in pulseless corona-assisted cone-jet (Ehouarn P. et al., 2001)**

As reported and modelled for cone-jet without discharge, the spray development in the gas depends on the initial droplet velocity and related inertia balanced by drag and electrical forces from the total electric field including the Lagrangian one related to the voltage and the space charge fields (Snarski et al., 1991; Hartmann et al., 1999a; Deng et al., 2007; Grifoll et al., 2012; Yang WW et al., 2012). The latest arises here from positive droplets and corona ions. Axial velocities decrease within a few ms from a few to a fraction of $m.s^{-1}$ on the spray axis over a few centimeters, while negative velocities of droplets flowing back to the ring are reported on the edges of the spray (see Figure 6). Droplet concentration (not presented here) decreases from a $10^4$-$10^5$ to $10^2$ in the first few centimeters from the jet on the spray axis with specific surface up to 1000 $m^2.m^{-3}$ (Ehouarn P. et al., 2001).

### *3.3.2 Steady water ES in cone-jet mode without discharge*

Steady water ES in cone-jet can also be performed without discharges in ambient air by acting (i) on liquid surface tension (ii) on threshold field of discharge and (iii) on the field profile around the liquid cone-jet using fine spraying nozzles (< 100 µm).

(i) The water surface tension can be lowered by organic surfactants or organic solvents to decrease the onset voltage of cone-jet. For such aqueous solutions with surface tension below 50 $mN.m^{-1}$, the threshold voltage of cone-jet and multi-cone-jet modes are smaller than the discharge one and both modes can be induced in air without discharges (Smith, 1986; Ehouarn P. et al., 1999).

(ii) To increase the dielectric strength of the gas i.e. the threshold reduced field of discharge (E/N in $V.m^{-4}$, (Nasser, 1986)), water ES has been performed in $CO_2$ or $SF_6$ at atmospheric pressure or at higher pressure in air (Smith, 1986; Hayati et al., 1987b; Bailey, 1988), (Yamashita et al., 1984; Tang K et al., 1994b, 1995). Then, the steady cone-jet is reported without discharge .

(iii) Otherwise, using smaller capillaries (<100 µm), the steady ES in cone-jet mode without discharges in ambient air has also been successfully tested by (Lopez-Herrera et al., 2004), as reported by (Cloupeau et al., 1989). In this case, the faster decrease of the electric field in the gap quenches the development of transient plasma filament since the field never overcomes the threshold field of ionization, further than a few micrometers from the liquid surface (see Figure 3a, dashed blue field profile). Then, eventual shorter avalanches produce less concentrated space charges without streamer formation due to insufficient number of electrons created on this sub-critical length of ionization discussed above from Figure 3b. This is used in commercial ES aerosol generator (Fu et al., 2011) with smaller capillaries and flowrates down to $nL.h^{-1}$ on 4 µm capillaries (Radionova et al., 2016) and even less in (Marginean et al., 2014). This applies to analytical methods based on mobility analysis either of droplets in atmospheric pressure ES-DMA (Liu Q et al., 2014b; Almaier, 2018) or of ions in low pressure ES-Ionization (Gibson et al., 2009).

### *3.3.3 Operating conditions for steady Water ES in cone-jet mode with and without discharges*

Steady production of droplets with constant size and charge distributions can be achieved in ambient air by water ES in cone-jet mode with pulseless corona or without discharges (see Figure 7).

**Figure 7: conditions for water ES in steady cone-jet modes with (white) and without discharges (blue) in air**

| **Steady cone-jet mode of ES** | Conductivity | Flowrate | $d_{out}$/ $d_{in}$ | $d_{drop}$ (µm) |
|---|---|---|---|---|

https://doi.org/10.1016/j.jaerosci.2018.04.005

| ***without discharge*** | ***with discharge*** | (mS.m$^{-1}$) | **nL/min$^{-1}$** | **µL.min$^{-1}$** | **µm** | **mm** | |
|---|---|---|---|---|---|---|---|
| (Cloupeau et al., 1989)<br>water + 0..5% surfactant | | 0.5-1.5 | 600 | | 120/ < 40 | | by lowering surface tension<br>→ $d_{drop\ Vol.}$ = 1µm (1.5 mS.m$^{-1}$) |
| (Tang K et al., 1994b)<br>*in CO2 at 0.5 % vol* | | 10<br>0.1 | 3<br>5-50 | | 0.4/ 0.15 | | → $d_{drop}$ = 2 µm<br>6 &10µm at 20 & 40µL.min$^{-1}$ |
| (Ehouarn et al . 2001<br>Borra 1997, 1999a-c, 2004) | | 0.04-5 | 500-3300 | | [0.4-1.8] / [0.25-0.2] | | [50-130] µm |
| (Jaworek 1997 & 1999) | | 1 | 2000-3000 | | 0.9/ 0.65 | | |
| (Lopez-Herrera et al., 2004) | | 150 &1800 | 0.06 & 0.018 | | 0.050/ 0.020 | | |
| (Lastow et al., 2007) | | 0.1 & 10 | 0.5-4 & 0.5-1 | | NA/ 0.11-0.2 | | |
| (Lopez-Herrera et al., 2004) | | 0.36-1800 | 0.1-240 | | 50/ 20 | | |
| (Marginean et al., 2007) | | | 10-100 | | NA/ 20 | | |
| (Kelly et al., 2008) | | | 50-950 | | 150/ 20 | | |
| (Li JL et al., 2008) | | 0.81 | 300 | | 900/600 +90 µm fiber | | ($d_{virtual\ cap} \approx d_{fiber}$) |
| (Gibson et al., 2009) | | NA | 0.3 | | 4 | | 0.2 µm |
| (Marginean et al., 2014) | | NA | 0.4¸ 20 & 200 | | NA/ 2, 5 & 10 | | |
| (Park I et al., 2015) | | 0.12 | 1700-67000 | | 50/ 20 | | |

In both cases, streamer and subsequent disruption of the EHD equilibrium are avoided, due to diverging fields induced on smaller radius, as in point-to-plane discharges (Goldman et al., 1978; Hartman, 1984). Indeed, small discrepancies in nozzle geometry make big differences as far as corona discharge are involved due to the double constraint for EHD equilibrium with water in air. The first one on the onset voltage of cone-jet formation, as defined in 3.2. The second condition concerns the spatial evolution of the electric field around the liquid, defining the ionization length and the corresponding discharge regime. As addressed in 3.3.1.2, smaller outer and inner nozzle diameters induce finer and longer jet, quenching the discharge on shorter ionization length than required for streamer development, even for liquid voltage higher than the threshold for cone-jet formation. In that case, the steady cone-jet mode is established without discharge.

The nozzle geometry affects the functioning flowrate and voltage of water ES in air, as depicted in Figure 7, for both steady cone-jet modes with and without discharges. Since the minimum flowrate depends on the conductivity, steady ES of more conductive water solutions can be achieved at lower flowrates with smaller capillaries for both steady cone-jet with and without discharges. *Then, as a rule of thumb, for inner diameters larger than 0.1 mm, pulseless corona-assisted cone-jet can be performed down to 0.5 µL.min$^{-1}$ flowrates, while steady water ES in cone-jet mode without discharges can be performed down to nL.min$^{-1}$ for inner diameters smaller than 100µm, with even more diverging field to quench the discharge*. Steady ES in cone-jet mode can be used for the production of water droplets in ambient air with unimodal or even monodisperse size distributions. Monodisperse submicron-sized sprays are achieved at lower flowrates for higher conductivities with small capillaries in ***cone-jet mode without discharges.***

Larger droplets from a few micrometers at 3 µL.min$^{-1}$ to 100 µm for a few mL.min$^{-1}$, with still unimodal size distributions are produced ***in pulseless corona-assisted cone-jet mode*** using capillaries with inner diameter from 0.12 to 0.5 mm and outer diameters smaller than 2mm, for water conductivities from 0.1 to 10 mS.m$^{-1}$. With charge levels close to the Rayleigh limit, the corona-assisted cone-jet mode is well adapted for physical studies of such suspended charged droplets and for the development of enhanced efficiencies interfacial processes, such as electro-scrubbing.

This particular mode of steady ES in cone-jet mode stabilized by a corona discharge has thus been tested for filtration by bipolar-scrubbing for filtration of fumes or ambient aerosol at lab-scale with mL.h$^{-1}$ water flow rate (see next section 4). Steady ES without discharge has impacted the rapidly growing market of high sensitivity analysis of biological aqueous solution by ESI-MS performed at much lower flowrates down to sub-nL.min$^{-1}$ (Gibson et al., 2009). Otherwise, Water ES with electrical discharges and more generally plasma-droplets interaction are studied to take advantage of the large interfacial exchanges between self-dispersed droplets and the gaseous plasma species like electrons, radicals, excited species or ions, with ozone and other nitrogen oxides/acids, as discussed above for surface and water decontamination and in conclusions for the development of new *plasma-based aerosol processes*, especially for material coating and deposition processes .

https://doi.org/10.1016/j.jaerosci.2018.04.005

Other modes than this steady mono cone-jet have recently been reinvestigated to achieve higher flowrate ES applications: the multi-jet first and the simple jet modes, described by Hayati, Cloupeau and others since the 1980', respectively for high added value applications of tailored monodisperse droplets (Duby et al., 2006) and for metal recovery from used water and as the evaporation step in desalination process to achieve ES of high conductivity water up to 600 $mL.h^{-1}$ (Agostinho et al., 2018). In both cases, the monodispersity of droplets is conserved. In the first case, similar monodisperse micron-sized droplet are produced than in cone-jet ES with higher throughout, while in the second, bigger droplets are achieved (> 200 µm).

Other applications of steady cone-jet mode of ES could be achieved at lower voltages and higher flowrates even for "dirty" water with conductivity around $S.m^{-1}$, with higher corona current in the same configuration, or by playing with corona ion space charge location and density around the liquid for different geometries and locations of ring(s), collecting i.e. driving ions on defined pathways "drawn by field lines". *Steady water ES in corona assisted cone-jet mode may advantageously be applied to water desalination* by droplet evaporation, all the more efficient with smaller droplets than in the simple-jet mode, already used to achieve the production of "clean" condensed water (Agostinho et al., 2018).

Nozzleless ES devices, with needles under the liquid surface, has been reinvestigated for multi-ES, self-fed in pure de-ionized water condensed from air (Pyrgiotakis et al., 2014). In terms of installation and maintenance cost, this system may find applications to avoid steps to control the water conductivity with a de-ionization step and the water feeding with flowrate retro-controlled by conductivity measurements.

## 4 Water ES for high efficiency bipolar-scrubbing of submicron-sized particles from gases

With charge levels close to the Rayleigh's limit, the steady water ES in the corona-assisted cone-jet mode is adapted for physical studies of electrical properties of charged droplets as well as for the development of efficient interfacial processes based on electrical forces. This section addresses such ES application for gas filtration by bipolar scrubbing to remove suspended particles from fume, smoke or ambient aerosols flows.

### 4.1 Filtration: goals, means and limits

The removal of particles suspended in gases was already a concern in the 1900's to prevent smog formation next to urban areas (Hinds, 1982). Since then, air quality has become a priority, with ever more accurate aerosol characterization tools and epidemiological studies of respiratory diseases. New tools for the missing range of size measurements down to sub-nanometer clusters (Intra et al., 2007), just confirmed high concentration of nanoclusters in towns "loaded" with combustion aerosols (Rönkkö et al., 2017).

*Fabrics filters and wet scrubbers* collect particles from gas stream on fibers or droplets mainly by mechanical forces. Both are based on efficient diffusion of particles smaller than 100 nm, on inertial impaction of particles larger than 1 µm eventually combined with less efficient hydrodynamic interception for the intermediate size range. As a result, these mechanical filters lack of efficiency from 0.1 to 1 µm, for the Most Penetrating Particle Size -MPPS- around 0.3 µm (Baron et al., 2001).

In this size range, electrical forces are larger than gravity and thermophoresis and thus control the kinematics of particles suspended in gases and subsequent particle trajectories. More efficient electro-filtration devices have been developed (Parker, 1997; Jaworek et al., 2007; Borra et al., 2009; Jidenko et al., 2012). In Electro-Static Precipitators -ESP- particles are charged by corona ions and collected from the gas by electrical forces with lower pressure drop than in fabric filters (Cross, 1987; Parker, 1997). However, lower efficiencies in the same submicron size range arises from lower electrical mobility and related terminal velocities, with respect to the charging mechanisms, either by ion drift along field lines intercepting the surface of particles, or by ion diffusion, which is the unique charging process below 0.1 µm (Wu D et al., 1987; Biskos et al., 2005; Park D et al., 2007). Filtration efficiencies are then reduced from 0.1 to 1 µm, since neither mechanical nor electrical collection are fully efficient, when used alone (Hinds, 1982).

Fabric filters induces high-pressure drop and usually works below 100 °C while ESP with lower pressure drop can be used for filtration of "hot" exhaust gases (incinerator, combustion power plants…). However, ESP requires maintenance and regulation since the surface potential of the collected dust layer increases

https://doi.org/10.1016/j.jaerosci.2018.04.005

and lowers the field in the gap. The voltage has to be raised to achieve stable corona discharge for continuous aerosol charging and collection. Then, to prevent from sparking due to back-discharges in the collected dust layer (Cross, 1987; Czech et al., 2011), different options have been developed, first by cyclic cleaning of electrodes, then with multi-step ESP, splitting charging and collection steps (Parker, 1997; Asbach et al., 2004; Jaworek et al., 2004). As an alternative to fabric filters and ESP, unipolar wet ESP were first developed to clean the collection electrode of particles charged with the same polarity as droplets (Eyraud et al., 1966; Lear et al., 1975; Xu DX et al., 2003).

***Wet electro-scrubbers*** have then been tested as hybrid systems combining advantages of wet scrubbers, for low pressure drop and simultaneous scrubbing of soluble gases ($SO_X$, $NO_X$) and ESP for efficient electro-collection in the submicron size range on larger surface of suspended droplets than in ESP (Pilat et al., 1974; Melcher et al., 1977; Ehouarn P. et al., 1997; Borra et al., 1999b; Unger et al., 2003; Jaworek et al., 2006a; Carotenuto et al., 2010b). With no more need to clean the electrodes as in ESP and reduced waste water per unit volume of filtered gas compared to wet scrubbing on neutral droplets, ***wet electro-scrubbers*** is a continuous on-line process for gas velocities in the order of $m.s^{-1}$, typical of large scale ESP, see 4.3.1.3.

## 4.2 Bipolar wet electro-scrubbers

### *4.2.1 Principle, mechanisms and models*

Based on Coulombian coagulation of oppositely charged particles and drops, wet electro-scrubbing is a continuous multi-step process for the removal of sub-micron sized atmospheric and combustion aerosol, depicted in Figure 8: suspended particles to be removed from the gas flow are first charged on-line by negative DC corona, injected in positive collecting water sprays dispersed in the scrubber by self-repulsions of unipolar droplets, collected from the gas by gravity and self-repulsion losses to the earthed walls.

Several wet electro-scrubber concepts are reviewed with one or both charged particle and collector either with the same or with opposite polarities respectively in unipolar and bipolar scrubbers (Allen, 1982; Jaworek et al., 2006b; Zhao et al., 2008). Different charge–to-mass ratio of the collecting droplets (see next section 4.2.2) and different concentrations from mg to $g.m^{-3}$ of sub-micron and micron sized particles, as discussed in section 4.3.2, have been tested over large range of exhaust aerosol flowrates. Wet electro-scrubbers have first been tested at higher flowrates up to 1700 $Nm^3.h^{-1}$ on exhaust aerosols from spark furnace, industrial boilers, diesel marine engines and other combustion sources (Penney, 1944; Eyraud et al., 1966; Pilat et al., 1974; Pilat et al., 1977; Metzler et al., 1997; Jaworek et al., 1998; Krupa et al., 2004; Jaworek et al., 2006a; Jaworek et al., 2007; Ha et al., 2010; Jaworek et al., 2011; Di Natale et al., 2013; Di Natale et al., 2015; Krupa et al., 2016). *The total collection efficiency*, defined in Figure 8, *increases with electrical forces*, especially for bipolar coagulation of oppositely charged particles and collecting droplets. Lab-scale systems have been tested at low flowrates (~ $m^3.h^{-1}$) for model validation (D'Addio et al., 2013) or to highlight the interest of ES for bipolar scrubbing (Borra et al., 1999c; Ehouarn P. et al., 2001).

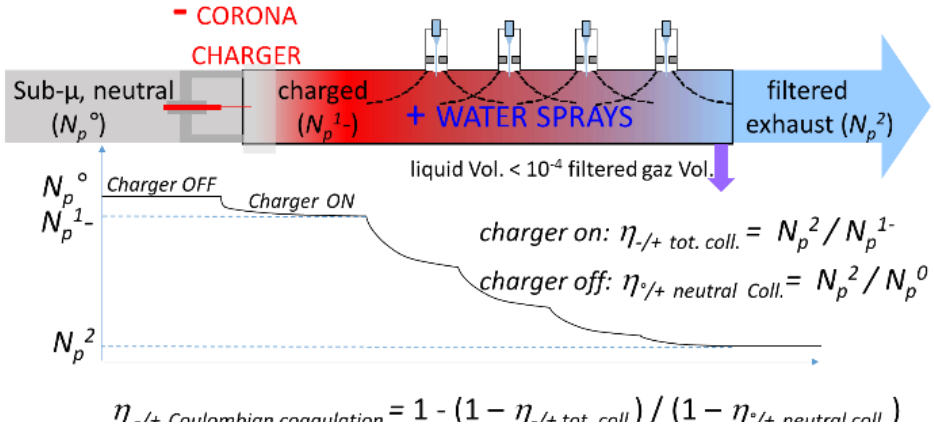


**Figure 8: Mean number concentration of particles (integrated on the cross section) along the Bipolar-scrubber**

https://doi.org/10.1016/j.jaerosci.2018.04.005

The *total collection efficiency*, defined in Figure 8, is used for comparison with other devices, including all collection mechanisms by mechanical, thermal and electrical forces, i.e. including diffusion, impaction and interception, as well as electro-coagulation by image and Coulombian forces. The Coulombian coagulation efficiency ($\eta_{-/+\ Coulombian\ coag.}$) is either derived from measured collection efficiencies of neutral and charged particles on positive droplets ($\eta_{\circ/+\ neutral\ coll.}$ and $\eta_{-/+\ tot.\ coll.}$), or calculated by theoretical analysis of Coulombian interaction between oppositely charged particles and droplets.

The theoretical analysis of electro-coagulation of oppositely charged particles was formalized by Fuchs (Fuchs, 1964). Models to account for collection of particles on a charged drop are reviewed in (Allen, 1982; Jaworek et al., 2006a; Carotenuto et al., 2010b). Three approaches have been used. Melcher discussed the scrubbing in terms of time constants of unipolar droplets repulsion and Coulombian coagulation (Melcher et al., 1977). The two other approaches rely on unitary or "single drop collection rate", then time integrated with respect to heterogeneous droplet concentration and evolving particle concentration along the scrubber (see 4.3.1). Here should be noted that it is most often assumed that the collecting field between a drop and a particle is not influenced by the background space charge field (Jaworek et al., 2013). Indeed, bipolar referred as Coulombian coagulation efficiencies have first been calculated for single falling or fixed drop (Kraemer et al., 1955; Nielsen et al., 1976a, b; Prem et al., 1978; Hara et al., 1984; Sumiyoshitani, 1996; Zuo et al., 2017). When considered as independent, the total single drop efficiency is defined as the sum of single drop collection efficiencies for each mechanism, if much smaller than unity (Kasper G et al., 1978; Brown, 1993). Otherwise, additional coupling terms are included for combined actions (Alonso et al., 2007), as for electro-collection by inter-particles image and Coulombian forces, eventually under additional Laplacian electric field imposed by polarized electrodes (Kraemer et al., 1955).

At first, based on process engineering analysis, simple semi-empirical expressions of the grade efficiency (i.e. efficiency per size range), were used for optimization and eventual scale up of lab-scale device. Collection efficiency of large scale bipolar-scrubber has been defined (Pilat et al., 1974; Calvert et al., 1978; Prem et al., 1978; Bertinat, 1980; Allen, 1982) using the macroscopic approach, by analogy to ESP efficiency calculations from Deutch-Andersen formalism (Hinds, 1982). Assuming that particles are first homogeneously distributed in the gas at the same velocity and then collected at its terminal electrical velocity (see 4.2.2 and 4.3.2), when approaching the droplet within the coagulation sphere (usually considered as one diameter away from the surface of the drop, (Jaworek et al., 2013)). *The single drop bipolar coagulation efficiency is related to the cylinder of gas swept by a drop per unit time, defined as the cross section of the coagulation sphere around each drop within which any particle with opposite polarity is collected, time the relative velocity between particle and drop (Kraemer et al., 1955; Melcher et al., 1977; Bertinat, 1980).* Replacing the collection surface of the ESP electrode by the surface of suspended droplets related to droplet concentration, the expression of the collection efficiency for ESP can be converted, as follows for collection by bipolar coagulation in electro-scrubbers (Bertinat, 1980; Allen, 1982). The Coulombian coagulation efficiency ($\eta_{-/+}$) is defined, neglecting other forces and losses to the walls, versus the mean product $<N_{drop}\ t_{scrubbing}>$, so averaged over the whole scrubber to account for variable droplet concentrations met along the scrubber, with respective transit times:

$$\eta_{Coulombian\ coagulation} = 1 - e^{-A\cdot\frac{\mu_p \cdot q_{drop} <N_{drop}\cdot t>}{\varepsilon_0}} \text{ (Bertinat, 1980)}$$

with $N_{drop}$ and $q_{drop}$, respectively the collecting water droplet number concentration ($m^{-3}$) and charge (C), $\mu_p$, the electrical mobility of particles ($m^2.V^{-1}.s^{-1}$), and $t$, the aerosol transit time in the scrubber.

This expression cannot be used for the design of electro-scrubbers as Deutsch equation for ESP, since the terms of the exponent are interdependent and do not include other collection mechanisms nor losses to the wall. However, a parameter (A) specific to each scrubber can be added to account for the spatial distribution of droplets defining the active volume of the scrubber for electro-coagulation (Allen, 1982). This parameter is defined by fitting Bertinat's law with defined charge per drop versus particle mobility and aerosol flowrate, i.e. versus mixing conditions and related $<N.t>$ products, to Coulombian coagulation efficiencies defined from measured total and neutral collection efficiencies. Despite the critical assumption of stationary particles swept by moving droplets, Bertinat's law is useful to define optimal conditions for collection of submicron particles (Allen, 1982; Cross, 1987) as detailed in 4.3.1 for ES application to bipolar scrubbing.

Otherwise, at last, Eulerian and Lagrangian methods (Carotenuto et al., 2010b; Jaworek et al., 2013; Di Natale et al., 2016a) can be combined to describe trajectories of micron-sized particles and water droplets (Beard, 1974; Nielsen et al., 1976a; Prem et al., 1978) and single drop collection efficiency (Bozorgi et al., 2006; Goniva et al., 2010; Jędrusik et al., 2013). This has been done first for neutral scrubbers (Wang A et al., 2016a, b) and atmospheric scavenging by falling droplets, adapted to ventury scrubbers (Yang HT et al., 2003; Bozorgi et al., 2006; Jaworek et al., 2006a; Carotenuto et al., 2010b; Di Natale et al., 2016a; Li X et al., 2016). Numerical calculation of single drop collision efficiency and related scavenging parameter have been performed (Zhao et al., 2008), for each collection mechanism with detailed numerical evaluation of these collisional efficiencies with references in (Carotenuto et al., 2010b). Fractional efficiency have first been calculated for different size and charge distributions (Eliasson et al., 1991) and improved with discrete (for each diameter), sectional (for size intervals) or continuous log normal size distributions, compared in (Park SH et al., 2005). Stochastic Monte Carlo methods can be used to define the single drop scavenging efficiency by population balance for time integration to account for actual droplet concentration and for decreasing concentration of particles along the scrubber (Zhao et al., 2008; Carotenuto et al., 2010b).

### *4.2.2 Methods for the production of charged water droplets for bipolar scrubbing*

Charged droplets can be produced by different processes with variable charge-to-mass ratio (Bailey, 1988; Vaaraslahti et al., 2002; Pilat et al., 2004; Krupa et al., 2013). Charged droplets may be produced without liquid polarization, by charge separation during breakup of the liquid double layer. First observed during the fragmentation of liquid films and jets with bursting bubbles (Iribarne et al., 1967) and with pneumatic nebulizers, specific charge from 1 to 100 $nC.kg^{-1}$ are reported for 100 µm droplets produced at a few $L.min^{-1}$ (Vaaraslahti et al., 2002). Such scrubber supplied by sea water have been tested (Ha et al., 2010).
Water droplets can also be charged by Corona ions (Xu DX et al., 2003) to lower levels than by the simplest *induction charging* by liquid polarization *in mechanical nebulizers*, *achieving* up to 10 % of the Rayleigh charge limit (Bailey, 1988). Charge-to-mass ratio from $10^{-3}$ to 1 $mC.kg^{-1}$ have been measured for 50 µm water droplets from pressure nebulizers where the liquid is pressurized across an orifice (Pilat et al., 2004; Krupa et al., 2013) and from pneumatic nebulizers (Metzler et al., 1997; Yang HT et al., 2003).
ES is used to achieve tunable and higher charge per drop -by induction charging as well-, but without dilution of the aerosol to be filtered by additional gas flow for the production of charged droplets (Lear et al., 1975; Hara et al., 1984). Electro scrubbing has been tested with water ES in other modes than the cone-jet mode, with less charged and larger drops, from 0.1 to 0.2 $mC.kg^{-1}$ for millimeter droplets produced *in the dripping mode* for model validation (D'Addio et al., 2013).
*The same EHD break up of jets as for ES in cone-jet mode* is used to achieve higher charge per drop:

- from 1 $mC.kg^{-1}$ for 100 µm droplets from a rotary cup nebulizer with multiple jets (Bailey, 1988; Balachandran et al., 2003), to a few $mC.kg^{-1}$ for 80 µm droplets assumed to carry half of the Rayleigh charge limit from ES *in precession mode* (Jaworek et al., 2006a), for static scrubbing in closed room.
- up to 12 $mC.kg^{-1}$ for 100 µm drop i.e. up to 70% of the Rayleigh charge limit, measured *in steady corona-assisted cone-jet mode*, (§3.3.1.4, (Ehouarn P. et al., 2001; Borra et al., 2004).

As expected for Coulombian coagulation, higher efficiencies are achieved for similar test aerosol collected by droplets with charge-to-mass ratio higher than by any other process by steady water ES, depicted below.

## 4.3 Electro-scrubbing by steady water ES in the corona-assisted cone-jet mode

Since no other data are available on the topic, here are presented results from two PhD researchers (Ehouarn P., 2001; Unger, 2001; Unger et al., 2003) with total collection efficiencies of this ES bipolar scrubber versus the aerosol mobility in Figure 9a with related Coulombian coagulation efficiencies on Figure 9a-b.
Properties of collecting water droplets and test aerosols (diameter, electrical charge, concentration), have been controlled independently from 0 to $10^{-6}$ $m^2.V^{-1}.s^{-1}$ for electrical mobilities of sub-micron aerosol charged by a wire-cylinder corona charger (Unger et al., 2004) and from 30 to 70 % of the Rayleigh charge limit for water drop, see section 3 (Ehouarn P. et al., 2001). A set of conditions to achieve steady water ES in corona assisted cone-jet (100 $mL.h^{-1}$, 200 $\mu S.m^{-1}$ water) is used to produce *90 µm droplets with 3.6 pC per drop (9.4 mC.kg $^{-1}$).* The charged aerosol is mixed with droplets of opposite polarity

produced by a line of four ES on top of an horizontal pipe of 7 cm diameter for 10 cm inter nozzle distance (appendix A1 and Fig.8).

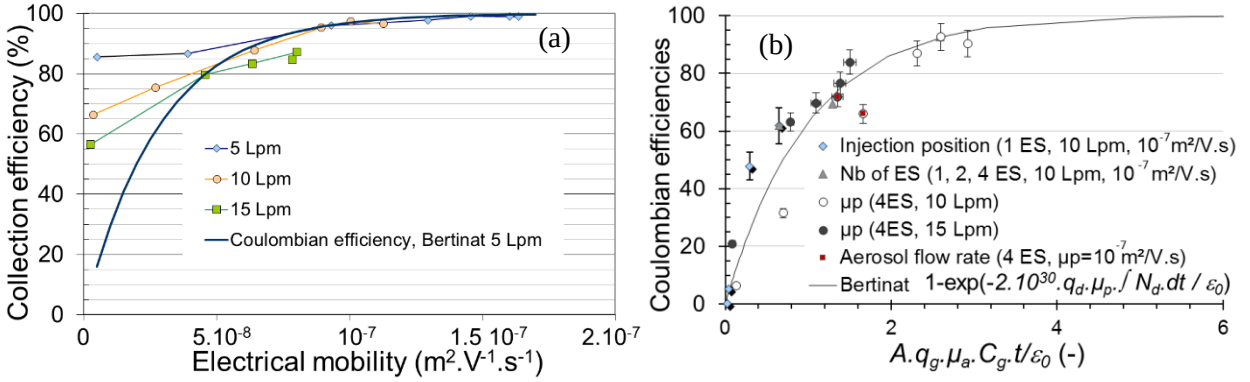


**Figure 9: in constant reference ES conditions, (a) Comparison of total collection and Coulombian coagulation efficiencies (points and line, respectively) of $10^6$ $cm^{-3}$ -i.e. 10-100 $mg.m^{-3}$- 0.44 µm monodisperse negative aerosol versus the electrical mobility for different flow rates with a line of 4 ES and (b) Coulombian coagulation efficiency versus the adimensional parameter $A \cdot q_g \cdot \mu_a \cdot \int c_g \cdot dt/\varepsilon_0$ (line with $A=2 \cdot 10^{30}$ from (Ehouarn P., 2001; Unger, 2001)), i.e. versus the mean $\langle N_{drop}.t \rangle$ product, controlled by injection of aerosol with constant mobility of $10^{-7}$ $m^2.V^{-1}.s^{-1}$ at 10 $L.min^{-1}$, in different initial mixing conditions at different heights from the spay injection, with different numbers of ES, as well as with different mobilities and flowrates (see legend for tuned parameter)**

### *4.3.1 Mixing conditions*

The ideal bipolar scrubber would consist of an injection of charged particles in spray with the highest droplet concentration, both being charged to maximal level with a large excess of charges with the polarity of collecting droplets. Then, with such unipolar net space charge, *the spatial dispersion of droplets in the scrubber has to be optimized for efficient interfacial processes, as electro-scrubbing of cross flow aerosol.* Indeed, one limit of electro-scrubbers results from repulsive losses to the walls increasing with the charge densities related to higher charge per drop. Nevertheless, large co- and reverse flow *unipolar scrubbers* have first been used for collection to the wall of aerosol with the same polarity as droplets with high efficiency in the sub-micron size range, using either ES in precession mode (Lear et al., 1975) or induction charging in ventury scrubber (Vicard, 1977). Even for bipolar scrubbing, electrostatic repulsions lowers the concentration of collecting droplets and the electro-coagulation efficiency (Melcher et al., 1977).

#### *4.3.1.1 Positive droplet space charge density in ES bipolar scrubber*

The dispersion of droplets in the scrubber depends on the total electric field including the space charge and eventual additional external field (Tang J et al., 1994a; Hartmann et al., 1999a; Deng et al., 2007; Wei et al., 2013). As a rule of thumb, ES can be considered as independent for larger inter nozzle distance than the pipe diameter, when the development of ES is unaltered by others. This is achieved in this water ES scrubber with space charge from $10^{11}$, close to the spray injection to $10^8$ $e.cm^{-3}$ (droplet charge of a few pC per droplet (~ $10^7$ e) and densities from $10^4$ to 10 $cm^{-3}$). Actually, *the spatial development of such unipolar sprays is self-induced by space charge (see section 3.3.1.5), unaffected up to gas velocities of a few* $m.s^{-1}$.

The injection of negative particles with eventual ions from the charger affects the space charge field and subsequent losses to the wall of unipolar particles before mixing in the scrubber, as well as the inter-particle field for coagulation in bipolar volumes, where both populations are mixed (see 4.3.2- Electrical mobility).

The coaxial ring used to shield the liquid cone-jet i.e. the production zone from variable space charge field in the scrubber, can be polarized with the same polarity than the nozzle to avoid the recollection of droplet on the ring and to disperse all droplets over the entire cross section of this earthed tubular scrubber, for cross flow mixing of charged aerosol and collecting droplets (Gan et al., 2016).

Besides, additional electrodes can be polarized in the scrubbers as well to control the electric field profile, intensity and dynamics necessarily affecting the bipolar coagulation (Kraemer et al., 1955; Nielsen et al., 1976a; Bertinat, 1980; Sumiyoshitani, 1996; Park SH et al., 2005). The field controls relative velocities for mixing initial unipolar space charges but also the transit time of particles around the coagulation

sphere to reach it (with 100% collection efficiencies). Depending on its intensity and frequency, it is beneficial for less charged particles and drops, but not anymore for more mobile particles and/or more charged droplets.

#### *4.3.1.2 Co-, cross- or reverse-flows*

Scrubbing has been tested with different spatial development of sprays and mixing conditions. Full or hollow conical sprays from pressure nebulizers have been compared for high flow applications (Jaworek et al., 2006b). Different scrubber geometries have also been compared for theoretical evaluation of optimal scrubbing conditions versus relative velocities of positive and negative species (Bertinat, 1980; Eliasson et al., 1991; Jaworek et al., 2006a). When both populations are produced by positive and negative DC ES ("Symmetric case" in (Eliasson et al., 1991)), Coulombian coagulation efficiencies of droplets with similar charge and size distributions decrease from 53 % for face-to-face to less than 20 % for parallel injection of unipolar sprays of both polarities (Borra et al., 1997a; Borra et al., 1999a). Despite a bit lower efficiency in cross than in reverse flow with "face-to-face" injections of charged droplets (Camelot, 1997; Chou, 1997; Fu et al., 2012), *cross flow has been selected for the bipolar scrubber (Unger et al., 2003)*. Actually, ES is more stable with vertical nozzles injecting sprays from the top of horizontal pipes. Counter flow is complex to handle when injectors of positive droplets and negative particles from the charger, have to be close for injection of particles in the highest concentration of droplets, as supported by Figure 9b for aerosol injection in the spray at different heights from the nozzle. Moreover, the parallel injection of oppositely charged species with different size and charge distributions of particles and droplets (asymmetric case) leads to smaller efficiencies than the cross one due to self-repulsion before mixing (Ehouarn P., 2001).

#### *4.3.1.3 Gas velocity (< m.s$^{-1}$) and aerosol dispersion*

Most filtration devices works at exhaust velocity around 1 m.s$^{-1}$ in scrubbers, fabric filters and ESP (Parker, 1997; Baron et al., 2001). E*lectro-scrubbing tests are thus often performed in this sub m*.s$^{-1}$ *range. Moreover,* steady ES in cone-jet is undisturbed up to gas velocities of 15 m.s$^{-1}$ (Allaf-Akbari et al., 2017).

Sprays are used for mixing of gases and gas scrubbing (Malet et al., 2015). With ES as well, the injection of aerosol perpendicularly to ES nozzle axis with droplets velocities from 8 to 1 m.s$^{-1}$ (see 3.3.1.5) along the diameter of the pipe induces cross flow due to the momentum transfer between droplets and gas (Hartmann et al., 1999a; Jaworek et al., 2013). In turns, this leads to turbulent mixing of particles within the droplets flux and probably accounts for the high efficiency achieved despite successive independent ES necessarily implying dead volumes in the scrubber with smaller droplet concentrations.

For faster velocities, the spray dispersion and the related collection efficiency evolve (e.g. in venturi (Ali et al., 2013) and electro-scrubbers (Carotenuto et al., 2010a; Di Natale et al., 2015; Di Natale et al., 2016b)).

With highly charged droplets produced by steady water ES in pulseless corona-assisted cone-jet and dispersed in the exhaust pipe with cross flow, *sub m*.s$^{-1}$ inlet velocities are used so that the spray expansion and deposition to the wall of the earthed pipe are unaffected by the aerosol flow.

### *4.3.2 Aerosol properties*

***Electrical mobility:*** In constant conditions of particle production, ES and mixing, the measured collection efficiencies increase with the electrical mobility of particles, as expected from Bertinat's law, above 5.10$^{-8}$ m².V$^{-1}$.s$^{-1}$. Longer transit times lead to higher efficiency all the more for lower mobilities. This is due to larger relative part of other collection mechanisms (diffusion, thermophoresis, impaction and interception, images forces and self repulsion losses) not included in Bertinat's law for bipolar coagulation alone (see Figure 9a, measured total collection efficiency > Coulombian efficiency). For mobilities above 10$^{-7}$ m².V$^{-1}$s$^{-1}$, the expected Coulombian coagulation efficiencies, fits to the measured collection efficiencies, over 95 % from 15 to 5 L.min$^{-1}$, even for sub-second transit times. The size integrated number efficiency overcomes 99.2 %, without pressure drop and only 0.4 water L.m$^{-3}$ of filtered aerosol.

Neglecting first, the turbulent mixing in this cross flow arrangement and the effect of decreasing particle concentration addressed in 4.3.1 and 4.3.2, the droplet concentration profile for this water ES (Ehouarn P. et al., 2001) has been discretized in different volumes with respective droplet concentrations and transit times of aerosol. Scrubbing efficiencies have then been calculated with respect to heterogeneous droplet concentration met across one spray, as detailed in (Ehouarn P., 2001). Despite numerous assumptions, the total collection efficiency follows roughly Bertinat's law for on-line particles removal from an aerosol

flow versus particle mobility, aerosol flowrate, number of ES and position of injection in the spray for different *Nt* products at constant charge per drop, with expected deviation between experimental data and calculations from these assumptions (see Figure 9b). When working with defined aerosol mobility and charge per drop as well as with a known profile of droplet concentration in the scrubber, this law enables one to define optimal mixing conditions (aerosol velocity, relative injection position in the spray, diameter of the exhaust pipe) for the selected cross flow scrubber. However, it is useless for other geometries and does not account for higher efficiencies with more concentrated industrial exhausts (from 0.1 to 100 $g.m^{-3}$). To do so, readers should use other approaches for efficiency calculation through single drop scavenging efficiency, to account for the related enhanced collision probability,(see 4.2.1).

***Aerosol concentration, size and charge:*** Coagulation of submicron sized bipolar aerosol is known to limit the maximum inlet concentration to $10^6$ $cm^{-3}$ for size distribution measurements without coagulation using radioactive neutralizers (Adachi M. et al., 1981; Maisels et al., 2004; Alonso et al., 2008) and to increase the ESP collection efficiency by shifting the inlet aerosol size from the MPPSize range to larger diameters (Zevenhoven et al., 1994; Watanabe et al., 1995).(Hara et al., 1984)

More concentrated aerosol generally leads to unimodal self-preserving size distribution by fast coagulation (Goudeli et al., 2015) which, in turns affects the charge of particles i.e. the negative current injected in the scrubber and the related droplet charge with subsequent spray dispersion. Indeed, injection of larger negative current lowers the collection efficiencies from 97 % without, to 91 % with co-injection of negative corona ions with charged particles (from sub-nA current for charged particles alone to -500 nA with ions, compared to +300 nA per ES, (Unger, 2001)). This may account for the dispersion of Coulombian coagulation efficiencies reported in Figure 9b, from measured collection efficiencies for neutral and charged particles at different flowrates, as well as assumptions on mixing conditions (see 4.2.1).

Finally, the current of negative particles injected in the scrubber (kept here below 0.1% of the spray current for maximal particle concentration 0.1 $g.m^{-3}$), also depends on the size-charge relation specific to the selected corona charger, with respect to particle concentrations and sizes i.e. with respect to the aerosol source (Biskos et al., 2005; Intra et al., 2009).

### *4.3.3 Fractional efficiencies (vs $d_p$) of bipolar scrubbers*

Fractional collection efficiency is calculated from number or mass concentration measurements versus particle size (Hinds, 1982; Baron et al., 2001), to depict size dependent properties of aerosol, e.g. with the Coulombian force for bipolar scrubbing (Carotenuto et al., 2010b; Chen TM et al., 2014). Fractional efficiencies are presented in Figure 10 for different bipolar-scrubbers using ES or induction charging for the production of charged water droplets from pressure and pneumatic nebulizers.

Higher efficiencies are achieved by lab-scale electro-scrubbing on highly charged droplets produced by ES in corona assisted cone-jet mode, than by induction charging. However, different objectives were targeted either for physical studies up to $m^3.h^{-1}$ or for applied scrubber optimization up to 100 times higher flowrates and 10 times higher aerosol concentrations. For comparison with emission limits from 10 to 100 $mg.Nm^{-3}$, efficiencies are often calculated as the ratio of final to initial mass concentrations. Bipolar scrubbing was developed for high flowrate (238 $m^3.h^{-1}$) particle removal from steel furnace exhaust (0.1 to 1 $g.m^{-3}$) with 94 % mass removal efficiency achieved by induction charging of 50 µm water drops from pressure nebulizer, with 2 $L.m^{-3}$ at 10 $W.m^{-3}$ (Pilat, 1978).

For similar flowrates of a few hundred $m^3.h^{-1}$, most bipolar scrubbers were designed with characteristic lengths of a few meters first to achieve transit times of at least a few seconds with aerosol velocities up to $m.s^{-1}$, as well as to reduce losses of droplets to the walls (Allen, 1982). To do so, classical pressure and pneumatic nebulizers with large gas flow rate and subsequent less diverging sprays dispersed in larger volumes than ES, (due to less charged, larger and faster droplets than with ES), are adapted for efficient collection at large flow rate. In large flowrate scrubbers, only few studies address fractional efficiencies for removal of *sub-micron particles* by droplets charged by induction (from 0.1 to 1 $mC.kg^{-1}$, Figure 10). Minimum collection efficiency above 80 % were achieved for submicron test aerosol with MPPS around 0.2 to 0.3 µm with 2 and 1.6 $L.m^{-3}$ of waste water per unit volume of filtered gas, respectively for pressure (Pilat et al., 1974) and pneumatic nebulizers (Calvert et al., 1978) (see apendix A1).

https://doi.org/10.1016/j.jaerosci.2018.04.005

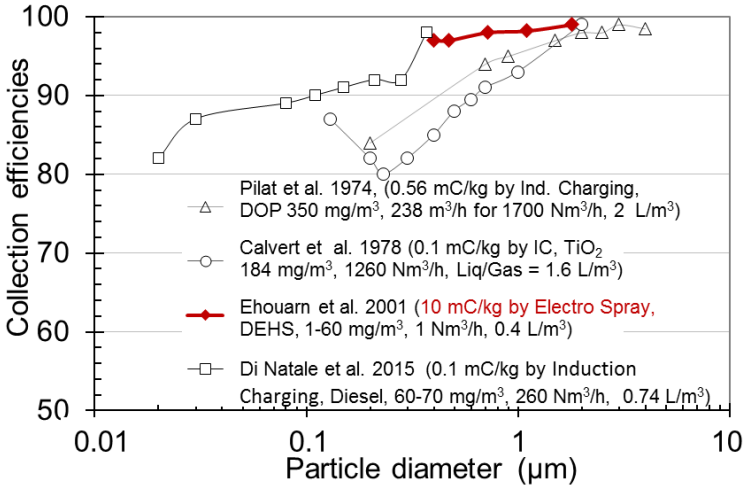


**Figure 10: Collection efficiencies versus particle size for four bipolar-scrubbers with different charge levels of water droplets from 0.1 mC.kg $^{-1}$ for induction charging of classical nebulizers at high liquid flowrates (200 L.h$^{-1}$), to 12 mC.kg$^{-1}$ for ES in corona assisted cone-jet at lower Liquid flowrate (0.4 L.h$^{-1}$)**

For real exhaust aerosol concentration from diesel engines, up to $10^{6\text{-}7}$ cm$^{-3}$ (~g.m$^{-3}$), similar pressure nebulizer with a full cone spray achieve 93% efficiency with 290 µm droplets (0.135 mC.kg$^{-1}$) for 0.2µm combustion aerosol with half the water consumption (Krupa et al., 2013; Di Natale et al., 2015; Di Natale et al., 2016b). For similar aerosol, the reader can also refer to (Ha et al., 2010) with sea water droplets.
With higher charge per drop from ES, faster self-repulsions lower the droplets concentration on smaller lengths, a few cm from the ES nozzle, than from other nebulisers, as depicted in 3.3.1.5. ES bipolar scrubbing is thus more efficient in smaller horizontal pipes to achieve particle injection in the spray above a minimal droplet concentration for efficient Coulombian coagulation (see section 4.3.1.2). *99.2% number efficiencies are achieved by bipolar scrubbing with* 4 water ES in corona assisted cone-jet, for aerosol concentrations up to $10^6$ cm$^{-3}$, with a minimum efficiency for the MPPS around 0.4 µm of 97%.
Higher exhaust gas flowrates, for real applications, are thus filtered with pressure and pneumatic nebulizers consuming more water for lower charge-to-mass ratio of droplets charged by induction, than in more efficient lab-scale ES scrubbers. Higher charge-to-mass ratio lowers the volume of waste water per cubic meter of filtered gas, at lower energetic cost (~ 0.03 kWh.m$^{-3}$), using steady water ES in corona assisted cone-jet than with induction charging of droplets from pressure or pneumatic nebulizers.

## 4.4 Conclusion

Bipolar wet scrubber using highly charged droplets produced by steady water ES in pulseless corona assisted cone-jet is more efficient (> 99 %) than other means to produce charged droplets for the removal of sub-micron particles from aerosol flows. Indeed, the selected cross flow configuration leads to turbulent mixing of particles within the droplet flux related to spray expansion (self-induced and unaffected up to 15 m.s$^{-1}$) and probably accounts for the high efficiency achieved despite successive independent ES necessarily implying dead volumes in the scrubber with smaller droplet concentrations.
With continuous production of self-dispersed charged droplets with low liquid consumption per unit gas volume, low-pressure drop, maintenance and exploitation cost, such ES scrubbing devices with a row of a few nozzles could be used in parallel for removal of particles from gases at higher flow rates than used for lab-scale proof of concept. Such ES bipolar scrubber could thus be considered not only as an additional last step downstream electrostatic precipitator to remove submicron particles but may be tested as High Efficiency Particulate Air (HEPA) Filter. This is all the more true that test were performed with immiscible oil droplet in water from ambient gas temperature for intermediate aerosol concentration from 1 to 10 mg.m$^{-3}$. Better efficiencies are expected on more concentrated particle in hot gases since the total collection efficiency is expected to increase for hotter exhaust aerosol due to thermophoresis pushing particles from hot gas to cool droplet surface (Di Natale et al., 2016a) and for higher concentrations than tested (> 2.10$^6$ cm$^{-3}$, 100 mg.m$^{-3}$). Water consumption can also be reduced with smaller droplets produced by ES at lower water flowrate and/or higher conductivities leading to larger collecting surface per unit water volume. Horizontal ES bipolar scrubber has proved to be efficient and can still be optimized using curtain-like sprays for cross flow injection of particles in more concentrated collecting droplets. It has to

be emphasized that larger flow rates can be treated in co-/reverse-flow, suitable for larger scale scrubbers, as already performed with success in the first unipolar ES scrubber (Lear et al., 1975), still to be tested for bipolar ES scrubbing.
The spray current has to be larger than the current of charged particles injected with eventual post-corona ions to be taken into account to avoid the reduction of the droplet charge, critical for electro collection.
Corona field chargers, where aerosol are injected in the discharge gap as used here for test on aerosol concentration from 0.1 mg to 100 $mg.m^{-3}$, are useless at higher concentrations with respect to deposition on electrodes and subsequent unsteady corona and charge of particles (Parker, 1997; Unger et al., 2000; Unger et al., 2004). Reliable post-discharge diffusion charger are available for lab-scale studies (Unger, 2001) up to commercial devices for low flow rate application to size distribution measurement (Biskos et al., 2005) and scaled-up for industrial two-steps ESP at larger flow rates (Asbach et al., 2004).
The development of these efficient bipolar scrubbers implies to achieve efficient particle charging up to $10^{-7}$ $m^2.s^{-1}.V^{-1}$ mobilities, for higher flowrate and concentration of suspended submicron particles, ideally up to $m^3.s^{-1}$ and $g.m^{-3}$. The critical size-mobility relation from different DC corona and/or AC Dielectric Barrier Discharges for bipolar charging still has to be addressed for high aerosol flowrate applications. Then, high flowrate and particle loading could be studied taking into account the evolution of the size-mobility relation with concentration, expected from self-repulsion losses of such unipolar aerosol clouds reported for charge density higher than $10^7$ $e.cm^{-3}$ (Whitby K. T. , 1961; Whitby K. T. et al., 1965; Kasper G., 1981; McMurry et al., 1985; Stratmann et al., 1992; Bouarouri et al., 2016).

## 5 Conclusions and perspectives

Some applications of electrosprays of Water or aqueous solutions have been reviewed with special attention for material production and bio-applications and a focus on particle filtration. As a continuous process, water ES in cone-jet mode (with and without discharge) can be used for the production of monodisperse/unimodal size distributions of self-dispersed unipolar water droplets.
Means to achieve these two steady modes of water ES in ambient air have been presented with respect to electrical discharges in the gas around the liquid cone and jet. Filamentary streamer discharges with transient and asymmetric space charges disrupt the EHD equilibrium required for steady cone-jet mode, while the axisymmetric and quasi-stationary space charge is required to achieve *steady water electrospray in ambient air in the pulseless corona-assisted cone-jet mode.*
Subsequent conditions to achieve *steady water ES in cone-jet mode without discharge* are then related (i) to lower onset electric field of cone-jet formation for aqueous mixtures with smaller surface tension than pure water and/or (ii) to higher discharge onset by playing either on the dielectric strength and density of the gas or on the electric field profile around the liquid cone-jet using fine spraying nozzles (< 100 µm).
Scaling laws between regulation parameters and droplet properties are reminded for steady water ES in cone-jet mode with pulseless corona and without discharge. Unimodal droplet size and charge distributions are achieved with modal diameters over three orders of magnitude from 0.2 µm droplets without discharge from nano-emitters at $5.10^{-12}$ $L.s^{-1}$, to 10-150 µm droplets in pulseless corona-assisted cone-jet at $10^{-4}$ $L.s^{-1}$.
Other than the cone-jet modes tested for application of electrical properties of monodisperse droplets to filtration by electro-scrubbing from tens to hundreds $mL.h^{-1}$ or used for rapidly growing market of high sensitivity analysis by ESI-MS down to sub-$nL.min^{-1}$ flowrates, the multi-jet first and the simple jet modes, have recently been reinvestigated to achieve higher liquid flowrate ES applications.
High filtration efficiencies by wet bipolar-scrubbing (> 99%) reported for classical pollutant concentration in lab-scale prototype supports that Water ES could be applied to air cleaning with low water and energy consumptions., mainly conditioned by the development of plasma charger to overcome $5.10^{-8}$ $m^2.V^{-1}.s^{-1}$, independently of the inlet concentration and of the nature of particles to be removed from the gas.
New ES facilities will emerge with new applications of bipolar coagulation for droplets neutralization to reduce self-repulsion and losses, for controlled kinetics in micro-reactor droplets as in micro-fluidic devices and more generally for interfacial processes as bipolar scrubbing, as well as for electric field driven deposition for coating, 3D printing and pulsed drop-on demand.

Based on the well-controlled ES current versus electric field, ES with micrometer gap has been tested as a scanning microscopy to measure the surface topography with resolution in the µm range, linking the ES current evolution with the electric field i.e. with the gap length above surface defaults (Yuill et al., 2015). Moreover, ES has been tested with magnetic fluids, as a tunable current source from simultaneous ES and electrical discharge versus the magnetic field intensity to control the shape of cones, the subsequent discharge regimes and related ozone production for gas depollution purposes (Uehara et al., 2015).
In terms of applications, ES with electrical discharges, proposed for plasma-based aerosol production and coating processes are studied to take advantage of the high interfacial exchange surface between the droplets and the plasma gaseous by-products (radicals, excited species, and electron or ions as well as ozone and other nitrogen oxides and corresponding acids with hydrogen peroxide). Similar species are formed in gas phase in humid air and in liquid water droplets, and can advantageously be produced simultaneously by ES with different discharges (corona, streamers and sparks) depicted in section 3.3.1. Chemical reactions can be induced in droplets, e.g. with bio decontamination of water droplets (see section 2.3 and 3.3.3). *Plasma-based aerosol processes* with droplet injection in plasma are developed for $SiO_X$ or polymer particle production and deposition, as coating processes (Fanelli et al., 2014; Brunet et al., 2017), to trigger either the polymerization of organic monomer precursor (Ward et al., 2003a; Tatoulian et al., 2006) or sol-gel reactions for oxide formation from organo-metal precursor, as reported by droplet injection in (Ward et al., 2003b; Jacopo et al., 2017) and downstream atmospheric pressure plasmas (Borra et al., 2012; Post et al., 2016). For more details, the reader can refer to a special session on the topic held in EAC 2016. ES is well adapted for such interfacial reactive plasma process, as just performed in microfluidic plasma devices (Zhang et al., 2017). In that respect, turbulent mixing from cross flow injection of ES into the gas, downstream a plasma, may be used to induce any chemical reaction in droplets. Coupled with controlled drying and eventual coating steps, these plasmas with interfacial suspended exchange surfaces for plasma-based reactivity with controlled kinetics will probably soon emerge as large-scale continuous production processes of tailored particles, powders and coatings.
At last, despite abundant literature on the structures and properties of water, water drop deformation still is triggering curious minds since the first observation. No doubt that the best is yet to come in terms of ES applications for material production with finely tuned properties (composition, size, structure) in association with plasma, or in small portable units possibly achieved with "nano-emitters" at low voltages, but more probably for larger production units at enhanced production rates from high interfacial exchange surface of self-dispersed droplets, as already started for patch production.

**ACKNOWLEDGEMENTS:** Here are acknowledged (i) the French ministry of Research and Education for the salary of one of both PhD devoted to this project, (ii) EDF and (iii) CNRS with ECODEV-ADEME for the financial support as part of an ARC research program from 1996 to 2003, and CNRS alone for the international patent. For their confidence to support the first study of the Bipolar wet scrubber, I thank Professors Fauchais and Amouroux. I take advantage of this review to acknowledge Gildas Hartman, Max and Alice Goldman, Emmanuel Marode for sharing their experience on dc corona, streamers and sparks. Denis Boulaud from IRSN, Brian Scarlett and Jan Marijnissen from TU Delft on aerosol science and technology. I thank Damien Camelot, Rob Hartmann, Najim Benali, Djamal Djermoun, Pascale Ehouarn, Lomig Unger, the PhD students who contribute to this work, and especially Nicolas Jidenko for his help for this review. At last, I am grateful to Professor Weber for proposing the special issue.

## 6 References

Adachi, M., Okuyama, K., & Kousaka, Y. (1981). Electrostatic coagulation of bipolarly charged aerosol particles. *Journal of Chemical Engineering of Japan, 14*(6), 467-473. doi: 10.1252/jcej.14.467

Adachi, M., Okuyama, K., & Kousaka, Y. (1983). Electrical neutralization of charged aerosol-particles by bipolar ions. *Journal of Chemical Engineering of Japan, 16*(3), 229-235. doi: 10.1252/jcej.16.229

Adachi, M., Pui, D. Y. H., & Liu, B. Y. H. (1993). Aerosol Charge Neutralization by a Corona Ionizer. *Aerosol Science and Technology, 18*(1), 48 - 58.

Agostinho, L. L. F., Marijnissen, J. C. M., Kamau, A., & B., B. (2018). Simple-jet mode electrosprays with water. Description, characterization and application in a single effect evaporation chamber. *J. Aerosol Sci., present Special Issue*, pp to be filled.

Alasri, A., Roques, C., Michel, G., Cabassud, C., & Aptel, P. (1992). Bactericidal properties of peracetic acid and H2O2, alone and in combination, and chlorine and formaldehyde against bacterial water strains. . *Can. J. Microbiol. , 38*(635-42).

Alexander, M. S., Smith, K. L., Paine, M. D., & Stark, J. P. W. (2007). Voltage-modulated flow rate for precise thrust control in colloid electrospray propulsion. *Journal of Propulsion and Power, 23*(5), 1042-1048.

Ali, M., Yan, C., Sun, Z., Gu, H., & Mehboob, K. (2013). Dust particle removal efficiency of a venturi scrubber. *Annals of Nuclear Energy, 54*, 178-183. doi: https://doi.org/10.1016/j.anucene.2012.11.005

Allaf-Akbari, E., & Ashgriz, N. (2017). An electrospray in a gaseous crossflow. *Journal of Aerosol Science, 114*, 233-243. doi: 10.1016/j.jaerosci.2017.09.021

Allen, R. (1982). Electrostatically Augmented Wet Dedusters. *Filtration Separation*, 330-340.

Almaier, G. (2018). Nano ES coupled to DMA (GEMMA) for the characterization of proteinaceous nanoparticles - from small peptides to functional protein complexes: A review. *J. Aerosol Sci., present special issue*, pp to be filled (STILL TO BE CONFIRMED).

Alonso, M., & Alguacil, F. (2008). Particle size distribution evolution during and after electrical charging: comparison of a corona ionizer and a radioactive neutralizer. *Aerosol and Air Quality Research, 8*(4), 366-380.

Alonso, M., Alguacil, F. J., Santos, J. P., Jidenko, N., & Borra, J. P. (2007). Deposition of ultrafine aerosol particles on wire screens by simultaneous diffusion and image force. *Journal of Aerosol Science, 38*(12), 1230-1239.

Asbach, C., Kuhlbusch, T. A. J., & Fissan, H. (2004). Development of a highly efficient electrostatic partitioner of gas and particles with minimal effect on the gas phase. *Aerosol Science and Technology, 38*(4), 322-329.

Ashgriz, N. (2011). *Handbook of atomization and sprays: theory and applications*.

Bacher, G., Szymanski, W. W., Kaufman, S. L., Zollner, P., Blaas, D., & Allmaier, G. (2001). Charge-reduced nano ES ionization combined with DMA of peptides, proteins, glycoproteins, noncovalent protein complexes and viruses. *Journal of Mass Spectrometry, 36*(9), 1038-1052. doi: 10.1002/jms.208

Bailey, A. G. (1988). *Electrostatic spraying of liquids*. Taunton, Somerset, England: Research Studies Press LTD.

Balachandran, W., Jaworek, A., Krupa, A., Kulon, J., & Lackowski, M. (2003). Efficiency of smoke removal by charged water droplets. *Journal of Electrostatics, 58*(3-4), 209-220. doi: 10.1016/S0304-3886(03)00049-4

Baron, P. A., & Willeke, K. (2001). *Aerosol measurement: principles, techniques, and applications*: Wiley.

Bastide, S., Duphil, D., Borra, J. P., & Levy-Clement, C. (2006). WS2 closed nanoboxes synthesized by spray pyrolysis. *Advanced Materials, 18*(1), 106-109. doi: 10.1002/adma.200501735

Beard, K. V. (1974). Experimental and numerical collision efficiencies for sub-micron particles scavenged by small raindrops. *J. Atmosperic Science, 31*, 1595-1603.

Bertinat, M. P. (1980). Charged-droplet scrubbing for controlling sub-micron particle emissions. *Journal of Electrostatics, 9*(2), 137-158. doi: https://doi.org/10.1016/0304-3886(80)90046-7

Biskos, G., Reavell, K., & Collings, N. (2005). Unipolar diffusion charging of aerosol particles in the transition regime. *Journal of Aerosol Science, 36*(2), 247-265. doi: http://dx.doi.org/10.1016/j.jaerosci.2004.09.002

Blanchard, D. C. (1989). The ejection of drops from the sea and their enrichment with bacteria and other materials-A review. *Estuaries, 12*(3), 127-137. doi: 10.2307/1351816

Boda, S. K., & Xie, Y. M. (2018). Electrospraying an enabling technology for pharmaceutical and biomedical applications: A review. *J. Aerosol Sci., present Special Issue*, pp to be filled.

Borner, A., Li, Z., & Levin, D. A. (2013). Prediction of fundamental properties of ionic liquid electrospray thrusters using molecular dynamics. *Journal of Physical Chemistry B, 117*(22), 6768-6781.

Borra, J. P., Camelot, D., Chou, K. L., Kooyman, P. J., Marijnissen, J., & Scarlett, B. (1999a). Bipolar coagulation for powder production: Micro-mixing inside droplets. *Journal of Aerosol Science, 30*(7), 945-958.

Borra, J. P., Camelot, D., Marijnissen, J., & Scarlett, B. (1997a). A new production process of powders with defined properties by EHD atomization of liquids and electrical mixing. *Journal of Electrostatics, 40-1*, 633-638.

Borra, J. P., & Ehouarn, P. (1999b). Moyens de pulverisation electrohydrodynamique: Google Patents.

Borra, J. P., Ehouarn, P., & Amouroux, J. (1999c). *Electro-hydrodynamic pulverisation of charged water droplets for the reduction of particulate plasma by-products in Progress in Plasma Processing of Materials 1999*. New York: Begell House, Inc.

Borra, J. P., Ehouarn, P., & Boulaud, D. (2004). Electrohydrodynamic atomisation of water stabilised by glow discharge - operating range and droplet properties. *Journal of Aerosol Science, 35*(11), 1313-1332.

Borra, J. P., Goldman, A., Goldman, M., & Boulaud, D. (1998). Electrical discharge regimes and aerosol production in point-to-plane dc high-pressure cold plasmas. *Journal of Aerosol Science, 29*(5-6), 661-674.

Borra, J. P., Hartmann, R., Marijnissen, J., & Scarlett, B. (1996). Destabilisation of sprays in the cone-jet mode by electrical dicharges on the jet. *Journal of Aerosol Science, 27*(SUPPL.1), S203-S204.

Borra, J. P., Jidenko, N., & Bourgeois, E. (2009). Atmospheric pressure plasmas for aerosols processes in materials and environment. *European Physical Journal-Applied Physics, 47*(2). doi: 10.1051/epjap/2009088

Borra, J. P., Roos, R. A., Renard, D., Lazar, H., Goldman, A., & Goldman, M. (1997b). Electrical and chemical consequences of point discharges in a forest during a mist and a thunderstorm. *Journal of Physics D-Applied Physics, 30*(1), 84-93. doi: 10.1088/0022-3727/30/1/011

Borra, J. P., Tombette, Y., & Ehouarn, P. (1999d). Influence of electric field profile and polarity on the mode of EHDA related to electric discharge regimes. *Journal of Aerosol Science, 30*(7), 913-925.

Borra, J. P., Valt, A., Arefi-Khonsari, F., & Tatoulian, M. (2010). Polymer surface processing by atmospheric pressure DBD for post-discharge grafting of washing-resistant functional coatings. In T. Chandra, N. Wanderka, W. Reimers & M. Ionescu (Eds.), *Thermec 2009, Pts 1-4* (Vol. 638-642, pp. 524-+).

Borra, J. P., Valt, A., Arefi-Khonsari, F., & Tatoulian, M. (2012). Atmospheric Pressure Deposition of Thin Functional Coatings: Polymer Surface Patterning by DBD and Post-Discharge Polymerization of Liquid Vinyl Monomer from Surface Radicals. *Plasma Processes and Polymers, 9*(11-12), 1104-1115.

Bouarouri, A., Jidenko, N., Gensdarmes, F., Maro, D., Boulaud, D., & Borra, J. P. (2016). Ion current density profiles in negative corona gaps versus EHD confinements. *Journal of Electrostatics, 82*, 88-95.

Bozorgi, Y., Keshavarz, P., Taheri, M., & Fathikaljahi, J. (2006). Simulation of spray scrubber with Eulerian/Lagrangian approach in aerosol removal. *Journal of Hazardous Materials, 137*(1), 509-517.

Brown, R. (1993). *Air Filtration: An Integrated Approach to the Theory and Applications of Fibrous Filters.* . Oxford: Pergamon Press.

Bruggeman, P., Graham, L., Degroote, J., Vierendeels, J., & Leys, C. (2007). Water surface deformation in strong electrical fields and its influence on electrical breakdown in a metal pin-water electrode system. *Journal of Physics D: Applied Physics, 40*(16), 4779-4786.

Brunet, P., Rincon, R., Margot, J., Massines, F., & Chaker, M. (2017). Deposition of homogeneous carbon-TiO2 composites by atmospheric pressure DBD. *Plasma Processes and Polymers, 14*(7).

Burayev, T. K., & Vereshchagin, I. P. (1972). Physical processes during electrostatic atomization of liquids. *Fluid Mech. - Sov. Res.; (United States)*, Medium: X; Size: Pages: 56-66.

Calvert, S., Yung, S. C., Barbarika, H., & Patterson, R. G. (1978). Evaluation of four novel fine particulate collection devices. San Diego, California: Air pollution Tehcnology, Inc.

Camelot, D. (1997). *Bipolar coagulation for the production of controlled powders.* Ph-D, TU Delft, Delft.

Camelot, D., Borra, J. P., Marijnissen, J. C. M., & Scarlett, B. (1998). Bipolar coagulation: Charge distribution of coagulated droplets. *Journal of Aerosol Science, 29*(SUPPL.2), S979-S980.

Camelot, D., Marijnissen, J. C. M., & Scarlett, B. (1999). Bipolar coagulation process for the production of powders. *Industrial and Engineering Chemistry Research, 38*(3), 631-638.

Carotenuto, C., D'Addio, L., Capocelli, M., & Di Natale, F. (2010a). *Diesel particle abatement by wet electrostatic scrubbing.* Paper presented at the 19th International Congress of Chemical and Process Engineering, CHISA 2010 and 7th European Congress of Chemical Engineering, ECCE-7.

Carotenuto, C., Di Natale, F., & Lancia, A. (2010b). Wet electrostatic scrubbers for the abatement of submicronic particulate. *Chemical Engineering Journal, 165*(1), 35-45. doi: 10.1016/j.cej.2010.08.049

Carvalho, T. C., & McConville, J. T. (2016). The function and performance of aqueous aerosol devices for inhalation therapy. *Journal of Pharmacy and Pharmacology, 68*(5), 556-578. doi: 10.1111/jphp.12541

Castillo, J. L., Martin, S., D, R.-P., Higuera, F., & Garcia-Ybarra, P. (2018). Nanostructured porous coatings via electrospray atomization and deposition of nanoparticle suspensions,. *J. Aerosol Sci., present Special Issue*, pp to be filled.

Chalmers, J. A. (1967). *Atmospheric Electricity*. Oxford: Pergamon Press.

Chen, C. H., Emond, M. H. J., Kelder, E. M., Meester, B., & Schoonman, J. (1999). Electrostatic sol-spray deposition of nanostructured ceramic thin films. *Journal of Aerosol Science, 30*(7), 959-967.

Chen, D. R., & Pui, D. Y. H. (1997). Experimental investigation of scaling laws for electrospraying: Dielectric constant effect. *Aerosol Science and Technology, 27*(3), 367-380.

Chen, D. R., & Pui, D. Y. H. (2010). Electrospray and its medical applications *Nanoparticles in Medicine and Environment: Inhalation and Health Effects* (pp. 59-75).

Chen, D. R., Pui, D. Y. H., & Kaufman, S. L. (1995). Electrospraying of conducting liquids for monodisperse aerosol generation in the 4 nm to 1.8 μm diameter range. *Journal of Aerosol Science, 26*(6), 963-977.

Chen, T. M., Tsai, C. J., Yan, S. Y., & Li, S. N. (2014). An efficient wet electrostatic precipitator for removing nanoparticles, submicron and micron-sized particles. *Separation and Purification Technology, 136*, 27-35.

Chou, K.-L. (1997). *Synthesis of multicomponenoxides by means of bipolar mixing.* Master thesis, TU Delft.

Cloupeau, M. (1994). Recipes for use of EHD spraying in cone-jet mode and notes on corona discharge effects. *Journal of Aerosol Science, 25*(6), 1143-1157.

Cloupeau, M., & Prunet-Foch, B. (1989). Electrostatic spraying of liquids in cone-jet mode. *Journal of Electrostatics, 22*(2), 135-159.

Cloupeau, M., & Prunet-Foch, B. (1990). Electrostatic spraying of liquids: Main functioning modes. *Journal of Electrostatics, 25*(2), 165-184.

Cloupeau, M., & Prunet-Foch, B. (1994). Electrohydrodynamic spraying functioning modes: a critical review. *Journal of Aerosol Science, 25*(6), 1021-1036.

Coffee, R. A. (1981). ElectroDynamic crop spraying. . *Outlook on Agriculture, 10*(7), 350-356.

Cross, J. (1987). Electrostatics : principles, problems and applications. Bristol :: Adam Hilger.

Cui, H., Li, N., Peng, J., Cheng, J., Zhang, N., & Wu, Z. (2017). Modeling the particle scavenging and thermal efficiencies of a heat absorbing scrubber. *Building and Environment, 111*, 218-227.

Czech, T., Sobczyk, A. T., & Jaworek, A. (2011). Optical emission spectroscopy of point-plane corona and back-corona discharges in air. *European Physical Journal D, 65*(3), 459-474. doi: 10.1140/epjd/e2011-20196-x

D'Addio, L., Di Natale, F., Carotenuto, C., Balachandran, W., & Lancia, A. (2013). A lab-scale system to study submicron particles removal in wet electrostatic scrubbers. *Chemical Engineering Science, 97*, 176-185.

Da Vinci, L. (1513). *The codex Leicester*. Sidney: Powerhouse publishing.

DBVtechno. (Producer). Retrieved from https://www.dbv-technologies.com/fr/viaskin-technologie/production

De Juan, L., & Fernández de la Mora, J. (1996). On-line Sizing of Colloidal Nanoparticles via Electrospray and Aerosol Techniques *ACS Symposium Series* (Vol. 622, pp. 19-41).

De Juan, L., & Fernández De La Mora, J. (1997). Charge and size distributions of electrospray drops. *Journal of Colloid and Interface Science, 186*(2), 280-293.

de la Mora, J. F., & Loscertales, I. G. (1994). The current emitted by highly conducting Taylor cones. *Journal of Fluid Mechanics, 260*(special issue), 155-184.

Deng, W., & Gomez, A. (2007). Influence of space charge on the scale-up of multiplexed electrosprays. *Journal of Aerosol Science, 38*(10), 1062-1078. doi: 10.1016/j.jaerosci.2007.08.005

Di Natale, F., Carotenuto, C., D'Addio, L., Jaworek, A., Krupa, A., Szudyga, M., & Lancia, A. (2015). Capture of particles in a wet electrostatic scrubber. *Journal of Environmental Chemical Engineering, 3*(1), 349-356.

Di Natale, F., Carotenuto, C., D'Addio, L., & Lancia, A. (2016a). Effect of gas temperature on the capture of charged particles by oppositely charged water droplets. *Aerosol Science and Technology, 50*(2), 110-117.

Di Natale, F., Carotenuto, C., D'Addio, L., Lancia, A., Antes, T., Szudyga, M., . . . Abbod, M. (2013) New technologies for marine diesel engine emission control. *Vol. 32. Chemical Engineering Transactions* (pp. 361-366).

Di Natale, F., Carotenuto, C., Manna, L., Esposito, M., La Motta, F., D'Addio, L., & Lancia, A. (2016b). Water ES for Emission Control *International Journal of Heat and Technology, 34S*, 597-602.

Duby, M. H., Deng, W., Kim, K., Gomez, T., & Gomez, A. (2006). Stabilization of monodisperse electrosprays in the multi-jet mode via electric field enhancement. *Journal of Aerosol Science, 37*(3), 306-322.

Dunn, P. F., & Snarski, S. R. (1992). Droplet diameter, flux and total current measurements in an EHD Spray. *Journal of Applied Physics, 71*(1), 80-84. doi: 10.1063/1.350651

Ehouarn, P. (2001). *Pulvérisation électro-hydrodynamique de liquide stabilisée par décharges électriques pour le traitement d'effluents particulaires.* Ph-D, Univ. Paris-Sud, Orsay.

Ehouarn, P., & Borra, J.-P. (1997). Electro-pulvérisation de gouttelettes d'eau microniques et chargées électriquement. *Info-Chimie, 392* 102-106.

Ehouarn, P., Unger, L., & Borra, J. P. (1999). *EHD atomization - Stability domains and scaling laws of the cone-jet-glow mode.* Paper presented at the 15th French Congress on Aerosols.

Ehouarn, P., Unger, L., & Borra, J. P. (2001). Properties of water droplets produced by ehd pulverisation for the collection of particulate plasmas by-products. *High Temperature Material Processes, 5*(3), 333-344.

Eliasson, B., & Egli, W. (1991). Bipolar Coagulation - Modeling and Applications. *J. Aerosol Sci., 22*(4), 429-440.

English, W. N. (1948). Corona from a Water Drop. *Physical Review, 74*(2), 179-189.

Eyraud, C., Joubert, J., Morel, R., Henry, C., & Roumesy, B. (1966). *Study of a New Dust Collector Using Electrostatically Sprayed Water.* Paper presented at the Proceedings: Part I Int. Clean Air Congress, London.

Fanelli, F., Mastrangelo, A., & Fracassi, F. (2014). Aerosol-assisted atmospheric cold plasma deposition of superhydrophobic organic-inorganic nanocomposite thin films. *Langmuir, 30*(3), 857-865.

Farzaneh, M., Phan, L. C., & Ai, B. (1985). On the role of the space-charge produced by hanging water drops in the mechanism of the corona-induced vibration of HV conductors. *Journal of Electrostatics, 17*(3), 235-244.

Fenn, J. B., Mann, M., Meng, C. K., Wong, S. F., & Whitehouse, C. M. (1990). Electrospray ionization-principles and practice. *Mass Spectrometry Reviews, 9*(1), 37-70.

Foti, L., Sionek, A., Stori, E. M., Soares, P. P., Pereira, M. M., Krieger, M. A., . . . Saul, C. K. (2015). Electrospray induced surface activation of polystyrene microbeads for diagnostic applications. *Journal of Materials Chemistry B, 3*(13), 2725-2731. doi: 10.1039/c4tb01884b

Fu, H., Liu, Q., & Chen, D.-R. (2012). Performance study of a twin-head electrospray system. *Journal of Aerosol Science, 52*, 33-44. doi: https://doi.org/10.1016/j.jaerosci.2012.04.008

Fu, H., Patel, A. C., Holtzman, M. J., & Chen, D.-R. (2011). A New ES Aerosol Generator with High Particle Transmission Efficiency. *Aerosol science and technology, 45*(10), 1176-1183.

Fuchs, N. A. (1964). *The Mechanics of Aerosols*. Elmsford, NY Pergamon Press.

Gamero-Castaño, M. (2008). Characterization of the electrosprays of 1-ethyl-3-methylimidazolium bis(trifluoromethylsulfonyl) imide in vacuum. *Physics of Fluids, 20*(3).

Gan, Y., Zhang, X., Li, H., Tong, Y., Zhang, Y., Shi, Y., & Yang, Z. (2016). Effect of a ring electrode on the cone-jet characteristics of ethanol in small-scale electro-spraying combustors. *Journal of Aerosol Science, 98*, 15-29.

Ganán-Calvo, A. M. (2004). On the general scaling theory for ES. *Journal of Fluid Mechanics*(507), 203-212.

Gañán-Calvo, A. M. (1997). Cone-jet analytical extension of taylor's electrostatic solution and the asymptotic universal scaling laws in electrospraying. *Physical Review Letters, 79*(2), 217-220.

Gañán-Calvo, A. M., Dávila, J., & Barrero, A. (1997). Current and droplet size in the electrospraying of liquids. Scaling laws. *Journal of Aerosol Science, 28*(2), 249-275.

Ganan-Calvo, A. M., Lopez-Herrera, J. M., Herrada, M. A., & Montanero, J. M. (2018). Review on the physcis of electrospray: from electrokinetics to the operating conditions of Taylor cone-jets, and beyond. *J. Aerosol Sci., present Special Issue*, pp to be filled.

Ganan-Calvo, A. M., Lopez-Herrera, J. M., Rebollo-Munoz, N., & Montanero, J. M. (2016). The onset of electrospray: the universal scaling laws of the first ejection. *Scientific Reports, 6*. doi: 10.1038/srep32357

Gañán-Calvo, A. M., Rebollo-Muñoz, N., & Montanero, J. M. (2013). The minimum or natural rate of flow and droplet size ejected by Taylor cone-jets: Physical symmetries and scaling laws. *New Journal of Physics, 15*.

Ganesan, V. A., Citroen, P., Ondimu, O. M., Bahlman, R., Marijnissen, J., & Agostinho, L. (2016, sept.). *Investigation of EHDA for natural gas odorization.* Paper presented at the European Aerosol Conference, Tours, France.

Geerse, K., Marijnissen, J., Scarlett, B., Kerssies, A., Van Der Staaij, M., & Van Der Meer, C. (2000). A multiple EHDA system for selective deposition of pesticide in greenhouse. *Journal of Aerosol Science, 31*(S1), 660-661.

Gibson, G. T. T., Mugo, S. M., & Oleschuk, R. D. (2009). Nanoelectrospray emitters: Trends and perspective. *Mass Spectrometry Reviews, 28*(6), 918-936.

Goldman, M., & Goldman, A. (1978). Corona discharges In M. N. Hirsh & H. J. Ascam (Eds.), *Gaseous Electronics 1, Electrical discharges* (Vol. 89b, pp. 119-166). New York: Academics Press.

Goniva, C., Tukovic, Z., Feilmayr, C., & Pirker, S. (2010). Towards efficient simulation of off-gas scrubbing by a hybrid Eulerian Lagrangian model. *Progress in Computational Fluid Dynamics, 10*(5-6), 265-275.

Goudeli, E., Eggersdorfer, M. L., & Pratsinis, S. E. (2015). Coagulation-Agglomeration of Fractal-like Particles: Structure and Self-Preserving Size Distribution. *Langmuir, 31*(4), 1320-1327. doi: 10.1021/la504296z

Grace, J. M., & Dunn, P. F. (1996). Droplet motion in an electrohydrodynamic fine spray. *Experiments in Fluids, 20*(3), 153-164.

Grifoll, J., & Rosell-Llompart, J. (2012). Efficient Lagrangian simulation of electrospray droplets dynamics. *Journal of Aerosol Science, 47*, 78-93.

Ha, T. H., Nishida, O., Fujita, H., & Wataru, H. (2010). Enhancement of diesel particulate matter collection in an electrostatic water-spraying scrubber. *Journal of Marine Science and Technology, 15*(3), 271-279.

Hara, M., Ishibe, S., Sumiyoshitani, S., & Akazaki, M. (1980). Electrical corona and specific charge on water drops from a cylindrical conductor with high DC Voltage. *Journal of Electrostatics, 8*(2-3), 239-270.

Hara, M., Sumiyoshitani, S., & Akazaki, M. (1984, Nov. 1984). *Fundamental processes of fine particle collection by charged water droplets.* Paper presented at the Int. Conf. Electrostatic Precipitation.

Harpur, I. G., Bailey, A. G., & Hashish, A. H. (1996). A design method for the electrostatic atomization of liquid aerosols. *Journal of Aerosol Science, 27*(7), 987-996.

Hartman, G. (1984). Theoretical Evaluation of Peek's Law. *IEEE Transactions on Industry Applications, IA-20*(6), 1647-1651. doi: 10.1109/TIA.1984.4504655

Hartmann, R. P. A., Borra, J. P., Brunner, D. J., Marijnissen, J. C. M., & Scarlett, B. (1999a). The evolution of EHD sprays produced in the cone-jet mode, a physical model. *Journal of Electrostatics, 47*(3), 143-170.

Hartmann, R. P. A., Borra, J. P., Marijnissen, J. C. M., & Scarlett, B. (1996). Development of electrohydrodynamic sprays related to space charge effects. *Journal of Aerosol Science, 27*(SUPPL.1), S177-S178.

Hartmann, R. P. A., Brunner, D. J., Camelot, D., Marijnissen, J. C. M., & Scarlett, B. (1999b). EHD atomization in the cone-jet mode physical modeling of the liquid cone and jet. *Journal of Aerosol Science, 30*(7), 823-849.

Hartmann, R. P. A., Brunner, D. J., Camelot, D., Marijnissen, J. C. M., & Scarlett, B. (2000). Jet break-up in electrohydrodynamic atomization in the cone-jet mode. *Journal of Aerosol Science, 31*(1), 65-95.

Hartmann, R. P. A., Brunner, D. J., Marijnissen, J. C. M., & Scarlett, B. (1998). Scaling laws for droplet size and current produced in the cone-jet mode. *Journal of Aerosol Science, 29*(SUPPL.2), S977-S978.

Hartmann, R. P. A., Marijnissen, J. C. M., & Scarlett, B. (1997). Electro hydrodynamic atomization in the cone-jet mode. A physical model of the liquid cone and jet. *Journal of Aerosol Science, 28*(SUPPL. 1), S527-S528.

Hayati, I., Bailey, A. G., & Tadros, T. F. (1987a). Investigations into the mechanism of electrohydrodynamic spraying of liquids: II. Mechanism of stable jet formation and electrical forces acting on a liquid cone. *Journal of Colloid and Interface Science, 117*(1), 222-230. doi: https://doi.org/10.1016/0021-9797(87)90186-X

Hayati, I., Bailey, A. G., & Tadros, T. F. (1987b). Investigations into the mechanisms of electrohydrodynamic spraying of liquids. *Journal of Colloid and Interface Science, 117*(1), 205-221.

Higashiyama, Y., Nakajima, T., & Sugimoto, T. (2017). Influence of conductivity on corona discharge current from a water droplet and on ejection of nano-sized droplets. *Journal of Electrostatics, 88*, 65-70.

Higashiyama, Y., & Saito, S. (2013). Negative corona discharge from a water droplet under the pulsating DC field. *Journal of Electrostatics, 71*(3), 499-503.

Hinds, W. C. (1982). *Aerosol Technology: Properties, Behavior, and Measurement of Airborne Particles*: John Wiley & Sons.

Ho, H., & Lee, J. (2012). Redispersible drug nanoparticles prepared without dispersant by electro-spray drying. *Drug Development and Industrial Pharmacy, 38*(6), 744-751.

Hoenig, S. A., Sill, G. T., Kelley, L. M., & Garvey, K. J. (1980). Destruction of bacteria and toxic organic-chemicals by a corona discharge. *Journal of the Air Pollution Control Association, 30*(3), 277-278.

Hong, J.-T., Seo, H., Kim, H.-S., Lee, D.-G., Jang, J.-J., Xu, G.-C., & Kim, H.-J. (2011). Electrical sterilization of E. coli by electrostatic atomization with a photo-chemical catalyst. *Journal of Electrostatics, 69*(4), 328-332.

Huberman, M. N., Beynon, J. C., Cohen, E., Goldin, D. S., Kidd, P. W., & Zafran, S. (1968). Present status of colloid microthruster technology. *Journal of Spacecraft and Rockets, 5*(11), 1319-&.

Ijsebaert, J. C., Geerse, K. B., Marijnissen, J. C. M., & Scarlett, B. (1999). Electrohydrodynamic spraying of inhalation medicine. *30*(Suppl. 1), S825-S826.

Intra, P., & Tippayawong, N. (2007). An overview of aerosol particle sensors for size distribution measurement. *Maejo International Journal of Science and Technology, 1*(2), 120-136.

Intra, P., & Tippayawong, N. (2009). Progress in unipolar corona discharger designs for airborne particle charging: A literature review. *Journal of Electrostatics, 67*(4), 605-615. doi: 10.1016/j.elstat.2008.12.018

Iribarne, J., & Mason, B. (1967). Electrification accompanying the bursting of bubbles in water and dilute aqueous solutions. *Transactions of the Faraday Society, 63*, 2234-2245.

Jacopo, P., Simon, D., Olivier, L., Nicolas, N., Antoine, B., Luc, S., & Nicolas, G. (2017). Interaction of atomized colloid with acDBD for deposition of nanocomposite coating. *Journal of Physics D: Applied Physics, 50*(7), 075201.

Janischewskyj, W., & Arainy, A. (1981). Corona characteristicss of simulated rain. *IEEE Tans. on Power apparatus and Systems, 100*(2), 539-551.

Jaworek, A. (2007a). Electrospray droplet sources for thin film deposition. *Journal of Materials Science, 42*(1), 266-297. doi: 10.1007/s10853-006-0842-9

Jaworek, A. (2007b). Micro- and nanoparticle production by electrospraying. *Powder Technology, 176*(1), 18-35. doi: 10.1016/j.powtec.2007.01.035

Jaworek, A. (2011). *Electrospray technology for thin-film deposition*.

Jaworek, A., Balachandran, W., Krupa, A., Kulon, J., & Lackowski, M. (2006a). Wet electroscrubbers for state of the art gas cleaning. *Environmental Science and Technology, 40*(20), 6197-6207. doi: 10.1021/es0605927

Jaworek, A., Balachandran, W., Lackowski, M., Kulon, J., & Krupa, A. (2006b). Multi-nozzle electrospray system for gas cleaning processes. *Journal of Electrostatics, 64*(3-4), 194-202. doi: 10.1016/j.elstat.2005.05.006

Jaworek, A., Czech, T., Rajch, E., & Lackowski, M. (2005). Spectroscopic studies of electric discharges in electrospraying. *Journal of Electrostatics, 63*(6-10), 635-641. doi: 10.1016/j.elstat.2005.03.029

Jaworek, A., & Krupa, A. (1996). Forms of the multijet mode of electrohydrodynamic spraying. *Journal of Aerosol Science, 27*(7), 979-986. doi: 10.1016/0021-8502(96)00042-0

Jaworek, A., & Krupa, A. (1997). Studies of the corona discharge in ehd spraying. *Journal of Electrostatics, 40-41*, 173-178.

Jaworek, A., & Krupa, A. (1999). Classification of the modes of EHD spraying. *Journal of Aerosol Science, 30*(7), 873-893. doi: 10.1016/S0021-8502(98)00787-3

Jaworek, A., & Krupa, A. (2011). Charged sprays generation and application *Sprays: Types, Technology and Modeling* (pp. 1-100).

Jaworek, A., Krupa, A., & Adamiak, K. (1998). Submicron charged dust particle interception by charged drops. *IEEE Transactions on Industry Applications, 34*(5), 985-991. doi: 10.1109/28.720438

Jaworek, A., Krupa, A., & Adamiak, K. (2004). *Dust particles removal by a novel two-stage electrostatic precipitator*. Paper presented at the Institute of Physics Conference Series.

Jaworek, A., Krupa, A., & Czech, T. (2007). Modern electrostatic devices and methods for exhaust gas cleaning: A brief review. *Journal of Electrostatics, 65*(3), 133-155. doi: 10.1016/j.elstat.2006.07.012

Jaworek, A., Krupa, A., Sobczyk, A. T., Marchewicz, A., Szudyga, M., Antes, T., . . . Carotenuto, C. (2013). Submicron particles removal by charged sprays. Fundamentals. *Journal of Electrostatics, 71*(3), 345-350.

Jaworek, A., Sobczyk, A., Czech, T., & Krupa, A. (2014). Corona discharge in electrospraying. *Journal of Electrostatics, 72*(2), 166-178. doi: 10.1016/j.elstat.2014.01.004

Jaworek, A., Sobczyk, A., & Krupa, A. (2018). Electrospray application to powder production and surface coating,. *J. Aerosol Sci., present Special Issue*, pp to be filled.

Jaworek, A., & Sobczyk, A. T. (2008). Electrospraying route to nanotechnology: An overview. *Journal of Electrostatics, 66*(3-4), 197-219. doi: 10.1016/j.elstat.2007.10.001

Jayasinghe, S. N. (2006). Electrospraying a nanoparticulate suspension. *International Journal of Nanoscience, 5*(1), 35-46.

Jayasinghe, S. N., & Edirisinghe, M. J. (2005a). Electrostatic atomization of a ceramic suspension at pico-flow rates. *Applied Physics A: Materials Science and Processing, 80*(2), 399-404.

Jayasinghe, S. N., & Edirisinghe, M. J. (2005b). Jet break-up in nano-suspensions during electrohydrodynamic atomization in the stable cone-jet mode. *Journal of Nanoscience and Nanotechnology, 5*(6), 923-926.

Jayasinghe, S. N., Edirisinghe, M. J., & De Wilde, T. (2002). A novel ceramic printing technique based on electrostatic atomization of a suspension. *Materials Research Innovations, 6*(3), 92-95.

Jędrusik, M., Świerczok, A., & Jaworek, A. (2013). Collection of low resistivity fly ash in an electrostatic precipitator. *Journal of Physics: Conference Series, 418*(1). doi: 10.1088/1742-6596/418/1/012069

Jidenko, N., & Borra, J. P. (2012). Self-cleaning, maintenance-free aerosol filter by non-thermal plasma at atmospheric pressure. *Journal of Hazardous Materials, 235*, 237-245. doi: 10.1016/j.jhazmat.2012.07.055

Joffre, G. H., & Cloupeau, M. (1986). Characteristic forms of electrified menisci emitting charges. *Journal of Electrostatics, 18*(2), 147-161. doi: https://doi.org/10.1016/0304-3886(86)90002-1

Jung, J. H., Lee, J. E., & Kim, S. S. (2009). Generation of Nonagglomerated Airborne Bacteriophage Particles Using an Electrospray Technique. *Analytical Chemistry, 81*(8), 2985-2990. doi: 10.1021/ac802584z

Juraschek, R., & Röllgen, F. W. (1998). Pulsation phenomena during electrospray ionization. *International Journal of Mass Spectrometry, 177*(1), 1-15.

Kamphoefner, F. J. (1972). Ink jet printing. *Ieee Transactions on Electron Devices, ED19*(4).

Kanev, I. L., ..., & Morozov, N. (2014). Are reactive Oxygen species generated in ES at low current ? *Analytical Chemistry*, 1511-1517.

Kasper, G. (1981). Electrostatic dispersion of homopolar charged aerosols. *Journal of Colloid and Interface Science, 81*(1), 32-40. doi: 10.1016/0021-9797(81)90298-8

Kasper, G., Preining, O., & Matteson, M. (1978). Penetration of a multistage diffusion battery at various temperatures. *Journal of Aerosol Science, 9*(4), 331-338.

Kaufman, S. L. (1998). Analysis of biomolecules using electrospray and nanoparticle methods: The gas-phase electrophoretic mobility molecular analyzer (GEMMA). *Journal of Aerosol Science, 29*(5-6), 537-552.

Kaufman, S. L. (2000). Electrospray diagnostics performed by using sucrose and proteins in the gas-phase electrophoretic mobility molecular analyzer (GEMMA). *Analytica Chimica Acta, 406*(1), 3-10.

Kaufman, S. L., Kuchumov, A. R., Kazakevich, M., & Vinogradov, S. N. (1998). Analysis of a 3.6-MDa hexagonal bilayer hemoglobin from Lumbricus terrestris using a gas-phase electrophoretic mobility molecular analyzer. *Analytical Biochemistry, 259*(2), 195-202.

Kaufman, S. L., Skogen, J. W., Dorman, F. D., Zarrin, F., & Lewis, K. C. (1996). Macromolecule analysis based on electrophoretic mobility in air: Globular proteins. *Analytical Chemistry, 68*(11), 1895-1904.

Kavadiya, S., & Biswas, P. (2018). Electrospray deposition of biomolecules: applications, challenges, and recommendations. *J. Aerosol Science, present Special Issue*, pp to be filled.

Kawamoto, H., Umezu, S., & Koizumi, R. (2005). Fundamental investigation on electrostatic ink jet phenomena in pin-to-plate discharge system. *Journal of Imaging Science and Technology, 49*(1), 19-27.

Kelder, E., Marijnissen, J., Waiyego Karuga, S., & al., e. (2018). EDHA for Energy Production, Storage and Conversion Devices , . *J. Aerosol Sci., present Special Issue*, pp to be filled.

Kelly, R. T., Page, J. S., Marginean, I., Tang, K. Q., & Smith, R. D. (2008). Nanoelectrospray emitter arrays providing interemitter electric field uniformity. *Analytical Chemistry, 80*(14), 5660-5665. doi: 10.1021/ac800508q

Kelvin, S. W. T.-L. (1867). On a Self-Acting Apparatus for Multiplying and Maintaining Electric Charges, with Applications to Illustrate the Voltaic Theory *Proceedings of the Royal Society*.

Kim, H. H., Kim, J. H., & Ogata, A. (2011). Time-resolved high-speed camera observation of electrospray. *Journal of Aerosol Science, 42*(4), 249-263.

Kim, H. H., Teramoto, Y., Negishi, N., Ogata, A., Kim, J. H., Pongrac, B., . . . Ganan-Calvo, A. M. (2014). Polarity effect on the electrohydrodynamic (EHD) spray of water. *Journal of Aerosol Science, 76*, 98-114.

Kim, K., Kim, W., Hwa Yun, S., Hyun Lee, J., Kim, S., & Lee, B. U. (2008). Use of an electrospray for the generation of bacterial bioaerosols. *Journal of Aerosol Science, 39*(4), 365-372.

Kodas, T. T., & Hampden-Smith, M. J. (1971). *Aerosol processing of materials*: New York (N.Y.) : Wiley.

Korkut, S., Saville, D. A., & Aksay, I. A. (2008). Enhanced Stability of Electrohydrodynamic Jets through Gas Ionization. *Physical Review Letters, 100*(3), 034503.

Kraemer, H. F., & Johnstone, H. F. (1955). Collection of Aerosol Particles in Presence of Electrostatic Fields. *Industrial & Engineering Chemistry, 47*(12), 2426-2434. doi: 10.1021/ie50552a020

Krella, A. K., Krupa, A., Gazda, M., Sobczyk, A. T., & Jaworek, A. (2017). Protective properties of Al2O3+TiO2 coating produced by ES deposition method. *Ceramics International, 43*(15), 12126-12137.

Krupa, A., Jaworek, A., Czech, T., Lackowski, M., & Luckner, J. (2004). *Dust particle removal by wet-type electrostatic scrubber*. Paper presented at the Institute of Physics Conference Series.

https://doi.org/10.1016/j.jaerosci.2018.04.005

Krupa, A., Jaworek, A., Sobczyk, A. T., Marchewicz, A., Szudyga, M., & Antes, T. (2013). Charged spray generation for gas cleaning applications. *Journal of Electrostatics, 71*(3), 260-264. doi: 10.1016/j.elstat.2012.11.022

Krupa, A., Jaworek, A., Szudyga, M., Czech, T., Sobczyk, A. T., Marchewicz, A., . . . D'Addio, L. (2016). Diesel nanoparticles removal by charged spray. *International Journal of Plasma Environmental Science and Technology, 10*(2).

Ku, B. K., & Kim, S. S. (2002). Electrospray characteristics of highly viscous liquids. *Journal of Aerosol Science, 33*(10), 1361-1378.

Lastow, O., & Balachandran, W. (2007). Novel low voltage EHD spray nozzle for atomization of water in the cone jet mode. *Journal of Electrostatics, 65*(8), 490-499.

Law, S. E. a. L., M. D. (1982). Electrostatic deposition of pesticide sprays onto ionising targets: charge and mass transfert analysis. *IEEE Tans., IA-I8*(6), 673-679.

Lear, C. W., Krieve, W. F., & Cohen, E. (1975). Charged droplet scrubbing for fine particle control. *J. Air Pollution Control Assoc., 25*(2), 184-189.

Lecuiller, M., & Goldman, M. (1988). Analysis of regimes and zones of corona discharge from the point of view of ozone production. *Journal of Physics D-Applied Physics, 21*(1), 51-56.

Lee, H.-K., & Lee, J.-G. (2005). Effect of electrostatic atomization on electrical sterilization. *Journal of Electrostatics, 63*(3), 329-336. doi: https://doi.org/10.1016/j.elstat.2004.11.002

Lee, H. K. (2001). Electrical sterilization of Escherichia coli by electrostatic atomization. *Journal of Electrostatics, 51*, 71-75. doi: 10.1016/s0304-3886(01)00066-3

Lenggoro, I. W., Okuyama, K., De La Mora, J. F., & Tohge, N. (2000). Preparation of ZnS nanoparticles by electrospray pyrolysis. *Journal of Aerosol Science, 31*(1), 121-136.

Lewis, K. C., Dohmeier, D. M., Jorgenson, J. W., Kaufman, S. L., Zarrin, F., & Dorman, F. D. (1994). ES-CPC: A molecule counting LG detector for macromolecules *Analytical Chemistry, 66*(14), 2285-2292.

Li, J. L., & Tok, A. (2008). Electrospraying of water in the cone-jet mode in air at atmospheric pressure. *International Journal of Mass Spectrometry, 272*(2-3), 199-203.

Li, X., Wei, T., Wang, D., Hu, H., Kong, L., & Xiang, W. (2016). Study of gas–liquid two-phase flow patterns of self-excited dust scrubbers. *Chemical Engineering Science, 151*, 79-92.

Liu, B. Y. H., & Pui, D. Y. H. (1974). Electrical neutralization of aerosols. *Journal of Aerosol Science, 5*(5), 465-472. doi: https://doi.org/10.1016/0021-8502(74)90086-X

Liu, Q., Budiman, T., & Chen, D. R. (2014a). Evaluation of twin-head electrospray nanoparticle disperser for nanotoxicity study. *Journal of Nanoparticle Research, 16*(8).

Liu, Q., & Chen, D. R. (2014b). An electrospray aerosol generator with X-ray photoionizer for particle charge reduction. *Journal of Aerosol Science, 76*, 148-162.

Loeb, L. B. (1965). *Electrical Coronas, Their Basic Physical Mechanisms*: University of California Press.

Loo, J. A., Berhane, B., Kaddis, C., Wooding, K., Xie, Y. M., Kaufman, S., & Chernushevich, I. (2005). ESI-MS and ion mobility analysis of proteasome complex. *Journal of the American Society for Mass Spectrometry, 16*(7), 998-1008.

Lopez-Herrera, J. M., Barrero, A., Boucard, A., Loscertales, I. G., & Marquez, M. (2004). An experimental study of the electrospraying of water in air at atmospheric pressure. *Journal of the American Society for Mass Spectrometry, 15*(2), 253-259. doi: 10.1016/j.jasms.2003.10.018

Lowke, J. J., & D'Alessandro, F. (2003). Onset corona fields and electrical breakdown criteria. *Journal of Physics D-Applied Physics, 36*(21), 2673-2682. doi: 10.1088/0022-3727/36/21/013

Machala, Z., Tarabova, B., Hensel, K., Spetlikova, E., Sikurova, L., & Lukes, P. (2013). Formation of ROS and RNS in water ES through spark in air and bactericidal effect. *Plasma Processes and Polymers, 10*(7), 649-659.

Maisels, A., Kruis, F. E., & Fissan, H. (2004). Coagulation in bipolar aerosol chargers. *Journal of Aerosol Science, 35*(11), 1333-1345. doi: http://dx.doi.org/10.1016/j.jaerosci.2004.05.009

Maißer, A., Attoui, M., Gañán-Calvo, A., & Szymanski, W. (2013). EHD generation of monodisperse nanoparticles in sub-10 nm size range from electrolytic salt solution. *Journal of Nanoparticle Research, 15*(1).

Malet, J., Mimouni, S., Manzini, G., Xiao, J., Vyskocil, L., Siccama, N. B., & Huhtanen, R. (2015). Gas entrainment by one French PWR spray, SARNET-2 spray benchmark. *Nuclear Engineering and Design, 282*, 44-53.

Marginean, I., Kelly, R. T., Page, J. S., Tang, K. Q., & Smith, R. D. (2007). ES characteristic curves: In pursuit of improved performance in the nanoflow regime. *Analytical Chemistry, 79*(21), 8030-8036.

Marginean, I., Tang, K. Q., Smith, R. D., & Kelly, R. T. (2014). Picoelectrospray Ionization-MS using narrow-Bore chemically etched emitters. *Journal of the American Society for Mass Spectrometry, 25*(1), 30-36.

Marijnissen, J. C. M., Mollinger, A. M., & Vercoulen, P. (1993a). Generation of (sub)micron droplets in an electrostatic precipitator by ES. *Journal of Aerosol Science, 24-S1*, S23-S24.

Marijnissen, J. C. M., Mollinger, A. M., & Vercoulen, P. H. W. (1993b). 04 O 03 The generation of (sub)micron droplets in an electrostatic precipitator by electro-spraying. *Journal of Aerosol Science, 24*(SUPPL. 1), S23-S24.

Marode, E. (1975a). Mechanism of spark breakdown in air at atmospheric-pressure between a positive point and plane .1. experimental - nautre of streamer track. *Journal of Applied Physics, 46*(5), 2005-2015.

Marode, E. (1975b). Mechanism of spark breakdown in air at atmospheric-pressure between a positive point and plane .2. theoretical -computer-simulation of streamer track. *Journal of Applied Physics, 46*(5), 2016-2020.

Mathon, R., Jidenko, N., & Borra, J. P. (2017). Ozone-free post-DBD aerosol bipolar diffusion charger: Evaluation as neutralizer for SMPS size distribution measurements. *Aerosol Science and Technology, 51*(3), 282-291. doi: 10.1080/02786826.2016.1265082

McMurry, P. H., & Rader, D. J. (1985). Aerosol Wall Losses in Electrically Charged Chambers. *Aerosol Science and Technology, 4*(3), 249-268. doi: 10.1080/02786828508959054

Meek, J. M. (1940). A Theory of Spark Discharge. *Physical Review, 57*(8), 722-728.

Meek, J. M., & Craggs, J. D. (1978). *Electrical breakdown of gases*: Wiley.

Meesters, G. M. H., Vercoulen, P. H. W., Marijnissen, J. C. M., & Scarlett, B. (1992). Generation of micron-sized droplets from the Taylor cone. *Journal of Aerosol Science, 23*(1), 37-49.

Melcher, J. R., Sachar, K. S., & P., W. E. (1977). Electrostatic devices for controll of submicrometer particles. *Peroc IEEE, 65*(12), 1659-1669.

Messing, G. L., Zhang, S.-C., & Jayanthi, G. V. (1993). Ceramic Powder Synthesis by Spray Pyrolysis. *Journal of the American Ceramic Society, 76*(11), 2707-2726. doi: 10.1111/j.1151-2916.1993.tb04007.x

Metzler, P., Weiss, P., Buttner, H., & Ebert, F. (1997). Electrostatic enhancement of dust separation in a nozzle scrubber. *Journal of Electrostatics, 42*(1-2), 123-141. doi: 10.1016/s0304-3886(97)00135-6

Morozov, V. (2011). *Generation of biologically active nano-aerosol by an electrospray-neutralization method* (Vol. 42).

Morozov, V. N., & Vsevolodov, N. N. (2007). Electrospray-Neutralization Method for Manufacturing Free and Supported Nanomats. *Advanced Materials, 19*(24), 4381-4386. doi: 10.1002/adma.200701606

Morris, T., Malardier-Jugroot, C., & Jugroot, M. (2013). Characterization of electrospray beams for micro-spacecraft electric propulsion applications. *Journal of Electrostatics, 71*(5), 931-938.

Mouradian, S., Skogen, J. W., Dorman, F. D., Zarrin, F., Kaufman, S. L., & Smith, L. M. (1997). DNA analysis using an ES scanning mobility particle sizer. *Analytical Chemistry, 69*(5), 919-925.

Naqwi, A. A., Hartman, R. P. A., & Marijnissen, J. (1996). Basic studies of EHD atomization process using phase Doppler measurement *Particle and Particle Systems Characterization, 13*(2), 143-149.

Nasser, E. (1986). *Fundamentals of Gaseous Ionization and Plasma Electronics*: University Microfilms.

Nielsen, K. A., & Hill, J. C. (1976a). Capture of particles on spheres by inertial and electrical forces. *Industrial & Engineering Chemistry Fundamentals, 15*(3), 157-163. doi: 10.1021/i160059a002

Nielsen, K. A., & Hill, J. C. (1976b). Collection of inertialess particles on spheres with elecrical forces. *Industrial & Engineering Chemistry Fundamentals, 15*(3), 149-157. doi: 10.1021/i160059a001

Noymer, P. D., & Garel, M. (1999). Stability and atomization characteristics of electrohydrodynamic jets in the cone-jet and multi-jet modes. *Journal of Aerosol Science, 31*(10), 1165-1172.

Odic, E., Goldman, A., Goldman, M., Delaveau, S., & Le Hegarat, F. (2002). Plasma sterilization technologies and processes. *High Temperature Material Processes, 6*(3), 12.

Okuyama, K., Wuled Lenggoro, I., Tagami, N., Tamaki, S., & Tohge, N. (1997). The formation of ultrafine particles of metal sulfide by the ES pyrolysis method. *KONA Powder and Particle Journal, 15*(May), 227-234.

Olumee, Z., Callahan, J. H., & Vertes, A. (1998). Droplet dynamics changes in electrostatic sprays of methanol-water mixtures. *Journal of Physical Chemistry A, 102*(46), 9154-9160. doi: 10.1021/jp982027z

Park, D., Kim, S., An, M., & Hwang, J. (2007). Real-time measurement of submicron particles with log-normal size distribution by unipolar diffusion and field charger. *Journal of Aerosol Science, 38*(12), 1240-1245.

Park, I., Kim, S. B., Hong, W. S., & Kim, S. S. (2015). Classification of EHD spraying modes of water in air at atmospheric pressure. *Journal of Aerosol Science, 89*(Supplement C), 26-30.

Park, S. H., Lee, K. W., Shimada, M., & Okuyama, K. (2005). Coagulation of bipolarly charged ultrafine aerosol particles. *Journal of Aerosol Science, 36*(7), 830-845.

Parker, K. R. (1997). *Applied Electrostatic Precipitation*: Springer.

Parmentier, D., Rybałtowska, A., van Smeden, J., Kroon, M., Marijnissen, J., & Lemos, L. (2016). EHDA for enhance mass transfer of metal salts from aqueous phase towards ionic liquids. *Journal of Electrostatics, 80*, 1-7.

Penney, G. W. (1944). Electrified liquid spray dust precipitator: Google Patents.

Pfeifer, R. J., & Hendrick.Cd. (1968). Parametric studies of EHD spraying. *Aiaa Journal, 6*(3), 496-+.

Pilat, M. J. (1978). USA Patent No. Brit. pat Spec.: W. University.

Pilat, M. J., Jaasund, S. A., & Sparks, L. E. (1974). Collection of aerosol particles by electrostatic droplet spray scrubbers. *Environmental Science & Technology, 8*(4), 360-362. doi: 10.1021/es60089a006

Pilat, M. J., & Lukas, J. C. (2004). Droplet charging for wet scrubbers. *Journal of the Air & Waste Management Association, 54*(1), 3-7.

Pilat, M. J., & Prem, A. (1977). Effect of diffusiophoresis and thermophoresis on overall particle collection efficiency of spray droplet scrubbers. *Journal of the Air Pollution Control Association, 27*(10), 982-988.

Pohl, P., & al., e. (2017). Crtical evaluation of Low power APGD between a flowing liquid cathode and a metal anode for element analysis by optical emission spectroscopy. *Trends in Analytical Chemistry, 88*, 119-133.

Pongrác, B., Kim, H. H., Janda, M., Martišovitš, V., & Machala, Z. (2014). Fast imaging of intermittent electrospraying of water with positive corona discharge. *Journal of Physics D: Applied Physics, 47*(31).

Pongrác, B., Krčma, F., Dostál, L., Kim, H. H., Homola, T., & Machala, Z. (2016). Effects of corona space charge polarity and liquid phase ion mobility on the shape and velocities of water jets in the spindle jet and precession modes of water electro-spray. *Journal of Aerosol Science, 101*, 196-206.

Pongrac, B. P., & MacHala, Z. (2011). Electrospraying of water with streamer corona discharge. *IEEE Transactions on Plasma Science, 39*(11 PART 1), 2664-2665.

Post, P., Jidenko, N., Weber, A. P., & Borra, J. P. (2016). Post-Plasma SiOx Coatings of Metal and Metal Oxide Nanoparticles for Enhanced Thermal Stability and Tunable Photoactivity Applications. *Nanomaterials, 6*(5).

Pozniak, B. P., & Cole, R. B. (2004). Negative ion mode evolution of potential buildup and mapping of potential gradients within the ES emitter. *Journal of the American Society for Mass Spectrometry, 15*(12), 1737-1747.

Pozniak, B. P., & Cole, R. B. (2007). Current Measurements within the Electrospray Emitter. *Journal of the American Society for Mass Spectrometry, 18*(4), 737-748.

Prajapati, B. G., & Patel, M. (2010). A technology update: Electro spray technology. *International Journal of Pharmaceutical Sciences Review and Research, 1*(1), 11-13.

Prem, A., & Pilat, M. J. (1978). Calculated particle collection efficiencies by single droplets considering inertial impaction brownian diffusion and electrostatics. *Atmospheric Environment, 12*(10), 1981-1990.

Pyrgiotakis, G., McDevitt, J., Bordini, A., Diaz, E., Molina, R., Watson, C., . . . Demokritou, P. (2014). A chemical free, nanotechnology-based method for airborne bacterial inactivation using engineered water nanostructures. *Environmental Science-Nano, 1*(1), 15-26. doi: 10.1039/c3en00007a

Pyrgiotakis, G., McDevitt, J., Yamauchi, T., & Demokritou, P. (2012). *Bacterial inactivation by engineered water nanostructures generated by electrospraying*.

Pyrgiotakis, G., Vedantam, P., Cirenza, C., McDevitt, J., Eleftheriadou, M., Leonard, S. S., & Demokritou, P. (2016). Optimization of a nanotechnology based antimicrobial platform for food safety applications using Engineered Water Nanostructures (EWNS). *Scientific Reports, 6*. doi: 10.1038/srep21073

Quang Tran Si, B., Byun, D., & Lee, S. (2007). Experimental and theoretical study of cone-jet for ES microthruster considering the interference effect in an array of nozzles. *Journal of Aerosol Science, 38*(9), 924-934.

Radionova, A., Greenwood, D. R., Willmott, G. R., & Derrick, P. J. (2016). Dual nano-electrospray and mixing in the taylor cone. *Mass Spectrometry Letters, 7*(1), 21-25.

Raether, H. (1964). *Electron Avalanches and Breakdown in Gases*: Butterworths.

Rai, P., Gautam, N., & Chandra, H. (2017). An Experimental Approach of Generation of Micro/Nano Scale Liquid Droplets by EHDA Process. *Materials Today-Proceedings, 4*(2), 611-620.

Rayleigh, L. (1879). *Proc. Ryal Soc., 29*, 71.

Rayleigh, L. (1882). XX. On the equilibrium of liquid conducting masses charged with electricity. *The London, Edinburgh, and Dublin Philosophical Magazine and Journal of Science, 14*(87), 184-186.

Rönkkö, T., Kuuluvainen, H., Karjalainen, P., Keskinen, J., Hillamo, R., Niemi, J., . . . Dal Maso, M. (2017). Traffic: major source of atmospheric nanocluster. *Proceedings of National Academy of Science, 114*(29), 7549-7554.

Rosell-Llompardt, J., Bodnar, E., & grifoll, J. (2018a). Polymer solution electrospraying: A tool for engineering particles and films with controlled morphology. *J. Aerosol Sci., present Special Issue*, pp to be filled.

Rosell-Llompardt, J., Grifoll, J., & Loscertales, I. (2018b). Electrosprays in the cone-jet mode: from Taylor cone formation to spray development, . *J. Aerosol Sci., present Special Issue*, pp to be filled

Rulison, A. J., & Flagan, R. C. (1994). Synthesis of yttria powders by electrospray pyrolysis. *Journal of the American Ceramic Society, 77*(12), 3244-3250.

Savart, F. (1833). Mémoire sur la constitution des veines liquides lancées par des orifices circulaires en mince paroi *Annales de chimie et de physique* (pp. 337-386): Masson.

Shi, F., Chen, M., Xu, Z., Sun, X., Chen, X., & Gao, X. (2011). Investigation of ES and application for the synthesis of fine ceramic powder. *Journal of Shenyang Jianzhu University (Natural Science), 27*(6), 1127-1136.

Shirai, N., Matsui, K., Ibuka, S., & Ishii, S. (2011). Atmospheric negative corona discharge observed at tip of taylor cone using PVA solution. *IEEE Transactions on Plasma Science, 39*(11 PART 1), 2210-2211.

Shirai, N., Sekine, R., Uchida, S., & Tochikubo, F. (2014). Atmospheric negative corona discharge using Taylor cone as a liquid cathode. *Japanese Journal of Applied Physics, 53*(2 PART 1).

Shiryaeva, S. O., & Grigorev, A. I. (1995). The semiphenomenological classification of the modes of electrostatic dispersion of liquids. *Journal of Electrostatics, 34*(1), 51-59. doi: 10.1016/0304-3886(94)00041-t

Sigmund, S., Akgun, E., Meyer, J., Hubbuch, J., Worner, M., & Kasper, G. (2014a). Defined polymer shells on nanoparticles via a continuous aerosol-based process. *Journal of Nanoparticle Research, 16*(8).

Sigmund, S., Yu, M. Z., Meyer, J., & Kasper, G. (2014b). An Aerosol-Based Process for Electrostatic Coating of Particle Surfaces with Nanoparticles. *Aerosol Science and Technology, 48*(2), 142-149.

Sisterson, D. L., & Liaw, Y. P. (1990). An evaluation of lightning and corona discharge on thunderstorm air and precipitation chemistry. *Journal of Atmospheric Chemistry, 10*(1), 83-96.

Smith, D. P. H. (1986). The EHD atomization of liquids. *IEEE Transactions on industry applications, IA*(28).

Snarski, S. R., & Dunn, P. F. (1991). Experiments characterizing the interaction between 2 sprays of electrically charged liquid droplets. *Experiments in Fluids, 11*(4), 268-278.

Song, Y., Chan, Y. K., Ma, Q. M., Liu, Z., & Shum, H. C. (2015). All-Aqueous Electrosprayed Emulsion for Fabrication of Cytocompatible Microcapsules. *Acs Applied Materials & Interfaces, 7*(25), 13925-13933.

Stachewicz, U., Yurteri, C. U., Frits Dijksman, J., & Marijnissen, J. C. M. (2010). Single event electrospraying of water. *Journal of Aerosol Science, 41*(10), 963-973.

Stratmann, F., Otto, E., & Fissan, H. (1992). Theoretical investigation of ion and particle transport in space charge fields. *Journal of Aerosol Science, 23, Supplement 1*, 101-104.

Sugimoto, T., Asano, K., & Higashiyama, Y. (2001). Negative corona discharge at a tip of water cone deformed under dc field. *Journal of Electrostatics, 53*(1), 25-38.

Sumiyoshitani, S. (1996). Three-dimensional model for analyzing charge carrier motion around a charged spherical object in the presence of flow and electric field. *Aerosol Science and Technology, 24*(4), 279-289.

Sun, M., Borocilo, D., Harvel, G. D., Ibe, M., Matsubara, H., Fanson, P., . . . Chang, J. S. (2011). Two-phase flow regimes and discharge characteristics of a plasma electrohydrodynamic atomization. *Plasma Science and Technology, 13*(1).

Sweet, M. L., Pestov, D., Tepper, G. C., & McLeskey Jr, J. T. (2014). Electrospray aerosol deposition of water soluble polymer thin films. *Applied Surface Science, 289*, 150-154.

Sweet, R. G. (1965). High Frequency recording with electrostatically deflected ink-jets. *Review of Scientific Instruments, 36*(131-136).

Tai, J. T., Lai, C. S., Ho, H. C., Yeh, Y. S., Wang, H. F., Ho, R. M., & Tsai, D. H. (2014). Protein Silver Nanoparticle Interactions to Colloidal Stability in Acidic Environments. *Langmuir, 30*(43), 12755-12764.

Tang, H. B., Qin, C. J., & Liu, Y. (2011). Characterization of colloid thruster beams and plumes. *Journal of Aerosol Science, 42*(2), 114-126.

Tang, J., & Gomez, A. (1994a). Structure of an ES of monodisperse droplets. *Physics of Fluids, 6*(7), 2317-2332.

Tang, J., Liu, W., Wang, H. L., & Gomez, A. (2016). High Performance Metal Oxide-Graphene Hybrid Nanomaterials Synthesized via Opposite-Polarity Electrosprays. *Advanced Materials, 28*(46), 10298-10303.

Tang, J., Wang, H. C., & Gomez, A. (2017a). Controlled nanoparticle synthesis via opposite-polarity electrospray pyrolysis. *Journal of Aerosol Science, 113*, 201-211.

Tang, J., Wang, H. L., & Gomez, A. (2017b). Controlled nanoparticle synthesis via opposite-polarity electrospray pyrolysis. *Journal of Aerosol Science, 113*, 201-211. doi: 10.1016/j.jaerosci.2017.07.001

Tang, K., & Gomez, A. (1994b). Generation by electrospray of monodisperse water droplets for targeted drug delivery by inhalation. *Journal of Aerosol Science, 25*(6), 1237-1249. doi: 10.1016/0021-8502(94)90212-7

Tang, K., & Gomez, A. (1995). Generation of Monodisperse Water Droplets from Electrosprays in a Corona-Assisted Cone-Jet Mode. *Journal of Colloid And Interface Science, 175*(2), 326-332.

Tang, K., & Gomez, A. (1996). Monodisperse electrosprays of low electric conductivity liquids in the cone-jet mode. *Journal of Colloid and Interface Science, 184*(2), 500-511.

Tatoulian, M., Arefi-Khonsari, F., Tatoulian, L., Amouroux, J., & Borra, J. P. (2006). Deposition of poly(acrylic acid) films by EHDA in postdischarge at atmospheric pressure in air. *Chemistry of Materials, 18*(25), 5860-5863.

Taylor, G. I. (1964). Disintegration of water drops in an electric field. *Proceeding of the Royal Society of London , Mathematical and Physical Sciences, A280*, 383-397.

Thompson, S. P., & Prewett, P. D. (1984). The dynamics of liquid metal ion sources. *Journal of Physics D: Applied Physics, 17*(11), 2305-2321.

Townsend, J. S. (1915). *Electricity in Gases*: Clarendon Press.

Tsai, D. H., DelRio, F., Pettibone, J., Lin, P. A., Tan, J. J., Zachariah, M., & Hackley, V. (2013). T-programmed ES-DMA for characterization of ligated nanoparticles in complex media. *Langmuir, 29*(36), 11267-11274.

Tsai, D. H., Zangmeister, R. A., Pease, L. F., Tarlov, M. J., & Zachariah, M. R. (2008). Gas-phase ion-mobility characterization of SAM-functionalized Au nanoparticles. *Langmuir, 24*(16), 8483-8490.

Uehara, S., Itoga, T., & Nishiyama, H. (2015). Discharge and flow characteristics using magnetic fluid spikes for air pollution control. *Journal of Physics D-Applied Physics, 48*(28). doi: 10.1088/0022-3727/48/28/282001

Unger, L. (2001). *Charge d'aérosol par décharge électrique pour la filtration d'effluents particulaires* PhD, Paris-South University, Orsay.

Unger, L., Boulaud, D., & Borra, J. P. (2004). Unipolar field charging of particles by electrical discharge: effect of particle shape. *Journal of Aerosol Science, 35*(8), 965-979. doi: 10.1016/j.jaerosci.2004.01.0060

Unger, L., Ehouarn, P., & Borra, J. P. (1999). *Influence of submicron aerosols on the operation of a wire-cylinder discharge.* Paper presented at the 15th French Congress on Aerosols.

Unger, L., Ehouarn, P., & Borra, J. P. (2000). Influence of aerosol deposition on the charging efficiency of a corona charger. *Journal of Aerosol Science, 31, Supplement 1*(0), 612-613.

Unger, L., Ehouarn, P., & Borra, J. P. (2003, 31st Aug.-5th Sept.). *Filtration of submicron sized particles by electro-coagulation.* Paper presented at the European Aerosol Conference, Madrid.

Vaaraslahti, K., Laitinen, A., & Keskinen, J. (2002). Spray charging of droplets in a wet scrubber. *Journal of the Air & Waste Management Association, 52*(2), 175-180.

Vehring, R. (2008). Pharmaceutical Particle Engineering via Spray Drying. *Pharmaceutical Research, 25*(5), 999-1022. doi: 10.1007/s11095-007-9475-1

Velásquez-García, L. F., Akinwande, A. I., & Martínez-Sánchez, M. (2006). A planar array of micro-fabricated ES emitters for thruster applications. *Journal of Microelectromechanical Systems, 15*(5), 1272-1280.

Verdoold, S., Agostinho, L. L. F., Yurteri, C. U., & Marijnissen, J. C. M. (2014). A generic electrospray classification. *Journal of Aerosol Science, 67*, 87-103. doi: 10.1016/j.jaerosci.2013.09.008

Verdoold, S., & Marijnissen, J. C. M. (2011). Modeling a bipolar-coagulation reactor using coupled population balances. *Journal of Electrostatics, 69*(3), 240-254. doi: 10.1016/j.elstat.2011.03.018

Verdoold, S., Marijnissen, J. C. M., & Scarlett, B. (2000). Scaling-up the bipolar coagulation process. *Journal of Aerosol Science, 31*(SUPPL.1), S857-S858.

Vicard, J. (1977). *Resultats et Experience Acquise avec un Nouveau Depoussiereur Electrique á Grande Vitesse: Le Venturi Electro-Dynamique.* Paper presented at the Proceedings of 4th Int. Clean Air Congress.

Vonnegut, B., & Neubauer, R. L. (1952). Production of monodisperse liquid particles by electrical atomization. *Journal Colloid Science, 7*, 616-622.

Wang, A., Song, Q., & Yao, Q. (2016a). Study on inertial capture of particles by a droplet in a wide Reynolds number range. *Journal of Aerosol Science, 93*, 1-15. doi: https://doi.org/10.1016/j.jaerosci.2015.11.010

Wang, A., Song, Q., & Yao, Q. (2016b). Thermophoretic capture of submicron particles by a droplet. *Atmospheric Environment, 147*, 157-165. doi: https://doi.org/10.1016/j.atmosenv.2016.10.001

Wang, D., Duan, H., Li, J., Liang, J., & Liu, C. (2011). EHDA deposition and patterning of a carbon nano-suspension. *Proceedings of the Institution of Mechanical Engineers, Part N, 225*(4), 149-154.

Wang, D., Wang, L., Liang, J., Xia, Z., Wang, S., Zhu, Y., . . . Sun, G. (2013). Formation of a catalyst membrane by EHDA Layer-by-Layer deposition for methanol fuel cells. *Journal of Power Sources, 224*, 202-210.

Wang, D. Z., Jayasinghe, S. N., & Edirisinghe, M. J. (2005). High resolution print-patterning of a nano-suspension. *Journal of Nanoparticle Research, 7*(2-3), 301-306.

Wang, D. Z., Jayasinghe, S. N., Edirisinghe, M. J., & Luklinska, Z. B. (2007a). Coaxial electrohydrodynamic direct writing of nano-suspensions. *Journal of Nanoparticle Research, 9*(5), 825-831.

Wang, L., Stevens, R., Malik, A., Rockett, P., Paine, M., Adkin, P., . . . Dobson, P. (2007b). High-aspect-ratio silica nozzle fabrication for nano-emitter ES applications. *Microelectronic Engineering, 84*(5-8), 1190-1193.

Ward, L. J., Schofield, W. C. E., Badyal, J. P. S., Goodwin, A., & Merlin, P. (2003a). Atmospheric pressure plasma deposition of structurally well-defined polyacrylic acid films. *Chemistry of Materials, 15*(7), 1466-1469.

Ward, L. J., Schofield, W. C. E., Badyal, J. P. S., Goodwin, A. J., & Merlin, P. J. (2003b). Atmospheric pressure glow discharge deposition of polysiloxane and SiOx films. *Langmuir, 19*(6), 2110-2114. doi: 10.1021/la0204287

Watanabe, T., Tochikubo, F., Koizumi, Y., Tsuchida, T., Hautanen, J., & Kauppinen, E. I. (1995). Submicron particle agglomeration by an electrostatic agglomerator. *Journal of Electrostatics, 34*(4), 367-383.

Wei, W., Gu, Z., Wang, S., Zhang, Y., Lei, K., & Kase, K. (2013). Numerical simulation of cone-jet formation and current in ES - Modeling of space charge. *Journal of Micromechanics and Microengineering, 23*(1).

Whitby, K. T. (1961). Generator for Producing High Concentrations of Small Ions. *Rev. Sci. Instrum., 32*, 1351-1355.

Whitby, K. T., Liu, B. Y. H., & Peterson, C. M. (1965). Charging and decay of monodispersed aerosols in presence of unipolar ion sources. *Journal of Colloid Science, 20*(6), 585-&.

Whitehouse, C. M., Dreyer, R. N., Yamashita, M., & Fenn, J. B. (1985). Electrospray interface for liquid chromatographs and mass spectrometers. *Analytical Chemistry, 57*(3), 675-679.

Wilhelm, O., & Mädler, L. (2006). Cone-jet and multijet electrosprays: Transport and evaporation. *Atomization and Sprays, 16*(1), 83-102.

Wilhelm, O., Mädler, L., & Pratsinis, S. E. (2003). Electrospray evaporation and deposition. *Journal of Aerosol Science, 34*(7), 815-836. doi: https://doi.org/10.1016/S0021-8502(03)00034-X

Wilm, M. S., & Mann, M. (1994). Electrospray and Taylor-Cone theory, Dole's beam of macromolecules at last? *International Journal of Mass Spectrometry and Ion Processes, 136*(2-3), 167-180.

Wu, D., McFarland, A. R., & Fjeld, R. A. (1987). Continuum field-diffusion charging of particles possessing non-zero initial charge. *Journal of Aerosol Science, 18*(4), 409-417.

Wu, Y. Q., & Clark, R. L. (2008a). EHD atomization: a versatile process for preparing materials for biomedical applications. *Journal of Biomaterials Science-Polymer Edition, 19*(5), 573-601.

Wu, Y. Q., & Clark, R. L. (2008b). Nanomaterials and biosensors ; EHD processing of Micro/Nanometer Biological materials. In X. L. P. K. Chu (Ed.), *Biomaterials fabrication and processing handbook*: Boca Raton, CRC Press/Taylor & Francis.

Xie, J., Jiang, J., Davoodi, P., Srinivasan, M. P., & Wang, C. H. (2015). EHD atomization: A two-decade effort to produce and process micro-/nanoparticulate materials. *Chemical Engineering Science, 125*, 32-57.

Xu, D. X., Li, J., Wu, Y., Wang, L. H., Sun, D. W., Liu, Z. Y., & Zhang, Y. B. (2003). Discharge characteristics and application for DC-ESP: corona with spraying electrodes. *Journal of Electrostatics, 57*(3-4), 217-224.

Xu, P., Zhang, B., Wang, Z., Chen, S., & He, J. (2017). Dynamic corona characteristics of water droplets on charged conductor surface. *Journal of Physics D: Applied Physics, 50*(8).

Xu, X., Lu, W., & Cole, R. B. (1996). On-Line Probe for Fast Electrochemistry/Electrospray Mass Spectrometry. Investigation of Polycyclic Aromatic Hydrocarbons. *Analytical Chemistry, 68*(23), 4244-4253.

Yamashita, M., & Fenn, J. B. (1984). NEGATIVE-ION PRODUCTION WITH THE ELECTROSPRAY ION-SOURCE. *Journal of Physical Chemistry, 88*(20), 4671-4675. doi: 10.1021/j150664a046

Yan, F., Farouk, B., & Ko, F. (2003). Numerical modeling of an electrostatically driven liquid meniscus in the cone-jet mode. *Journal of Aerosol Science, 34*(1), 99-116.

Yang, H. T., Viswanathan, S., Balachandran, W., & Ray, M. B. (2003). Modeling and Measurement of ES Behavior in a Rectangular Throat of Venturi Scrubber. *Environmental Science & Technology, 37*(11), 2547-2555.

Yang, W. W., Lojewski, B., Wei, Y., & Deng, W. W. (2012). Interactions and deposition patterns of multiplexed electrosprays. *Journal of Aerosol Science, 46*, 20-33. doi: 10.1016/j.jaerosci.2011.11.004

Yin, F. H., Farzaneh, M., & Jiang, X. L. (2017). Corona Investigation of an Energized Conductor under Various Weather Conditions. *Ieee Transactions on Dielectrics and Electrical Insulation, 24*(1), 462-470.

You, R., Li, M., Guha, S., Mulholland, G. W., & Zachariah, M. R. (2014). Bionanoparticles as Candidate Reference Materials for Mobility Analysis of Nanoparticles. *Analytical Chemistry, 86*(14), 6836-6842.

Yu, J. H., Kim, S. Y., & Hwang, J. (2007). Effect of viscosity of silver nanoparticle suspension on conductive line patterned by EHD jet printing. *Applied Physics A: Materials Science and Processing, 89*(1), 157-159.

Yuill, E. M., Shi, W. Q., Poehlrnan, J., & Baker, L. A. (2015). Scanning Electrospray Microscopy with Nanopipets. *Analytical Chemistry, 87*(22), 11182-11186. doi: 10.1021/acs.analchem.5b03399

Yunoki, A., Tsuchiya, E., Yu, F. K., Fujii, A., & Maruyama, T. (2014). Preparation of Inorganic/Organic Polymer Hybrid Microcapsules with High Encapsulation Efficiency by an Electrospray Technique. *Acs Applied Materials & Interfaces, 6*(15), 11973-11979. doi: 10.1021/am503030c

Zeleny, J. (1914). The Electrical Discharge from Liquid Points, and a Hydrostatic Method of Measuring the Electric Intensity at Their Surfaces. *Physical Review, 3*(2), 69-91.

Zeleny, J. (1917). Instability of Electrified Liquid Surfaces. *Physical Review, 10*(1), 1-6.

Zevenhoven, C. A. P., Wierenga, R. D. J., Scarlett, B., & Yamamoto, H. (1994). An evaluation of the Masuda "boxer charger". *Journal of Electrostatics, 32*(2), 133-155.

Zhao, H. B., & Zheng, C. G. (2008). Modeling of Gravitational Wet Scrubbers with Electrostatic Enhancement. *Chemical Engineering & Technology, 31*(12), 1824-1837. doi: 10.1002/ceat.200800360

Zuo, Z., Wang, J., Huo, Y., & Xu, R. (2017). Numerical study of particle motion near a charged collector. *Particuology, 32*, 103-111. doi: https://doi.org/10.1016/j.partic.2016.05.017

https://doi.org/10.1016/j.jaerosci.2018.04.005

*LIST of FIGURES*

https://doi.org/10.1016/j.jaerosci.2018.04.005

# 7 Appendix A : Materials and methods for electro-scrubbing

Properties of collecting water droplets and test aerosols (diameter, electrical charge, concentration), have been controlled independently from 0 to $10^{-6}$ $m^2.V^{-1}.s^{-1}$ for electrical mobilities of sub-micron aerosol by a wire-cylinder corona charger (Unger et al., 2004) and from 30 to 70 % of the maximum Rayleigh charge limit for water drop, see section 3 (Ehouarn P. et al., 2001). A set of conditions to achieve steady water ES in corona assisted cone-jet (100 $mL.h^{-1}$, 200 $\mu S.m^{-1}$ water) is used to produce *90 µm droplets with 3.6 pC per drop (9.4 $mC.kg^{-1}$)*. The charged aerosol is mixed with droplets of opposite polarity produced by a line of four ES on top of an horizontal pipe of 7 cm diameter for 10 cm inter nozzle distance

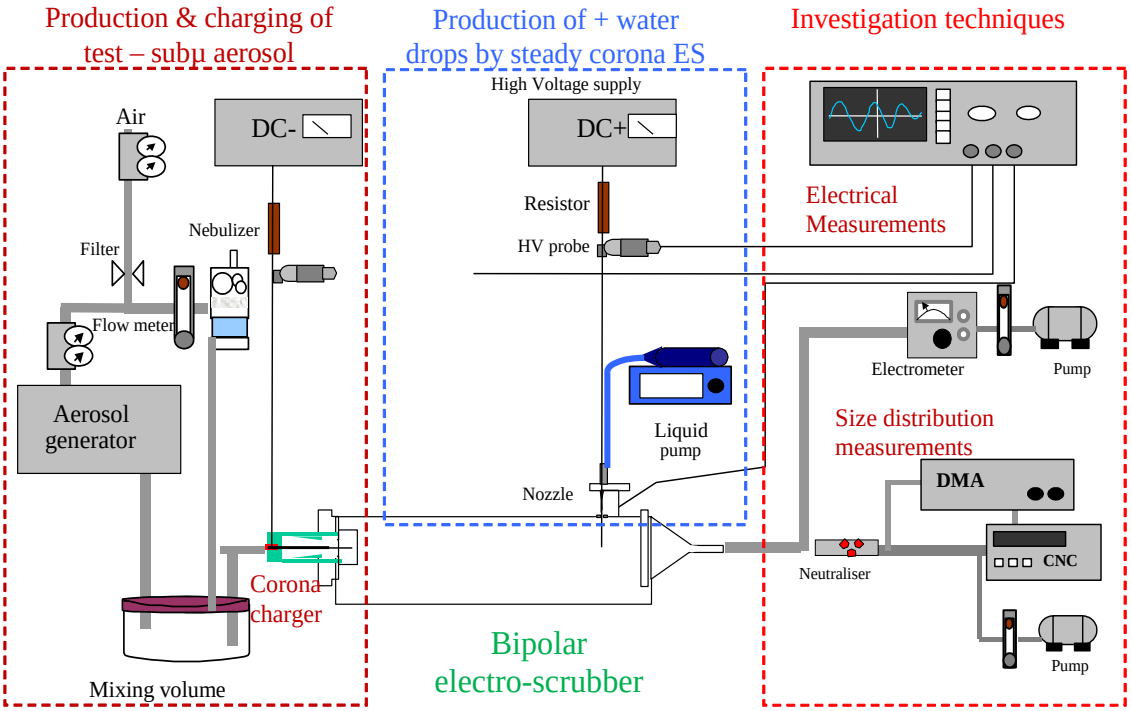


**Figure A1: Set-up for the production of water droplets**

The experimental set-up is classical for aerosol filtration studies (see Fig. A1) with:
- ***aerosol production***: A Sinclair-Lamer Generator is used to produce a monodisperse aerosol of Di-Ethyl-Hexyl-Sebacate with tunable modal diameters from 0.4 to 1.1 µm and a pneumatic nebulizer to achieve unimodal size distribution of 0.3 µm DEHS droplets or NaCl dissolved in water droplet leading to 30 to 70 nm salt crystals after evaporation versus the initial salt concentration in water, before nebulization). These aerosols generators are fed with dry filtered compressed air, with controlled relative humidity, critical in terms of corona charger stability with subsequent control of a steady charge diameter relation.

- ***aerosol charging:*** These test aerosols are then charged in a wire-cylinder corona discharge, detailed in Unger *et al.*, 2000, to produce sub-micron negative particles hereafter referred as the "test aerosol", detailed in (Ehouarn P. et al., 2001; Unger et al., 2004).
*Required ion collection downstream the corona charger to prevent competitive electro-scrubbing of negative gaseous ions and charged aerosol:* As expected, lower efficacies were reported with than without gaseous ions injection, probably due to higher mobility and resulting electro-coagulation on positive water droplets, reducing thus the mean charge per collecting drop.
This expected preliminary result leads to design a charged aerosol exhaust pipe from the corona charger within which gaseous ions were collected on the walls from the test charged aerosol with the same polarity before injection, mixing and electro-coagulation on water droplets charged in opposite polarity (see Fig. A2).

https://doi.org/10.1016/j.jaerosci.2018.04.005

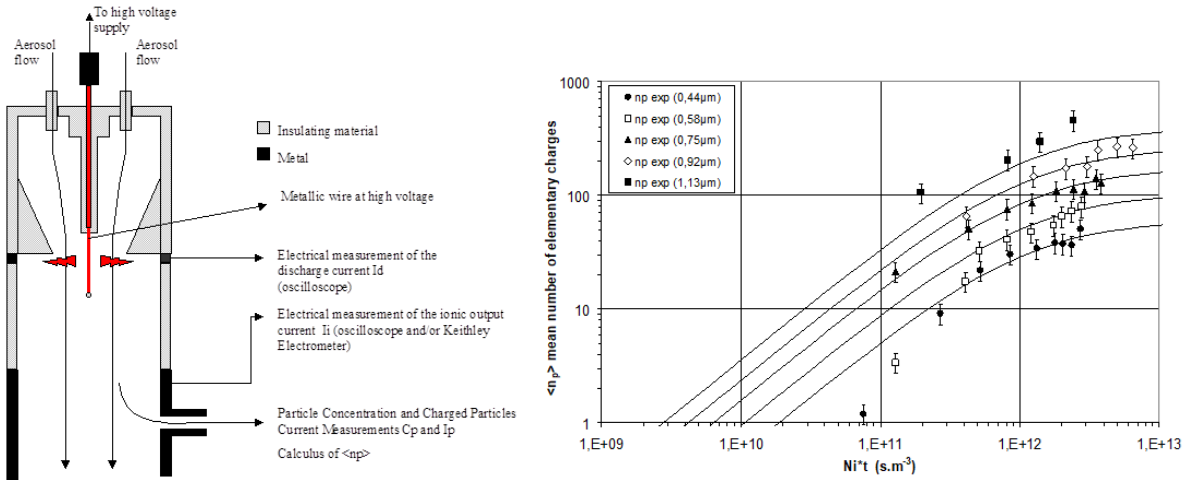


**Figure A2 : (a) Wire cylinder corona charger used to charge the submicron sized particles (b) measured and calculated charge versus particle diameter in reference conditions for electro-coagulation tests presented in the last section**

- ***Production of positive scrubbing water droplets****:* Different number and arrangements of ES nozzles were first tested versus ES liquid flowrate for fifteen different nozzle diameters to select one simple set of operating conditions - droplet characteristics at different liquid flowrates, and then in reference test conditions for ES (100 mL/h 200 µS/m), the number of ES nozzles, the symmetry and the density of the net of ES production nozzles with lines, circles and hexagonal nets from 250 to 5000 Nozzle / m²)

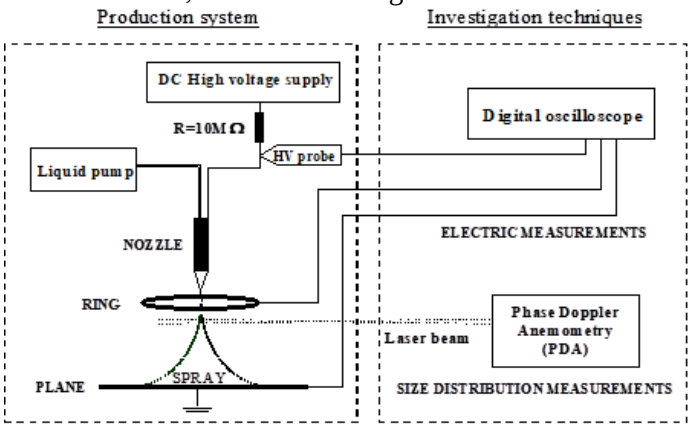


**Figure A3: Set-up for the production of water droplets**

Positive water droplets were produced by electrospray in the corona assisted cone-jet mode for liquid flow rates from a few tens to a few hundred mL/hour, as discussed in section 3 and detailed in Figure A3 (see Borra *et al.*, 1999 and Ehouarn *et al.*, 2001). Water with conductivities from 100 to 5000 µS/m, is electro sprayed with nozzle diameter 0.4 mm. Doing so, droplets with charge levels close to the maximum Rayleigh limit (from 30 to 70%) were produced to enhance electro-coagulation efficiency. Well-controlled water droplets properties (diameter, electrical charge, concentration), were then tuned by simple operating parameters such as the nozzle voltage and the liquid flow rate, as depicted in the previous section 3 and detailed in Table 1.

**Table 1: droplet and spray properties versus the water flow rate**

https://doi.org/10.1016/j.jaerosci.2018.04.005

| Qliq. (mL/h) | I total (µA) | I drops | Mean diameter | Prod.° Frequency | q drop | % qRayleigh | q/m | electrical mobility |
|---|---|---|---|---|---|---|---|---|
| | corona ions & drops | (µA) | (µm) | Qliq / drop vol. (Hz) | Idrop / Freq. (C ) | | (C/kg) | (m2.Volt-1.s-1) |
| 50 | 5,22 | 0,17 | 55,7 | 1,54E+05 | 1,11E-12 | 37% Qr | 1,23E-02 | 1,17E-04 |
| 60 | 5 | 0,19 | 65,7 | 1,12E+05 | 1,69E-12 | 45% Qr | 1,14E-02 | 1,52E-04 |
| 70 | 4,13 | 0,22 | 74,28 | 9,07E+04 | 2,43E-12 | 53% Qr | 1,13E-02 | 1,93E-04 |
| 75 | 3,87 | 0,225 | 77 | 8,72E+04 | 2,58E-12 | 54% Qr | 1,08E-02 | 1,98E-04 |
| 100 | 3 | 0,25 | 91,4 | 6,95E+04 | 3,60E-12 | 58% Qr | 9,02E-03 | 2,32E-04 |
| 150 | 2,1 | 0,27 | 114 | 5,37E+04 | 5,02E-12 | 58% Qr | 6,49E-03 | 2,60E-04 |
| 200 | 2 | 0,3 | 142 | 3,71E+04 | 8,09E-12 | 67% Qr | 5,41E-03 | 3,36E-04 |

***- Mixing and coagulation conditions for experimental investigation of electro-scrubbers***.
Droplet are characterized in terms of particle diameter, charge and concentration profile in the scrubber. The charged aerosol is mixed with water droplets of opposite polarities downstream the corona charger in different scrubbers, with coaxial or cross flow of aerosol related to the axis of ES nozzles.
Since most of particle filtration devices works at exhaust velocities in the order of meter per second in scrubbers, fabric filters and ESP, *electro-scrubbing test are frequently performed in this sub m/s range*, except in inertial Stokes impactor, cyclones and venturi scrubbers. Then, the continuous production of unipolar droplets is achieved in steady ES in pulseless corona assisted cone-jet mode for *sub m/s* inlet velocities, as reported up to cross flow velocities of 15 m/s, above which the gas flow interact with the liquid and modifies its shape affecting thus the capillary pressure and the cone-jet shape or even worst stability (Allaf-Akbari et al., 2017).
ES bipolar scrubbing has been performed in horizontal pipes to achieve particle injection in clouds of droplets above a minimal droplet concentration for efficient bipolar scrubbing (see section 4.3.1.2). Here for water ES, a pipe diameter of 7 cm with spray separated by a longer length to achieve self-induced development of the spray over a few cm.

The complete description of these experiments with additional results and detailed calculations on :
- droplet characteristics at different liquid flowrates, and then in reference test conditions for ES (100 mL/h 200 µS/m) versus the number of ES nozzles, the symmetry and the density of the net of ES production nozzles with lines, circles and hexagonal nets from 250 to 5000 Nozzle.m$^{-2}$)
- corona chargers with size-mobility relations for different aerosol nature and concentration
- droplet density profiles in two types of scrubbers with parallel or crossflow injections
Then in selected ES, corona and mixing test conditions, with one to four water ES nozzles (outer and inner diameters of 0.4/0.25 mm at 100 mL.h$^{-1}$ of 200 µS.m$^{-1}$ water), as the reference test conditions, filtration test have been performed versus:
- the electrical field profile in the scrubbers controlled by surface potential of walls and electrodes, positive and negative charge densities and distribution with different relative positions of injection of oppositely charged aerosol and droplets in the scrubber, aerosol flowrate, as well as with different ring voltages from 0 to 10 kV, focusing the spray and limiting its radial development,
- the concentration of aerosol to be filtered that affects the negative currents of charged species from the corona charger into the scrubber, reducing the positive space charge created by scrubbing droplets in the scrubber by co-injection of negative corona ions (from 0 to 500 nA compared to the 300 nA of charged droplets per ES).

https://doi.org/10.1016/j.jaerosci.2018.04.005

# Table des matières